Studies on Synthesis and Physicochemical Properties of Substituted [n]Phenacenes (n = 5 and 6) through Cross-Coupling Reaction/Double Cyclization Sequences

2013.9

Ning-hui CHANG

Graduate School of Natural Science and Technology
(Doctor's Course)
OKAYAMA UNIVERSITY

Contents

Abstract

Organic materials have attracted a great deal of attention as active layers in organic field-effect transistors (OFETs) and organic light-emitting diodes (OLEDs) because of their mechanical flexibility, light weight, large-area coverage, ambipolar property, and low-cost/low-temperature fabrication process. On the other hand, fused polycyclic aromatic compounds possessing an extended π-conjugation system have been developed owing to their potential application toward organic electronic devices. Development of methods to prepare various derivatives is of great interest because derivatization of the fused aromatic compounds may adjust their optical and electronic properties as well as their solubility and packing structures in the crystals.

This Ph.D Thesis describes novel and versatile methods for the synthesis of various [n]phenacenes (n = 5 and 6) derivatives by Suzuki-Miyaura coupling reactions of polyhalobenzenes with (*Z*)-alkenylboronates and sequential double cyclization via C−H bond activation. The physicochemical properties of [5]- and [6]phenacenes derivatives were modified by introducing different functional groups to the phenacene framework. All compounds have been evaluated by UV-vis and fluorescence spectra, and CV as well as DFT calculations.

Chapter 1 addresses an overview of organic field-effect transistors (OFETs) and the application of [n]phenacene in OFETs. Previous reported synthetic methods for the synthesis of [n]phenacenes are summarized. After the drawbacks of these methods are pointed out, novel and convenience methods are proposed.

Chapter 2 describes the detail exploration, optimization, and completion of the versatile synthetic method of picene ([5]phenacene) and its derivatives as new compounds. The appropriate and practical strategy for the formation of picene was explored. Initially, the Author exploited a direct cyclization of the precursor, 1,2-bis[(1*Z*)-2-phenylethenyl]benzene, which was readily prepared by coupling reaction of 1,2-

diiodobenzene with 2 equivalents of (*Z*)-phenylethenylboronates. In spite of irradiation and oxidation reaction for the precursor, no desired product was obtained. As an alternative synthetic route, two halogen atoms were introduced to 1,2-diiodobenzene to synthesize 1,4-dichloro-2,3-diiodobenzene. By using Suzuki-Miyaura coupling, 2,3-bis[(1*Z*)-2-arylethenyl]-1,4-dichlorobenzenes were prepared as the precursors, which were converted to picenes through the Pd-catalyzed intramolecular double cyclization. The physicochemical properties of the obtained picenes were varied by introducing a variety of functional groups into the picene framework. All compounds are evaluated by UV-vis and fluorescence spectroscopic measurements, CV, and DFT calculations. Based on this study, the effects of the structural variations of substituents on their electronic and electrochemical properties have emerged.

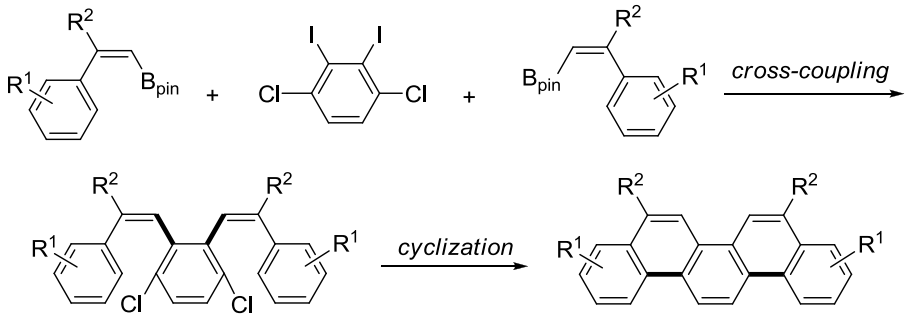

Chapter 3 describes development and application of aforementioned methodology to synthesis of [6]phenacenes. The results that the increased numbers of the benzene rings in [n]phenacene would have potentials to improve the FET characteristics imply that the synthesis of expanded [n]phenacenes is necessary. A new family of the unsymmetrically substituted [6]phenacenes were synthesized via Suzuki-Miyaura coupling of 1,4-dichloro-2,3-diiodobenzene with two alkenylboronates and the subsequent intramolecular cyclization. An introduction of methoxy and alkyl groups into [6]phenacene framework increased the solubility of [6]phenacenes. The physicochemical properties of the synthesized [6]phenacenes were also investigated by measurements of UV-vis and fluorescence spectra, CV, and DFT calculations.

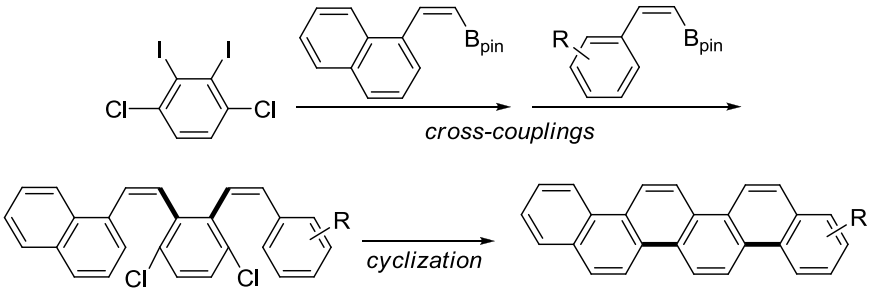

Chapter 4 summarizes the contents of this Thesis and a perspective of this research is described.

CHAPTER 1

General Introduction

1-1 A Brief Overview of Organic Field-Effect Transistors

A field-effect transistor (FET) is an electronic device that amplifies and switches electrical signals. Since the discovery of highly conducting polyacetylene by Shirakawa, MacDiarmid, and Heeger[1] in 1977, π-conjugated systems have attracted much attention as futuristic materials for the development and production of the next generation of electronics,[2] that is, organic electronics.[3] It means that we are facing a new technological evolution that could possibly impact on our lives—the emergence of flexible and printed electronics.[4]

Conceptually, organic electronics are quite different from conventional inorganic solid-state electronics because the structural versatility of organic semiconductors allows for the incorporation of functionality by molecular design. This versatility leads to a new era in the design of electronic devices. To date, a great number of π-conjugated semiconducting materials that have either been discovered or synthesized generate an exciting library of π-conjugated systems for use in organic electronics.[5]

Among them, organic field-effect transistors (OFETs) have been conceptualized and developed over the past two decades.[6,7] OFETs are devices consisting of an organic semiconducting layer, a gate insulator layer, and three terminals (drain, source, and gate electrodes) (Figure 1-1).

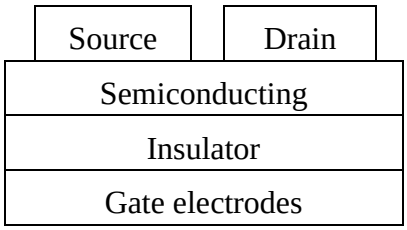

Figure 1-1. A schematic drawing of the top-contact OFET device.

OFETs are not only essential building blocks for the next generation of cheap and flexible organic circuits, but also provide an important insight into the charge transport of π-conjugated systems. Therefore, they act as strong tools for the exploration of the structure property relationships of π-conjugated systems, such as parameters of field-effect

mobility (μ, the drift velocity of carriers under unit electric field), current on/off ratio (the ratio of the maximum on-state current to the minimum off-state current), and threshold voltage (the minimum gate voltage that is required to turn on the transistor).[8]

Since the discovery of OFETs in the 1980s,[9] they have attracted much attention. Research on OFETs includes the discovery, design, and synthesis of π-conjugated systems for OFETs, device optimization, development of applications in radio frequency identification (RFID) tags, flexible displays,[10,11] electronic papers,[12,13] sensors,[14] and so forth.

1-2 Application of [n]Acenes and [n]Phenacenes in OFETs

It is no doubt that the semiconducting π-conjugated system incorporated into OFETs is one of the most important factors determining the ultimate performance of the device. In principal, the mobility of the organic semiconductor should be as high as possible so that an efficient charge transport from one molecule to another is attainable. This in turn is intimately related to the electron cloud on the molecule and the electron cloud splitting with its neighbor molecules. Two parameters, the transfer integral and the reorganization energy, are both believed to be highly important for the mobility of organic semiconductors. The transfer integral means the splitting of the highest occupied molecular orbital (HOMO) and the lowest unoccupied molecular orbital (LUMO). This in turn depends to a large extent on the π-overlap between neighboring molecules.[15] The reorganization energy is the energy loss when a charge carrier passes through a molecule and is dependent on the conjugation length, degree, and packing of the organic molecules.[16] Usually, the larger the transfer integral and the smaller the reorganization energy, the higher the mobility will be.[17]

Small molecule semiconductors have been widely studied because they are easy to purify and easily form crystalline films for the fabrication of the desired high performance devices. Typical [n]acenes and [n]phenacenes, as seen in Chart 1-1, show ideal transistor behaviors when employed in OFETs. Their π-conjugated systems are similar to that of

single layer of graphite, that is, graphene (to date, the aromatic compound with the highest mobility and which recently won its discoverers the 2010 Noble Prize in physics).

Anthracene has been examined in OFETs and its single crystal devices exhibited mobility at 0.02 $cm^2\ V^{-1}\ s^{-1}$ at low temperature.[18] Normally, with the expansion of the π-conjugated dimension, the intermolecular overlap of the electron cloud is increased, and this results in a larger transfer integral and lower reorganization energy.[19] Gundlach et al.[20] found that thin film field-effect transistors of tetracene showed a mobility of 0.1 $cm^2\ V^{-1}\ s^{-1}$ with a current on/off ratio over 10^6 on octadecyltrichlorosilane (ODTS)-modified SiO_2 substrates. Its single crystal transistors[21] provided a mobility of 2.4 $cm^2\ V^{-1}\ s^{-1}$ by using poly(dimethylsiloxane) (PDMS) as the dielectric layer. Thin film transistors[22] of pentacene demonstrated mobilities of up to 1.5 $cm^2\ V^{-1}\ s^{-1}$ with an on/off ratio over 10^8. Clearly, the field-effect mobility is increasing on going from anthracene to pentacene with the extension of the π-conjugated systems. This is attributed to the associated benefits of intermolecular π-orbital overlap and the fact that the charge transport is facilitated (for larger transfer integral and lower reorganization energy).

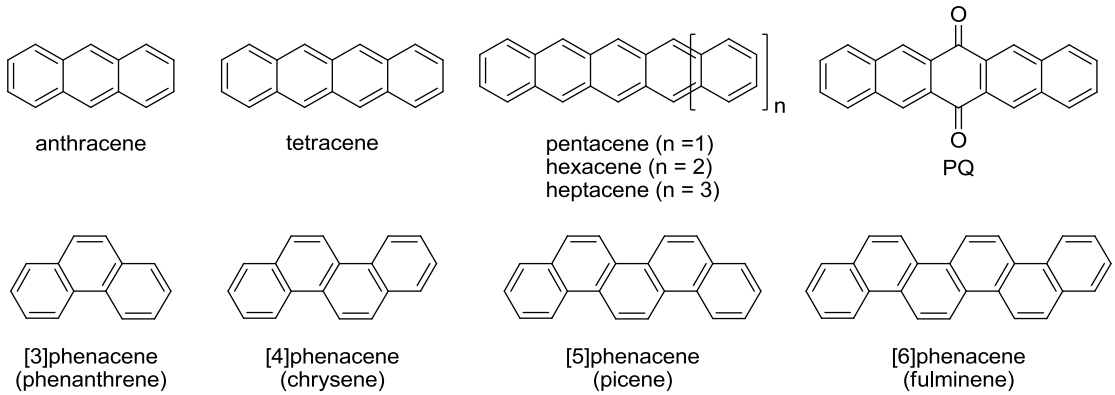

Chart 1-1. Structures of [n]acenes and [n]phenacenes.

However, one disadvantage of higher acenes is not only their high sensitivity to light because of their narrow energy gaps (from anthracene,[23] tetracene,[24] to pentacene:[25] 4.0, 2.6, and 1.8 eV, respectively) leading to easy molecular excitation by light but also their high HOMO energy levels (from anthracene,[23] tetracene,[24] to pentacene:[25] −5.7, −5.2, and −5.0

eV, respectively) which results in high oxidation sensitivity . For example, pentacene easily forms dimers and trimers under ambient conditions or can be oxidized into 6,13-pentacenequinone (PQ) (Chart 1-1). Moreover, a solubility of pentacene is also very poor in common organic solvents.[26] As a result, purification of pentacene is highly challenging (ultrapure pentacene is almost impossible to obtain due to the existence of PQ). With a further increase in the number of benzene rings for extension of the π-conjugated systems, the stability and solubility of the larger acenes become even poorer so that OFETs based on hexacene[27] and heptacene[28] have never been addressed.

By contrast, [n]phenacene molecules have high stability even against O_2 and H_2O. [n]Phenacenes as large as [11]phenacene have been synthesized,[29] while [9]acene (nonacene) has been the largest acene obtained to date. The stability of phenacenes has also been elaborated experimentally and theoretically.[30]

Picene (represented as [5]phenacene),[31a] an isomeric compound of pentacene, shows higher stability because its energy band gap is larger (Eg = 3.3 eV) and its ionization potential is higher (IP = 5.5 eV) than those of pentacene (Eg = 1.8 eV, IP = 5.0 eV). The OFET performance of picene exhibited typical p-channel characteristics with a mobility of 1.1 $cm^2\ V^{-1}\ s^{-1}$ and an on/off ratio of 10^5 under atmospheric conditions. The mobility was found to approach 3.2 $cm^2\ V^{-1}\ s^{-1}$ if the device was exposed to O_2 for oxygen doping.[31b]

More recently, the [6]phenacene thin film FET has been fabricated and its p-channel FET characteristics have been confirmed.[32] As expected from the molecular alignment in [6]phenacene thin films on SiO_2 surface, the μ value as high as 3.7 $cm^2\ V^{-1}\ s^{-1}$ has been realized, which is one of the highest in organic thin film FETs. The clear O_2 sensing properties are observed as in picene thin film FET. The high μ and clear O_2 sensing properties suggest that [6]phenacene is a promising material for practical high-performance organic FET.

1-3 Previous Reports on Synthesis of [n]Phenacenes

[n]Phenacenes such as picene have attracted less attention than acenes such as pentacene for use in organic electronic devices because only a few efficient synthetic methods are currently available for [n]phenacenes. The difficulty in obtaining large quantities of phenacenes has delayed their application in electronics. Synthetic pathways for picene so far reported are summarized in Figure 1-2.

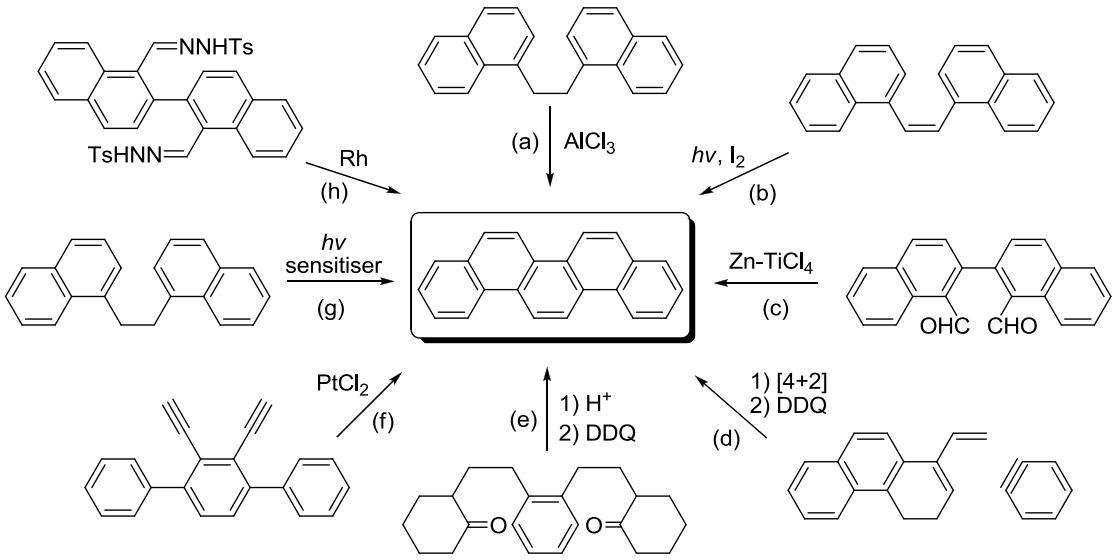

Figure 1-2. Previous synthesis routes to picene.

It has been reported that 1,2-dinaphthylethane underwent cyclization to picene in the presence of a Lewis acid (path a).[33] However, this acid-promoted cyclization has still not been reproduced. Photocyclization of stilbene to phenanthrene has been established as a procedure to construct the phenanthrene skeleton,[34] and this photoreaction was applied to a 1,2-dinaphthylethene system to produce picene (path b). But, this irradiation method is the limited application in large-scale synthesis. Intramolecular McMurry coupling of bi(β-naphthyl) can also produce picene in a moderate yield (path c).[35] [4 + 2] cycloaddition between benzyne and vinyl-substituted dihydrophenanthrene (path d)[36] and intramolecular Friedel–Crafts-type cyclization (path e)[37] were used to prepare the picene framework in the 1990s. Besides, Pt-catalyzed cycloaromatization of an ethynyl-substituted *p*-terphenyl has

been developed to synthesize picene derivatives (path f).[38] Recently, an one-step photochemical synthesis of picene was developed, in which 1,2-dinaphthylethane was irradiated in the presence of sensitizers to afford picene (path g).[39] Additionally, the rhodium(II)-catalyzed intramolecular cyclization of bis(*N*-tosylhydrazone)s provided an alternative strategy for the picene synthesis (path h).[40]

1-4 The Aims of This Research

As mentioned above, [n]phenacenes, arm-chair edged benzenoid compounds possessing extended π-conjugation, have attracted a great deal of attention as an active layer in organic field-effect transistors (OFETs), which can offer many attractions for unconventional electronic circuitry,[41] including solution-processability/printability,[42] mechanical flexibility,[43] fabrication at low temperatures,[44] low production costs via roll-to-roll printing,[45] biocompatibility,[46] and high performance.[47] However, the systematic modification of a [n]phenacene core has rarely been reported. In addition, there are several critical drawbacks in the reported synthetic methods for [n]phenacenes, such as limitation of irradiation for large-scale,[34,39] multi-steps for starting materials preparation, using expensive and unstable transition metals,[38] and a requirement of unstable precursors.[40] In addition, these methods are based on the naphthyl or phenanthryl motifs, which is difficult to introduce a variety of functional groups into the picene framework, compared to the benzene ring-based strategy.

On the other hand, solubilities of the unsubstituted [n]phenacenes dramatically decrease with an increasing n.[29] For instance, [5]phenacene (picene) is sparingly soluble in $CHCl_3$, whereas the $^{13}C\{^1H\}$ NMR spectrum of [6]phenacene cannot be obtained due to its extreme insolubility. This solubility problem can be overcome by incorporating alkyl substituents into the core. Since ideal OFETs are expected to be solution-processed and exhibit high carrier mobility, high solubility of the molecules in common organic solvents.

In order to solve the problems in previous reports, the Author aimed to develop a simple and convenient methodology that involves sequential Suzuki-Miyaura coupling of

polyhalobenzenes with (Z)-alkenylboronates and sequential intramolecular cyclization to synthesize [n]phenacenes (Scheme 1-1). For the further investigation, characterization through measurements of UV-vis, fluorescence spectra, cyclic voltammetry, and DFT calculations as well as X-ray diffraction analysis were carried out, and physicochemical properties of a series of novel substituted [n]phenacenes (n = 5, 6) were evaluated.

Scheme 1-1. A new methodology for synthesis of [n]phenacenes.

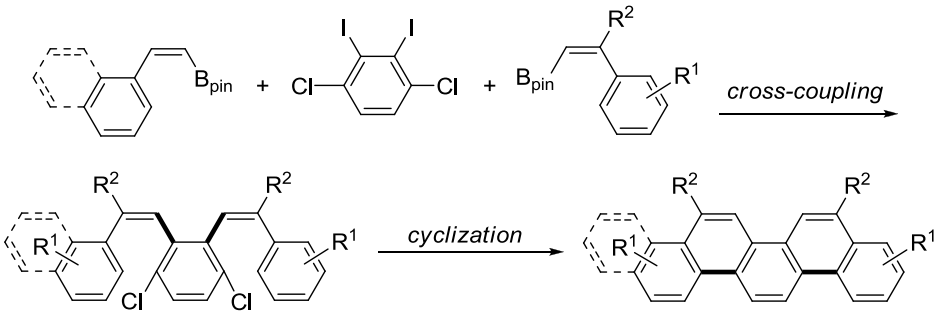

1-5 References and Notes

[1] Chiang, C. K.; Fincher, C. R.; Park, Y. W.; Heeger, A. J.; Shirakawa, H.; Louis, E. J.; Gau, S. C.; MacDiarmid, A. G. *Phys. Rev. Lett.* **1977**, *39*, 1098.

[2] Dimitrakopoulos, C. D.; Malenfant, P. R. L. *Adv. Mater.* **2002**, *14*, 99.

[3] Muccini, M. *Nat. Mater.* **2006**, *5*, 605.

[4] Mei, J.; Diao, Y.; Appleton, A. L.; Fang, L.; Bao, Z. *J. Am. Chem. Soc.* **2013**, *135*, 6724.

[5] (a) Anthony, J. E. *Chem. Rev.* **2006**, *106*, 5028. (b) Takimiya, K.; Kunugi, Y.; Otsubo, T. *Chem. Lett.* **2007**, *36*, 578. (c) Yamada, H.; Okujimaa, T.; Ono, N. *Chem. Commun.* **2008**, 2957. (d) Anthony, J. E. *Angew. Chem., Int. Ed.* **2008**, *47*, 452. (e) Blouin, N.; Leclerc, M. *Acc. Chem. Res.* **2008**, *41*, 1110. (f) Mas-Torrent, M.; Rovira, C. *Chem. Soc. Rev.* **2008**, *37*, 827. (g) Wu, W.; Liu, Y.; Zhu, D. *Chem. Soc. Rev.* **2010**, *39*, 1489. (h) Pron, A.; Gawrys, P.; Zagorska, M.; Djurado, D.; Demadrille, R. *Chem. Sov. Rev.* **2010**, *39*, 2577.

[6] Mallik, A. B.; Locklin, J.; Mannsfeld, S. C. B.; Reese, C.; Roberts, M. E.; Senatore, M. L.; Zi, H.; Bao, Z. In *Organic Field-Effect Transistors*; Zhenan, B., Locklin, J. J., Eds.; CRC Press: Boca Raton, FL, 2007, p 159−228.

[7] Wang, C.; Dong, H.; Hu, W.; Liu, Y.; Zhu, D. *Chem. Rev.* **2011**, *112*, 2208.

[8] (a) Strohriegl, P.; Grazulevicius, J. V. *Adv. Mater*. **2002**, *14*, 1439. (b) Sun, Y. M.; Liu, Y. Q.; Zhu, D. B. *J. Mater. Chem*. **2005**, *15*, 53. (c) Facchetti, A. *Mater. Today* **2007**, *10*, 28. (d) Murphy, A. R.; Frechet, J. M. J. *Chem. Rev.* **2007**, *107*, 1066. (e) Mishra, A.; Ma, C. Q.; Bauerle, P. *Chem. Rev*. **2009**, *109*, 1141. (f) Yamashita, Y. *Sci. Technol. Adv. Mater.* **2009**, *10*, 024313.

[9] (a) Tsumura, A.; Koezuka, H.; Ando, T. *Appl. Phys. Lett*. **1986**, *49*, 1210. (b) Madru, M.; Guillaud, G.; Sadoun, M. A.; Maitrot, M.; Clarisse, C.; Contellec, M. L.; Andre, J. J.; Simon, J. *Chem. Phys. Lett.* **1987**, *142*, 103.

[10] Gelinck, G. H.; Huitema, H. E. A.; van Veenendaal, E.; Cantatore, E.; Schrijnemakers, L.; van der Putten, J. B. P. H.; Geuns, T. C. T.; Beenhakkers, M.; Giesbers, J. B.; Huisman, B.-H.; Meijer, E. J.; Benito, E. M.; Touwslager, F. J.; Marsman, A. W.; van Rens, B. J. E.; de Leeuw, D. M. *Nat. Mater*. **2004**, *3*, 106.

[11] Huitema, H. E. A.; Gelinck, G. H.; van der Putten, J. B. P. H.; Kuijk, K. E.; Hart, C. M.; Cantatore, E.; Herwig, P. T.; van Breemen, A. J. J. M.; de Leeuw, D. M. *Nature* **2001**, *414*, 599.

[12] Rogers, J. A.; Bao, Z.; Baldwin, K.; Dodabalapur, A.; Crone, B.; Raju, V. R.; Kuck, V.; Katz, H.; Amundson, K.; Ewing, J.; Drzaic, P. Proc. *Natl. Acad. Sci. U. S. A.* **2001**, *98*, 4835.

[13] Comiskey, B.; Albert, J. D.; Yoshizawa, H.; Jacobson, J. *Nature* **1998**, *394*, 253.

[14] Sokolov, A. N.; Roberts, M. E.; Bao, Z. *Mater. Today* **2009**, *12*, 12.

[15] Bredas, J. L.; Calbert, J. P.; da Silva, D. A.; Cornil, J. *Proc. Natl. Acad. Sci. U. S. A.* **2002**, *99*, 5804.

[16] (a) Hutchison, G. R.; Ratner, M. A.; Marks, T. J. *J. Am. Chem. Soc.* **2005**, *127*, 2339. (b) Cornil, J.; Bredas, J. L.; Zaumseil, J.; Sirringhaus, H. *Adv.Mater.* **2007**, *19*, 1791.

[17] (a) Bromley, S. T.; Mas-Torrent, M.; Hadley, P.; Rovira, C. *J. Am. Chem. Soc.* **2004**, *126*, 6544. (b) Brédas, J.-L.; Beljonne, D.; Coropceanu, V.; Cornil, J. *Chem. Rev.* **2004**, *104*, 4971.

[18] Aleshin, A. N.; Lee, J. Y.; Chu, S. W.; Kim, J. S.; Park, Y. W. *Appl. Phys. Lett.* **2004**, *84*, 5383.

[19] da Silva Filho, D. A.; Kim, E.-G.; Brédas, J.-L. *Adv.Mater.* **2005**, *17*, 1072.

[20] Gundlach, D. J.; Nichols, J. A.; Zhou, L.; Jackson, T. N. *Appl. Phys. Lett.* **2002**, *80*, 2925.

[21] Reese, C.; Chung, W.-J.; Ling, M.-M.; Roberts, M.; Bao, Z. *Appl. Phys. Lett*. **2006**, *89*, 202108.

[22] Lin, Y. Y.; Gundlach, D. J.; Nelson, S. F.; Jackson, T. N. *IEEE Electron Device Lett.* **1997**, *18*, 606.

[23] Nayak, P. K.; Periasamy, N. *Org. Electron.* **2009**, *10*, 1396.

[24] Chen, Z.; Muller, P.; Swager, T. M. *Org. Lett.* **2006**, *8*, 273.

[25] Klauk, H.; Zschieschang, U.; Weitz, R. T.; Meng, H.; Sun, F.; Nunes, G.; Keys, D. E.; Fincher, C. R.; Xiang, Z. *Adv. Mater*. **2007**, *19*, 3882.

[26] Ito, K.; Suzuki, T.; Sakamoto, Y.; Kubota, D.; Inoue, Y.; Sato, F.; Tokito, S. *Angew. Chem., Int. Ed.* **2003**, *42*, 1159.

[27] Mondal, R.; Adhikari, R. M.; Shah, B. K.; Neckers, D. C. *Org. Lett*. **2007**, *9*, 2505.

[28] Mondal, R.; Shah, B. K.; Neckers, D. C. *J. Am. Chem. Soc.* **2006**, *128*, 9612.

[29] Mallory, F. B.; Butler, K. E.; Evans, A. C.; Brondyke, E. J.; Mallory, C. W.; Yang C.; Ellenstein, A. *J. Am. Chem. Soc.* **1997**, *119*, 2119.

[30] Portella, G.; Poater, J.; Bofill, J. M.; Alemany, P.; Sola, M. *J. Org. Chem.* **2005**, *70*, 2509.

[31] (a) Okamoto, H.; Kawasaki, N.; Kaji, Y.; Kubozono, Y.; Fujiwara, A.; Yamaji, M. *J. Am. Chem. Soc.* **2008**, *130*, 10470. (b) Kawasaki, N.; Kubozono, Y.; Okamoto, H.; Fujiwara, A.; Yamaji, M. *Appl. Phys. Lett*. **2009**, *94*, 043310

[32] Komura, N.; Goto, H.; He, X.; Mitamura, H.; Eguchi, R.; Kaji, Y.; Okamoto, H.; Sugawara, Y.; Gohda, S.; Sato, K.; Kubozono, Y. *Appl. Phys. Lett.* **2012**, *101*, 083301..

[33] Buu-Hoï, N. P.; Hoán, N. *J. Org. Chem.* **1949**, *14*, 1023.

[34] (a) Mallory, F. B.; Mallory, C. W. *Org. React.* **1984**, *30*, 1. (b) Mallory, F. B.; Mallory, C. W.; Regan, C. K.; Aspden, R. J.; Ricks, A. B.; Racowski, J. M.; Nash, A. I.; Gibbons, A. V.; Carroll, P. J.; Bohen, J. M. *J. Org. Chem.* **2013**, *78*, 2040.

[35] Some, S.; Dutta, B.; Ray, J. K. *Tetrahedron Lett.* **2006**, *47*, 1221.

[36] Minuti, L.; Taticchi, A.; Gacs-Baitz, E.; Marrocchi, A. *Tetrahedron* **1998**, *54*, 10891.

[37] Harvey, R. G.; Pataki, J.; Cortez, C.; Di Raddo, P.; Yang, C. X. *J. Org. Chem.* **1991**, *56*, 1210.

[38] Kitazawa, K.; Kochi, T.; Nitani, M.; Ie, Y.; Aso, Y.; Kakiuchi, F. *Chem. Lett.* **2011**, *40*, 300.

[39] Okamoto, H.; Yamaji, M.; Gohda, S.; Kubozono, Y.; Komura, N.; Sato, K.; Sugino, H.; Satake, K. *Org. Lett.* **2011**, *13*, 2758.

[40] Xia, Y.; Liu, Z.; Xiao, Q.; Qu, P.; Ge, R.; Zhang, Y.; Wang, J. *Angew. Chem., Int. Ed*. **2012**, *51*, 5714.

[41] (a) Cho, S.; Seo, J. H.; Park, S. H.; Beaupre, S.; Leclerc, M.; Heeger, A. J. *Adv. Mater*. **2010**, *22*, 1253. (b) Wen, Y. G.; Liu, Y. Q. *Adv. Mater.* **2010**, *22*, 1331. (c) Virkar, A. A.; Mannsfeld, S.; Bao, Z.; Stingelin, N. *Adv. Mater*. **2010**, *22*, 3857. (d) Anthony, J. E.; Facchetti, A.; Heeney, M.; Marder, S. R.; Zhan, X. W. *Adv. Mater*. **2010**, *22*, 3876. (e) Sirringhaus, H.; Bird, M.; Richards, T.; Zhao, N. *Adv. Mater.* **2010**, *22*, 3893. (f) Facchetti, A. *Chem. Mater.* **2011**, *23*, 733. (g) Spijkman, M. J.; Myny, K.; Smits, E. C. P.; Heremans, P.; Blom, P. W. M.; de Leeuw, D. M. *Adv. Mater*. **2011**, *23*, 3231. (h) Wen, Y. G.; Liu, Y. Q.; Guo, Y. L.; Yu, G.; Hu, W. P. *Chem. Rev.* **2011**, *111*, 3358.

[42] (a) Marks, T. J. *MRS Bull.* **2010**, *35*, 1018. (b) Arias, A. C.; MacKenzie, J. D.; McCulloch, I.; Rivnay, J.; Salleo, A. *Chem. Rev.* **2010**, *110*, 3. (c) Liu, C. A.; Minari, T.; Lu, X. B.; Kumatani, A.; Takimiya, K.; Tsukagoshi, K. *Adv. Mater.* **2011**, *23*, 523.

[43] (a) Street, R. A.; Wong, W. S.; Ready, S. E.; Chabinyc, I. L.; Arias, A. C.; Limb, S.; Salleo, A.; Lujan, R. *Mater. Today* **2006**, *9*, 32. (b) Zschieschang, U.; Ante, F.; Yamamoto, T.; Takimiya, K.; Kuwabara, H.; Ikeda, M.; Sekitani, T.; Someya, T.; Kern, K.; Klauk, H. *Adv. Mater.* **2010**, *22*, 982. (c) Gelinck, G.; Heremans, P.; Nomoto, K.; Anthopoulos, T. D. *Adv. Mater*. **2010**, *22*, 3778.

[44] Murphy, A. R.; Frechet, J. M. J. *Chem. Rev.* **2007**, *107*, 1066.

[45] (a) Kjellander, B. K. C.; Smaal, W. T. T.; Anthony, J. E.; Gelinck, G. H. *Adv. Mater*. **2010**, *22*, 4612. (b) Sun, J.; Zhang, B.; Katz, H. E. *Adv. Funct. Mater.* **2011**, *21*, 29. (c)

Shao, M.; Das, S.; Xiao, K.; Chen, J.; Keum, J. K.; Ivanov, I. N.; Gu, G.; Durant, W.; Li, D.; Geohegan, D. B. *J. Mater. Chem. C*, **2013**, *1*, 4384.

[46] (a) Roberts, M. E.; Sokolov, A. N.; Bao, Z. N. *J. Mater. Chem.* **2009**, *19*, 3351. (b) Irimia-Vladu, M.; Troshin, P. A.; Reisinger, M.; Shmygleva, L.; Kanbur, Y.; Schwabegger, G.; Bodea, M.; Schwodiauer, R.; Mumyatov, A.; Fergus, J. W.; Razumov, V. F.; Sitter, H.; Sariciftci, N. S.; Bauer, S. *Adv. Funct. Mater.* **2010**, *20*, 4069. (c) Sokolov, A. N.; Tee, B. C. K.; Bettinger, C. J.; Tok, J. B. H.; Bao, Z. *Acc. Chem. Res.* **2012**, *45*, 361.

[47] (a) Tsao, H. N.; Cho, D.; Andreasen, J. W.; Rouhanipour, A.; Breiby, D. W.; Pisula, W.; Mullen, K. *Adv. Mater.* **2009**, *21*, 209. (b) DiBenedetto, S. A.; Facchetti, A.; Ratner, M. A.; Marks, T. J. *Adv. Mater.* **2009**, *21*, 1407. (c) Osaka, I.; Zhang, R.; Sauve, G.; Smilgies, D. M.; Kowalewski, T.; McCullough, R. D. *J. Am. Chem. Soc.* **2009**, *131*, 2521. (d) Lee, W. H.; Cho, J. H.; Cho, K. *J. Mater. Chem.* **2010**, *20*, 2549. (e) Shao, W.; Dong, H. L.; Jiang, L.; Hu, W. P. *Chem. Sci.* **2011**, *2*, 590. (f) Giri, G.; Verploegen, E.; Mannsfeld, S. C. B.; Atahan-Evrenk, S.; Kim, D. H.; Lee, S. Y.; Becerril, H. A.; Aspuru-Guzik, A.; Toney, M. F.; Bao, Z. *Nature* **2011**, *480*, 504. (g) Ma, H.; Acton, O.; Hutchins, D. O.; Cernetic, N.; Jen, A. K.-Y. *Phys. Chem. Chem. Phys.* **2012**, *14*, 14110. (h) Ito, M.; Uemura, T.; Soeda, J.; Takeya, J. *Org. Electron.* **2013**, *14*, 2144. (i) Yuan, J.; Zang, Y.; Dong, H.; Liu, G.; Di, C.; Li, Y.; Ma, W. *Polym. Chem.* **2013**, *4*, 4199.

CHAPTER 2

Synthesis of [5]Phenacenes and Their Physicochemical Properties

2-1 Introduction

Fused polycyclic aromatic compounds have been attracting a great deal of interest in view of the application of organic materials for electronic devices such as organic field effect transistors (OFETs) and light-emitting diodes (OLEDs).[1] Among them, [n]phenacenes, arm-chair edged benzenoid compounds possessing extended π-conjugation, have attracted a great deal of attention as active layers in organic field-effect transistors (OFETs)[2] because of their advantages compared to conventional inorganic FET.

Picene ([5]phenacene, Figure 2-1, left) represents a novel and promising class of materials for organic electronics.[3] An OFET with a thin film of picene (Figure 2-1, right) showed a high μ value more than 1.1 $cm^2\ V^{-1}\ s^{-1}$ and the OFET device properties are clearly improved, not only the μ value but also the on-off ratio under air/O_2 conditions.[3a] Furthermore, alkali-metal, potassium or rubidium, doped picene exhibited superconductivity below 18 K.[3c] The development of methods to prepare various picene derivatives is of great interest because it may adjust their optical and electronic properties as well as their solubility and packing structures in the crystals.[4] However, the systematic modification of a picene core has rarely been reported.[5] In addition, there are several critical drawbacks for the established synthetic methods of picenes. Therefore, a simple and convenient strategy for the synthesis of various substituted picene derivatives is highly desirable in order to promote further investigations into its use in organic electronics.

In this Chapter, the Author discusses the synthesis, characterization, and physicochemical properties of a series of novel substituted picenes.

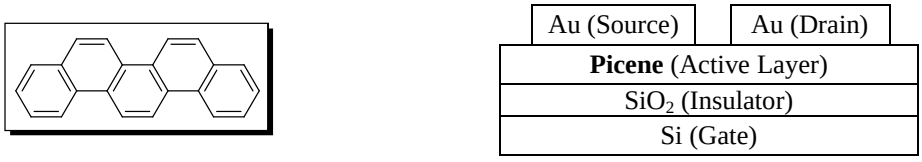

Figure 2-1. Structure of picene (left) and picene thin film FET device (right).

2-2 Results and Discussion

2-2-1 Exploration of a new synthetic route to picenes

An outline for retrosynthetic analysis of picene is shown in Scheme 2-1. In order to obtain picene as the target molecule through C−C bond formation, at least two pathways can be considered. In path a, after synthesis of (*Z*,*Z*)-*o*-styrylbenzene as a precursor, the desired product can be obtained through intramolecular C−H activation. In path b, an alternative synthetic route, two halogen atoms can be introduced into the precursor and the target molecule can also be obtained via intramolecular double cyclization. These two precursors can be readily synthesized by cross-coupling reactions of 2-fold excess of alkenylboronates with 1,2-diiodobenzene or 1,4-dibromo (or chloro)-2,3-diiodobenzene.

Scheme 2-1. A retrosynthetic analysis of picene.

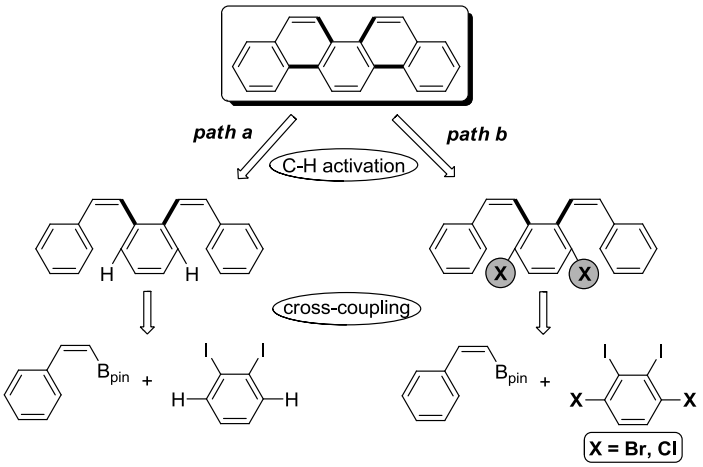

Firstly, Suzuki-Miyaura coupling reaction to synthesize the precursor of picene **3a'** was carried out. Examining various reaction conditions of 1,2-diiodobenzene (**1'**) with (*Z*)-phenylethenylboronates (**2a**) was initiated. Several reaction parameters, such as Pd catalysts, phosphine ligands, solvents, bases, temperatures, times, and the equivalent of substrates were optimized. The results were summarized in Table 2-1.

Among the tested Pd catalysts, PEPPSI-IPr[6] (Figure 2-2) gave the best result. When the reaction was conducted under 75 °C using toluene as the solvent, inexpensive K_2CO_3 as the base, the corresponding product was obtained in 82% GC yield after 3 h (entry 22). As

expected, when 2.2 equivs of **2a** was used, the yield of **3a'** was increased to 90% GC yield (entry 23). Under the optimization conditions, **3a′** was isolated in 78% yield by column chromatography.

Table 2-1. Optimization of Suzuki-Miyaura coupling reaction of **1'** with **2a**.

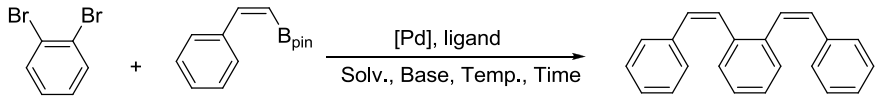

1' (1.0 eq) **2a** (X eq.) **3a'**

Entry	X	[Pd] (5 mol %) + ligand	Solvent	Base	Temp. (°C)	Time (h)	GC yield (%)
1	2.0	PEPPSI-IPr	THF	TBAF	50	3	72
2	2.0	$PdCl_2(dppf)CH_2Cl_2$	THF	K_2CO_3	75	24	72
3	2.0	$Pd(PPh_3)_4$	toluene	K_2CO_3	100	24	6
4	2.0	$PdCl_2(PPh_3)_2$	dioxane	K_2CO_3	100	24	32
5	2.0	$PdCl_2(dppf)CH_2Cl_2$	THF	TBAF	50	3	54
6	2.0	$PdCl_2(PPh_3)_2$	THF	TBAF	50	3	62
7	2.0	$PdCl_2$	THF	TBAF	50	3	22
8	2.0	$Pd(OAc)_2$ + dppf	THF	TBAF	50	3	<1
9	2.0	$Pd(OAc)_2$ + $Cp_2Fe[P(p\text{-}C_6H_4\text{-}CF_3)_2]_2$	THF	TBAF	50	3	22
10	2.0	$PdCl_2$ + dppf	THF	TBAF	50	3	<1
11	2.0	$PdCl_2$ + $Cp_2Fe[P(p\text{-}C_6H_4\text{-}CF_3)_2]_2$	THF	TBAF	50	3	5
12	2.0	$Pd(CH_3CN)_2Cl_2$	THF	TBAF	50	3	<1
13	2.0	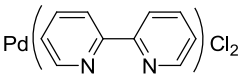	THF	TBAF	50	3	<1
14	2.0	$PdCl_2$(dppe)	THF	TBAF	50	3	45
15	2.0	$PdPhI(PPh_3)_2$	THF	TBAF	50	3	<1
16	2.0	$PdCl_2$ + dppp	THF	TBAF	50	3	25
17	2.0	$PdCl_2$ + dpppent	THF	TBAF	50	3	22
18	2.0	$PdCl_2$ + DIOP	THF	TBAF	50	3	<1
19	2.0	$PdCl_2$ + Xantphos	THF	TBAF	50	3	<1
20	2.0	$PdCl_2$ + 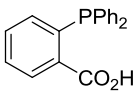	THF	TBAF	50	3	13
21	2.0	$PdCl_2$ + DtBPF	THF	TBAF	50	3	32
22	2.0	PEPPSI-IPr	toluene	K_2CO_3	75	3	82
23	2.2	PEPPSI-IPr	toluene	K_2CO_3	75	3	90

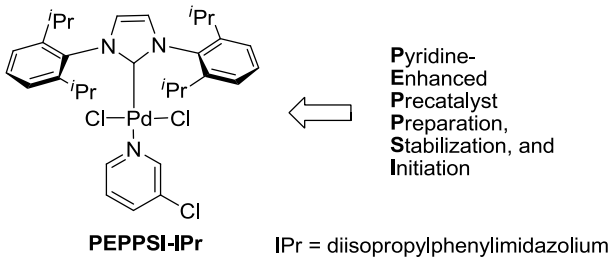

Figure 2-2. Structure of PEPPSI-IPr.

Next, C−H bond activation reaction was surveyed under oxidation[7] and irradiation[8] conditions (Scheme 2-2). Oxidation, Scholl reaction[7b] to the substrate **3a′** was subjected. $MoCl_5$, $FeCl_3$, and DDQ were investigated as the oxidants. Besides, the Author also applied photocyclization to this reaction. The reaction vessel was irradiated with 400 W high pressure mercury vapor lamp for several hours. The reactions were carried out using different solvents, such as toluene, hexane, and chloroform. Unfortunately, however, in spite of attempts of these reactions many times, no desired product was obtained. These results indicate that the substrate **3a′** is disfavored under these irradiation conditions. Therefore, the Author shifted to the *path b* as an alternative synthetic route.

Scheme 2-2. Examinations of C−H bond activation under oxidation and irradiation.

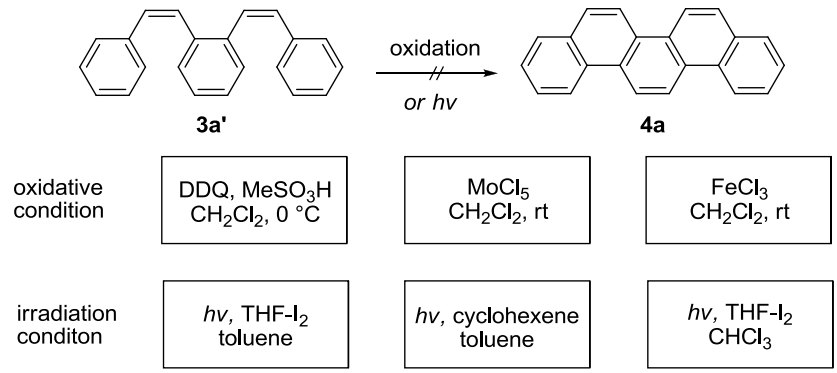

Based on the above investigation, it is necessary to introduce halogen atoms into substrate **3a′**. Meanwhile, in order to ensure the regioselectivity of Suzuki-Miyaura coupling reaction, 1,4-dibromo-2,3-diiodobenzene[9] (**1-Br**) was synthesized successfully as the cross-coupling partner, which can react with **2a** to give corresponding product **3a-Br**.

Under the reaction condition of entry 23 in Table 2-1, isomerization of the product **3a-Br** was observed because of high temperature. Therefore, further optimization of reaction conditions was investigated (Table 2-2). Under mild reaction conditions[10] at room temperature (entries 1−5), the reactions using different amounts of alkenylboronate **2a** and the different phosphorus ligands were performed. However, the yields of the desired product **3a-Br** were not satisfactory. Instead, the mono-substituted product and the homo-coupled product of **2a** were detected. Under harsh conditions in entries 6 and 7, the reactions were conducted at 110 °C using toluene as the solvent. In the presence of PEPPSI-IPr catalyst bearing NHC as the ligand, the better result was obtained when KOH was used as the base (entry 7).

Table 2-2. Optimization of cross-coupling reaction of **1-Br** with **2a**.

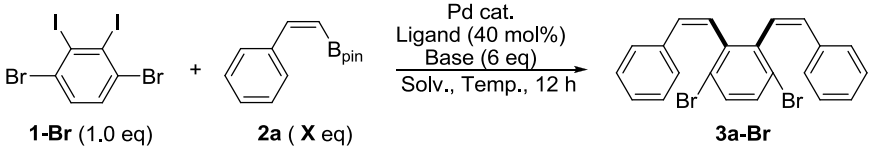

1-Br (1.0 eq) **2a** (**X** eq) **3a-Br**

Entry	X	Pd cat.[a]	Ligand	Base	Solv.	Temp. (°C)	Yield (%)[b]
1	2.0	$Pd(dba)_2$	$[HP^tBu_2Me]BF_4$	KOH	THF	rt	11
2	2.0	$Pd(dba)_2$	P^iPr_3	KOH	THF	rt	12
3	2.0	$Pd(dba)_2$	P^tBu_3	KOH	THF	rt	24
4	2.2	$Pd(dba)_2$	P^tBu_3	KOH	THF	rt	30
5	2.4	$Pd(dba)_2$	P^tBu_3	KOH	THF	rt	30
6	2.2	PEPPSI-IPr	-	K_2CO_3	toluene	110	43[c]
7	**2.2**	**PEPPSI-IPr**	**-**	**KOH**	**toluene**	**110**	**34**

[a] 20 mol% of $Pd(dba)_2$ and 10 mol% of PEPPSI-IPr were used respectively.
[b] Isolated yields. [c] Stereoisomer was contaminated (*ZZ:ZE:EE* = 2:1:1).

After the precursor was synthesized, the Author carried out Pd-catalyzed intramolecular double cyclization. Although there have been no examples of the application of Pd-catalyzed C−H arylation to the picene synthesis, to the best of his knowledge, it would be a powerful method for the construction of the desired framework.[11] The reaction conditions were examined and the results are shown in Table 2-3. Various catalysts, ligands, bases, solvents were screened under different temperatures and reaction times. Among these

catalyst systems, the *in situ* generated $PdCl_2(PCy_3)_2$ from $PdCl_2(NCPh)_2$ and PCy_3 and pivalic acid as the additive was found to be the best.[12]

Table 2-3. Examination of Pd-catalyzed intramolecular double cyclization.

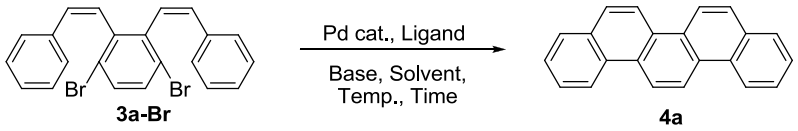

3a-Br **4a**

Entry	Pd cat.	Ligand	Base	Solvent	Temp. (°C)	Time (h)	Result
1	$Pd(OAc)_2$	LiCl, $^nBu_4NBr$	K_2CO_3	DMF	110	15	SM remain
2	$PdCl_2(NCPh)_2$	$P(3,5\text{-}(CF_3)_2C_6H_3)_3$	Cs_2CO_3	toluene	110	15	SM remain[a]
3	$PdCl_2$	PCy_3	DBU/Cs_2CO_3	DMF	150	24	No SM[b]
4	$PdCl_2(NCPh)_2$	PCy_3	DBU/Cs_2CO_3	DMA	150	15	debromination occured
5[c]	$PdCl_2(NCPh)_2$	PCy_3	Cs_2CO_3	DMA	150	24	picene formed[d]

[a] At 130 °C, GC-MS showed the SM was consumed, but ^{1}H NMR showed no signal of picene.

[b] Identification of the ^{1}H NMR is difficult due to the low concentration.

[c] PivOH was used as the additive.

[d] GC-MS showed the peak of m/z = 278, around 60 min (retention time), and the signals of picene can be detected by ^{1}H NMR. The pure picene can be obtained after purification by HPLC.

The data of the product **4a** is consistent with the desired structure. ^{1}H NMR spectrum of **4a** is identical to that of a commercially available sample (Figure 2-3). The aromatic proton signals at δ 8.80, 8.87, and 8.97 are characteristic signals of the picene backbone.

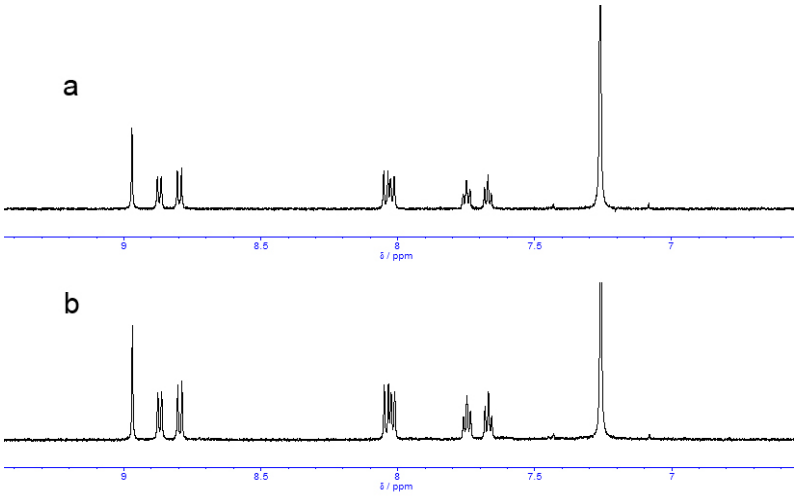

Figure 2-3. ^{1}H NMR spectra (600 MHz, $CDCl_3$, rt) of picene (**4a**):
(a) material purchased from TCI, (b) sample prepared by the present method.

2-2-2 Synthesis of picene derivatives

Encouraged by a successful synthesis of picene **4a**, the substrate scope was explored through this methodology. The Author expected that physicochemical properties of the parent picene can be modified by introducing functional groups into the picene framework.

Firstly, 1,4-dichloro-2,3-diiodobenzene (**1-Cl**) was also synthesized as an alternative coupling partner. A series of the stereodefined (*Z*)-alkenylboronates **2b**-**2f** were successfully prepared by Rh-catalyzed stereoselective hydroboration of terminal alkynes[13] or the zirconocene-mediated synthesis from an alkynylboronate[14] (Scheme 2-3).

Scheme 2-3. Synthesis of alkenylboronates **2a**−**2f**.

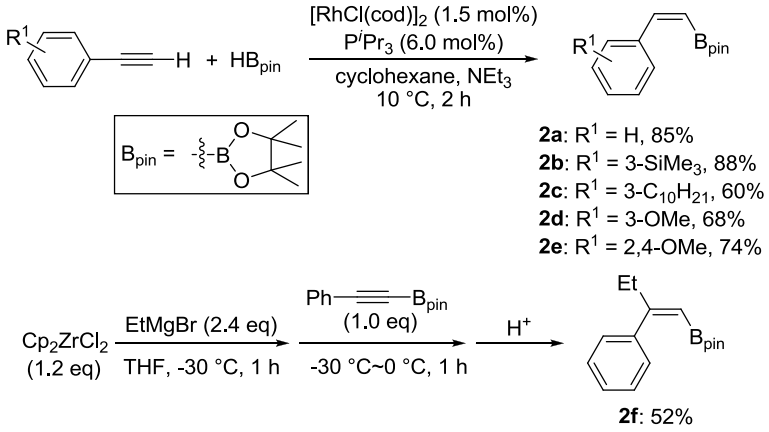

Next, based on the previous result (Table 2-2, entry7), cross-coupling reaction conditions were further optimized using **1-Cl** and trimethylsilane-substituted alkenylboronate **2b** as the starting materials (Table 2-4). The Author examined an amount of the base, catalyst, water and an equivalent of the substrates. As a result, the yields of the corresponding product were slightly lower when the amount of the Pd catalyst and the base were decreased (entries 2 and 3). An appropriate amount of water is important in this reaction system because the solubility of KOH is increased (entries 4 and 5). Besides, a little excess amount of **2b** is necessary to increase the yield of the product (entry 6). Overall, the use of PEPPSI-IPr/KOH systems with a mixture of toluene and H_2O as the co-solvents has been proved to be the most efficient conditions for the formation of the cross-coupled product.

Table 2-4. Optimization of cross-coupling reaction conditions of **1-Cl** with **2b**.

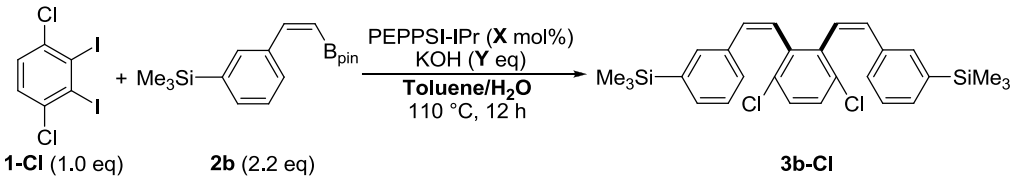

1-Cl (1.0 eq) **2b** (2.2 eq) **3b-Cl**

Entry	PEPPSI-IPr (**X** mol%)	KOH (**Y** eq)	Toluene/H_2O (mL/mL)	Yield (%)[a]
1	10	6	10/1	63
2	10	3	10/1	44
3	5	6	10/1	43
4	10	6	without H_2O	nd[b]
5	**10**	**6**	**10/2**	**68**
6[c]	10	6	10/2	51

[a] Isolated yields. [b] nd: not detected. [c] 2.0 eq of **2b** was used.

With the optimized conditions in hand, Suzuki-Miyaura coupling reactions of **1** with **2a**−**2f** catalyzed by PEPPSI-IPr gave the corresponding **3a**−**3f** as the precursors in moderate to high yields (Scheme 2-4). As a result, the Author noticed that in the cases of chlorides, the desired products were obtained in better yields compared with bromides. These results are ascribed to the reactivity of the halogen atoms in cross-coupling reactions. A competitive reaction occurs among chlorides, bromides and iodides. Because the reactivity of chlorides is much lower than the corresponding bromides, alkenylboronates readily reacted with iodides to give a less amount of by-products. So other picene precursors were directly synthesized using 1,4-dichloro-2,3-diiodobenzene.

For the synthesis of picene, the reaction conditions were further examined using the different substrates based on previous investigations (Table 2-5). The Author checked the amounts of catalysts, ligands, and bases. In comparison of the result in entry 2 with that in entry 3, when the amounts of the catalyst and the ligand were decreased to a half, the yields were comparable. In a sharp contrast, when the amount of the base was decreased (entry 4) and the reaction temperature was lowered (entry 5), the results became worse. Therefore, the condition shown in entry 3 was chosen as the optimized reaction conditions.

Scheme 2-4. Synthesis of picene precursors by cross-coupling reactions.

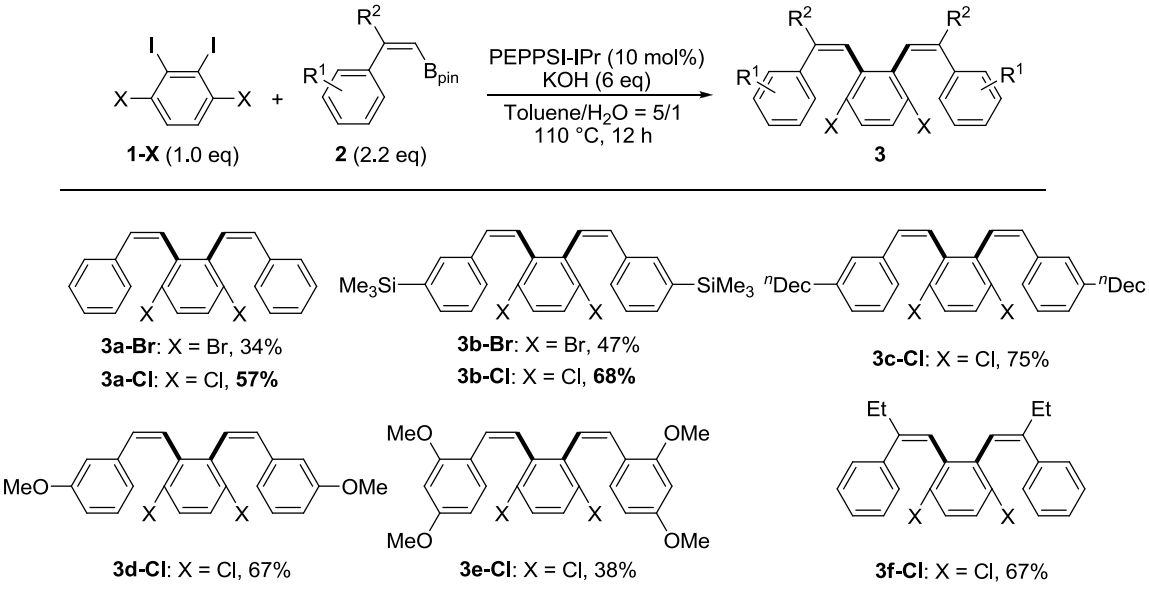

A series of picene derivatives **4b**−**4f** were synthesized in reasonable and moderate yields under optimized reaction conditions (Scheme 2-5).[15] Several different functionalities, such as TMS, Et, OMe, and decyl groups, could be introduced into the different positions of the picene framework. The Author considered the reason why the yield of cyclization is relative low, because the main by-product in the cyclization step is the protodehalogenated compound. This result indicates that after one C−C bond was formed, protodebromination (or protodechlorination) occurred.[16]

Table 2-5. Optimization of Pd-catalyzed intramolecular double cyclization.

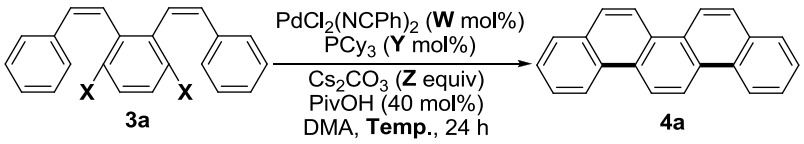

Entry	X	W	Y	Z	Temp. (°C)	Yield (%)[a]
1	Br	20	40	2	150	20
2	Cl	20	40	2	150	24
3	**Cl**	**10**	**20**	**2**	**150**	**23**
4	Cl	10	20	1	150	10
5	Cl	10	20	2	120	15

[a] Isolated yields.

Scheme 2-5. Synthesis of picenes **4a**−**4f**.

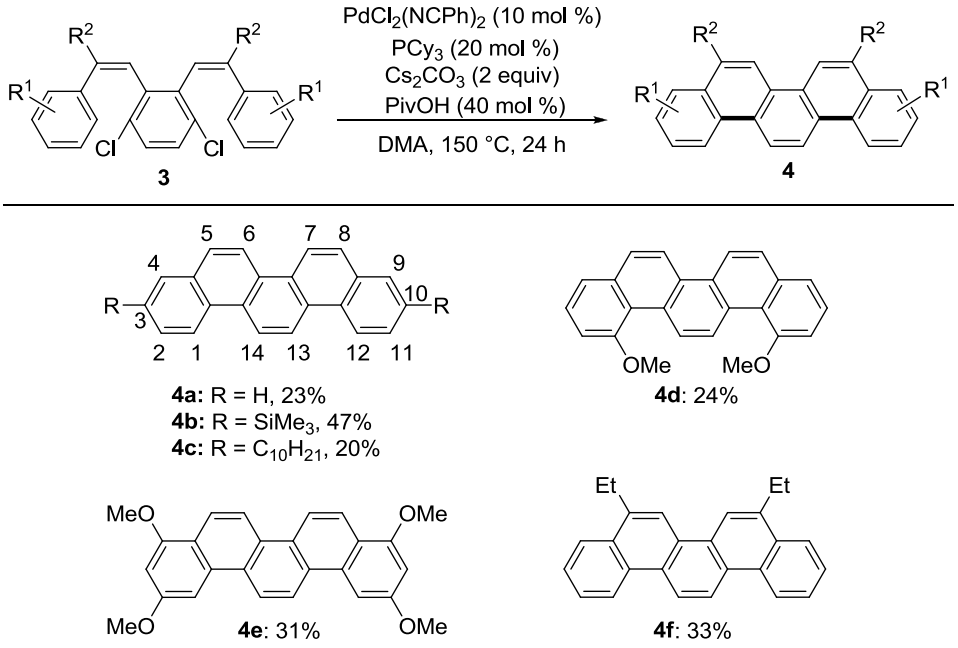

It is noteworthy that the structure of compound **4d** is different from an initial expectation that two methoxy groups would locate in the 3,10-positions by the C−H bond functionalization to avoid a steric congestion. However, as shown in Figure 2-4, X-ray structural analysis successfully clarified the structure of **4d**, in which two OMe groups are situated at the 1,12-positions. Moreover, the ^{1}H NMR measurement of **4d** showed a characteristic signal at 9.92 ppm, which is quite different from those in **4b** and **4c** bearing the substituents in the 3,10-positions.

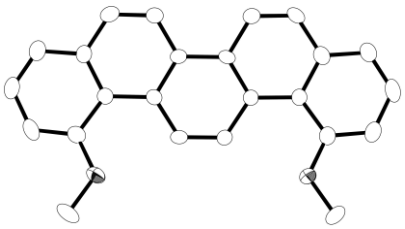

Figure 2-4. An ORTEP drawing of **4d** determined by X-ray crystallography with 30% thermal ellipsoidal plotting. Hydrogen atoms are omitted for simplicity.

The related crystallographic data of **4d** were listed as follows:

Empirical Formula	C24H18O2
Formula Weight	338.41
Crystal Color, Habit	colorless, prism
Crystal Dimensions	0.50 X 0.15 X 0.10 mm
Crystal System	Orthorhombic
Lattice Type	Primitive
No. of Reflections Used for Unit Cell Determination (2q range)	12327 (6.3 - 55.5^o)
Lattice Parameters	a = 17.528(2) Å b = 13.8570(16) Å c = 6.9178(8) Å V = 1680.2(3) Å^3
Space Group	Pna21 (#33)
Z value	4
D_{calc}	1.338 g/cm^3
F_{000}	712.00
m(MoKa)	0.837 cm^{-1}
Diffractometer	AFC7
Radiation	MoKa (l = 0.71075 Å) graphite monochromated
Take-off Angle	2.8^o
Detector Aperture	2.0 - 2.5 mm horizontal 2.0 mm vertical
Crystal to Detector Distance	21 mm
Temperature	24.9 ^{o}C
Scan Type	w-2q
$2q_{max}$	55.0^o
Corrections	Lorentz-polarization Absorption (trans. factors: 0.959 - 0.992)
Structure Solution	Direct Methods (SIR92)
Refinement	Full-matrix least-squares on F
Function Minimized	S w (|Fo| - |Fc|)^2
Least Squares Weights	1
2qmax cutoff	55.0^o
Anomalous Dispersion	All non-hydrogen atoms
No. Observations (I>2.00s(I))	3849
No. Variables	307
Reflection/Parameter Ratio	12.54
Residuals: R (I>2.00s(I))	0.0705
Residuals: Rw (I>2.00s(I))	0.1170
Goodness of Fit Indicator	1.064
Max Shift/Error in Final Cycle	0.001
Maximum peak in Final Diff. Map	0.16 e$^-$/Å^3
Minimum peak in Final Diff. Map	0.00 e$^-$/Å^3

2-3 Physicochemical Properties of Picenes

2-3-1 Measurements of UV-vis absorption spectra

The optical properties of **4a–4f** were studied by UV-vis spectroscopy. The observed optical properties are listed in Table 2-6. As shown in Figure 2-5(A), the wavelengths of maximum absorptions (λ_{max}^{abs}) of **4a–4f** are ca. 290 nm. The substituted picenes **4b–4f** exhibited absorption peaks at longer wavelengths, but their molar extinction coefficient ε values are smaller, compared to that of **4a**. These results indicate that an introduction of the substituents into a picene framework can affect the physical properties, since no concentration influence was observed when UV-vis spectra of **4a**–**4f** in different concentrations were measured[17] (Figure 2-6). The absorption spectra of the either edged- (as **4b** and **4c**) or side- (as **4d** and **4f**) substituents are similar in shape, possessing the main transition around 290 nm and at higher wavelengths the other transitions appeared as a shoulder.

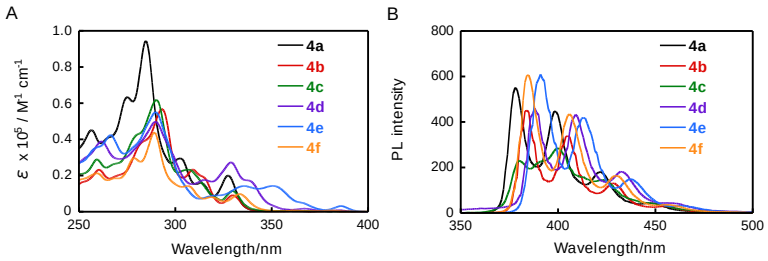

Figure 2-5. (A) Absorption spectra (1×10^{-5} M) and (B) Fluorescence emission spectra with excitation wavelength at λ_{max}^{abs} (5×10^{-7} M) of **4a**–**4f** in CH_2Cl_2.

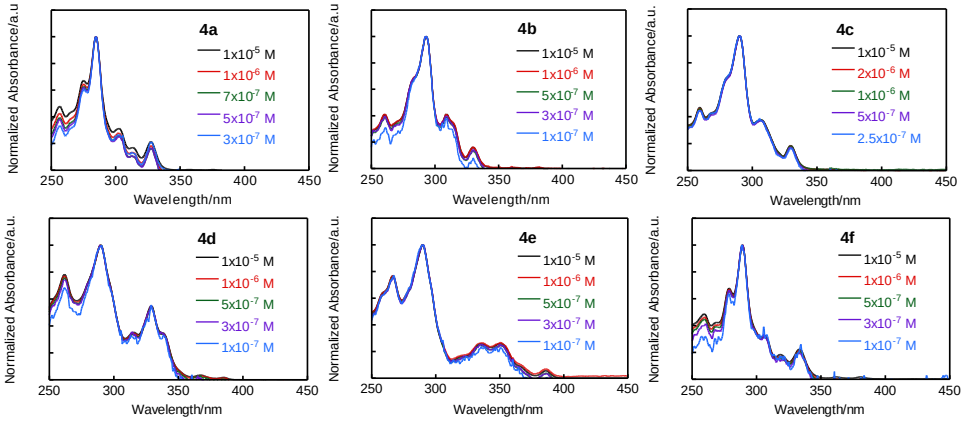

Figure 2-6. UV-vis spectra of **4a**–**4f** in different concentrations (10^{-5}-10^{-7} M).

2-3-2 Measurements of fluorescence spectra

Since all the compounds **4a**−**4f** are fluorescent, the measurements of steady-state fluorescence spectra were performed by using the diluted CH_2Cl_2 solution (5×10^{-7} M), as shown in Figure 2-5(B). The results are also summarized in Table 2-6. Using the λ_{max}^{abs} values of picenes as the 0-0 transition wavelength, the emission maxima (λ_{max}^{em}) displayed Stokes shifts by approximately 4 nm.[18] The relative fluorescence quantum yields (Φ_f) of **4a**−**4f** were estimated with Williams relative method.[19]

The substituents in the picene framework can significantly affect the Φ_f values. The Φ_f values of **4e** and **4f** were 0.18 and 0.13, respectively. An introduction of a methoxy or alkyl group decreased the Φ_f values of **4c** and **4d**. It is uncertain at present why the Φ_f value was changed by an introduction of these substituents.

Table 2-6. UV-vis[a] and fluorescence[b] data of picenes **4a**−**4f**.

Picenes	λ_{max}^{abs} /nm	ε /$M^{-1}\cdot cm^{-1}$	λ_{max}^{em} /nm[c]	Stokes shift /cm^{-1}	Φ_f[d]
4a	285	94300	378	212	0.07
4b	293	56800	384	274	0.10
4c	290	61800	380	209	0.05
4d	290	49700	388	201	0.06
4e	290	55100	391	331	0.18
4f	290	43700	385	273	0.13

[a] 1×10^{-5} M in CH_2Cl_2. [b] 5×10^{-7} M in CH_2Cl_2. [c] Wavelength of maximum fluorescence emission. [d] *p*-Terphenyl was used as a standard sample.

2-3-3 Measurements of cyclic voltammograms

The absorption band-edges (λ_{onset}) of picenes **4a**−**4f** and the corresponding optical band gaps (E_g^{opt}) calculated from $1240/\lambda_{onset}$ are summarized in Table 2-7. The electrochemical properties of **4a**−**4f** were also investigated by cyclic voltammetry (CV). The CV curves were recorded versus the potential of the Ag/Ag^+, which was calibrated by the ferrocene–ferrocenium (Fc/Fc^+) redox couple (−4.8 eV below the vacuum level).[20] The electrochemical data are also summarized in Table 2-7. The highest occupied molecular orbital (HOMO) energy levels were calculated from the CV data and the corresponding

LUMO levels were estimated from formula $E_{LUMO} = E_{HOMO} + E_g^{opt}$. The observed oxidation waves and no reduction waves in the CV measurements suggest that all compounds are p-type semiconductors, which have potent applications in organic electronics. Moreover, all picene derivatives exhibited quasi-reversible oxidation wave (Figure 2-7), reflecting that they possess an excellent electrochemical stability.

Table 2-7. Physicochemical properties of picenes **4a**–**4f**.

Picenes	E_{onset} (V)[a]	E_{HOMO} (eV)[b]	E_{LUMO} (eV)[c]	$E_g^{opt}/\lambda_{onset}$ [(eV)[d]/nm]	E_{HOMO} (eV)[e]	E_{LUMO} (eV)[e]	E_g (eV)[e]
4a	+0.88	–5.80	–2.57	3.23/384	–5.48	–1.27	4.21
4b	+0.86	–5.78	–2.60	3.18/390	–5.45	–1.25	4.20
4c	+0.85	–5.77	–2.56	3.21/386	–5.39	–1.18	4.18
4d	+0.59	–5.51	–2.38	3.13/396	–5.12	–1.02	4.10
4e	+0.37	–5.29	–2.21	3.08/402	–4.80	–0.84	3.96
4f	+0.74	–5.67	–2.52	3.15/393	–5.33	–1.19	4.14

[a] Obtained from cyclic voltammograms in CH_2Cl_2. Reference electrode: Ag/Ag^+. [b] All the potentials were calibrated with the Fc/Fc^+ ($E^{1/2}$ = -0.12 V measured under identical conditions). Estimated with a following equation: E_{HOMO} (eV) = –4.92 – E_{onset}. [c] Calculated according to the formula $E_{LUMO} = E_{HOMO} + E_g^{opt}$. [d] Optical band gap, $E_g^{opt} = 1240/\lambda_{onset}$. [e] Obtained from theoretical calculations.

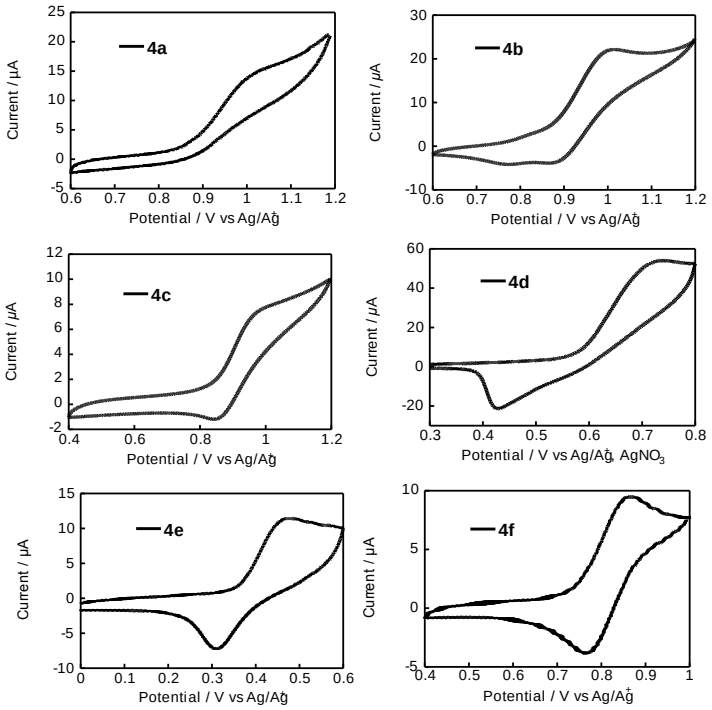

Figure 2-7. Cyclic voltammetry diagrams of compounds **4a**–**4f**.

Picene derivative **4b** and **4c** bearing the substituents in the 3,10-positions have the similar HOMO energy levels and slightly narrow optical band gaps than that of the parent picene **4a**. These results indicate that a substitution effect of a picene core in the 3,10-positions is rather small. In a sharp contrast, other substituted picenes, **4d**, **4e**, and **4f**, have higher HOMO energy levels and smaller optical band gaps than that of **4a**. Furthermore, their HOMO levels significantly elevate with increasing the number of the substituents. In these cases, methoxy groups were introduced into the picene framework in the 1,12-, 2,11-, and 4,9-positions act as strong electron-donating groups. New five picenes **4b**–**4f** could show better electron transfer capability in electronic devices since they showed relatively smaller the band gaps of than picene (3.23 eV).[21]

Table 2-8. B3LYP/6-31G (d) estimates of the reorganization energies of hole λ^h in **4a**–**4f**.

Compound	λ^h/meV
4a	185
4b	240
4c	188
4d	168
4e	277
4f	203

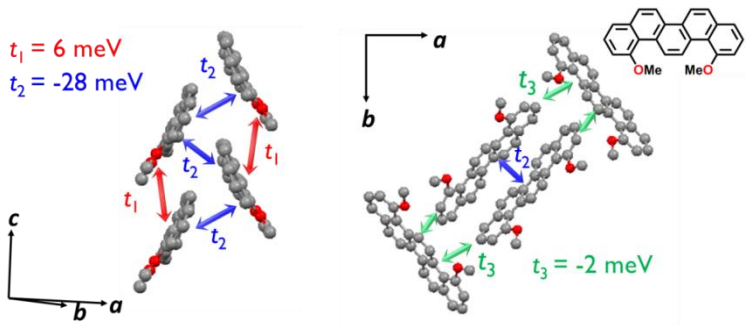

Figure 2-8. Transfer integrals of HOMO in **4d**.

Thus, the Author calculated molecular reorganization energy (λ), which may potentially affect the transport properties.[22] In the present p-channel organic semiconductor's cases, λ for hole (λ^h) should be in concern. From the results of λ^h (Table 2-8), **4d** should be advantageous for an efficient carrier transport. However, the calculated transfer integrals[23]

(t_{HOMO}s) of **4d** were found to be fairly small (Figure 2-8), because packing structure of **4d** is less effective for carrier transport, which was quite different from **4a** with high field-effect mobility.[24]

2-3-4 Density functional theory (DFT) calculation

Electronic structures of novel picenes **4a**−**4f** are theoretically investigated through calculation. The molecular geometries of **4a**−**4f** were optimized using density functional theory (DFT) at the B3LYP/6-31G(d) level using Gaussian 09, Revision A. 02.[25] The results are also listed in Table 2-7. The frontier molecular orbitals of the optimized molecules were also calculated, as shown in Figure 2-9. The theoretically calculated HOMO−LUMO gaps are higher than those obtained in the UV-vis spectroscopic measurements (E_g^{opt}) by ca. 1.0 eV. All the HOMOs and LUMOs of picenes **4a**−**4f** are evenly delocalized over the entire molecular π-frameworks. In addition, coefficients of picenes **4d**−**4f** reside on the 1,12-, 2,11-, and 4,9-methoxy and 5,8-alkyl groups in the HOMO. On the other hand, the carbon atoms in the 3,10-position in **4b** and **4c** have nodal planes in the HOMO. These results clearly support the similarity/difference of the energy levels of the frontier orbitals as well as the molecular electronic structures among **4a**−**4f**.

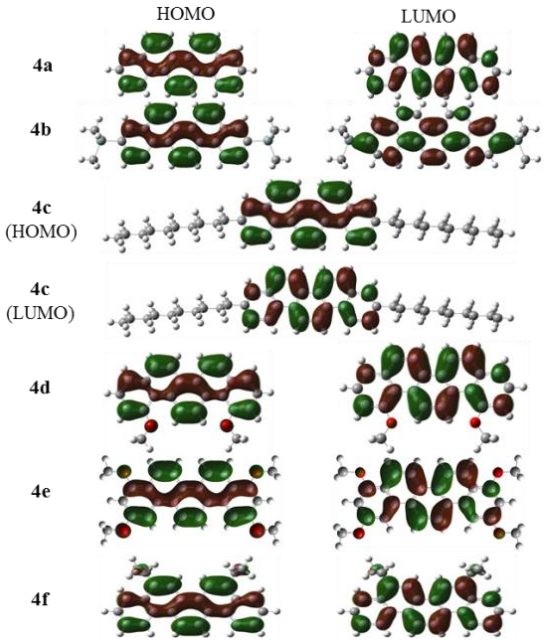

Figure 2-9. Wave functions for the HOMO and LUMO of **4a**−**4f**.

2-4 Summary

In summary, a novel and versatile synthetic method for the synthesis of various picene derivatives was developed through sequential Suzuki-Miyaura cross-coupling reaction and intramolecular C−H bond activation. The physicochemical properties of picene derivatives were modified by introducing different functional groups to the picene framework. All compounds have been investigated by UV-vis and fluorescence spectral measurements, CV, and DFT calculations as well as X-ray analyses. Based on this study, the clear pictures about the effects of the structural variations of substituents on their electronic and electrochemical properties have emerged.

1. No concentration influence was observed when UV-vis spectra of picenes were measured in different concentrations solution.

2. An introduction of the methoxy or alkyl group to the picene framework decreased the Φ_f values compared with that of the parent picene.

3. The observed oxidation waves and no reduction waves in the CV measurement suggest that all picene derivatives are p-type semiconductors, which have potent applications in organic electronics. Moreover, all compounds exhibited quasi-reversible oxidation wave, reflecting that they possess an excellent electrochemical stability.

4. After comparison of HOMO energy levels and optical band gaps between picene derivatives and the parent, it is found that the substitution effect of a picene core in the edge-positions is rather small. In a sharp contrast, other substituents in side-position of picenes, have lower HOMO energy levels and smaller optical band gaps than that of the parent. Furthermore, their HOMO levels significantly elevate with increasing the number of the substituents. In these cases, methoxy groups were introduced into the picene framework act as strong electron-donating groups. New five picenes would show better electron transfer capability in electronic devices since they showed relatively smaller the band gaps of than picene.

2-5 Experimental Section

2-5-1 General

All the reactions were carried out under an Ar atmosphere using standard Schlenk techniques. Glassware was dried in an oven (150 °C) and heated under reduced pressure before use. Dehydrated toluene, dichloromethane, hexane, and diethyl ether were purchased from Kanto Chemicals Co., Ltd. For thin layer chromatography (TLC) analyses throughout this work, Merck precoated TLC plates (silica gel 60 GF254, 0.25 mm) were used. Silica gel column chromatography was carried out using Silica gel 60 N (spherical, neutral, 40-100 μm) from Kanto Chemicals Co., Ltd. NMR spectra (^{1}H, ^{13}C{^{1}H}) were recorded on Varian INOVA-600 (600 MHz) or Mercury-300 (300 MHz) spectrometers. Infrared spectra were recorded on a Shimadzu IRPrestige-21 spectrophotometer. GC analyses were performed on a Shimadzu GC-14A equipped with a flame ionization detector using Shimadzu Capillary Column (CBP1-M25-025) and Shimadzu C-R6A-Chromatopac integrator. Melting Points were measured on a Yanagimoto micromelting point apparatus and are uncorrected. The GC yields were determined using suitable hydrocarbon internal standards. GC/MS analyses were carried out on a SHIMADZU GC-17A equipped with a SHIMADZU QP-5050 GC-MS system. Elemental analyses were carried out with a Perkin-Elmer 2400 CHN elemental analyzer.

2-5-2 Experimental procedures

Synthesis of catalysts

[Rh(cod)Cl]$_2$[26]

$$RhCl_3\cdot 3H_2O + cod \xrightarrow[EtOH/H_2O = 5/1,\ 90\ ^\circ C,\ 4\ h]{Na_2CO_3} [Rh(cod)Cl]_2$$

To a solution of $RhC1_3\cdot 3H_2O$ (4.53 g, 17.0 mmol), Na_2CO_3 (1.85g, 17.5 mmol), ethanol (20 mL), H_2O (5 mL), COD (η^4-1,5-cyclooctadiene, 7.5 mL, 61.1 mmol) was added. After refluxing at 90 °C for 4 h, the reaction cooled gradually to ambient temperature. The precipitate was filtered and washed with hexane (25 mL), MeOH/H_2O (5/1, 20 mL), and

Et_2O (10 mL). The residue was recrystallized (CH_2Cl_2/hexane) to give pure product (3.68 g, 88% yield) as an orange crystal.

$Pd(dba)_2$[27]

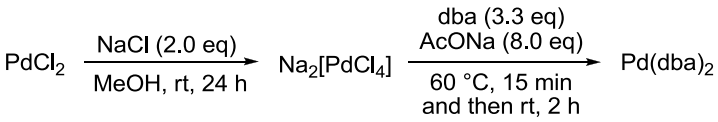

NaCl (0.59 g, 10 mmol) was added to a solution of $PdCl_2$ (0.89 g, 5 mmol) in methanol (30 mL) and stirred at ambient temperature under an inert atmosphere for 24 h. It was subsequently filtered through a plug of cotton wool and concentrated *in vacuo* to approximately half its original volume. The solution was warmed to 60 °C and then dibenzylidene acetone (3.87 g, 16.5 mmol) was added. The resulting mixture was stirred at 60 °C for 15 min, then sodium acetate was added, and the reaction cooled gradually to ambient temperature. The mixture was stirred at ambient temperature for 2 h until a dark red precipitate was observed. The precipitate was filtered and washed with methanol (2 × 15 mL), water (2 × 15 mL), and finally acetone (2 × 5 mL). The product was partially dried under suction and then the solid was added to a Schlenk flask which was placed under a flow of nitrogen with stirring overnight. This gave the desired complex as a maroon/purple microcrystalline solid (2.56 g, 89% yield).

$PdCl_2(NCPh)_2$[28]

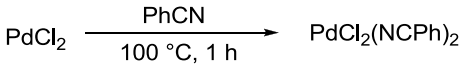

$PdCl_2$ (2.0 g, 11 mmol) was dissolved in 35 ml benzonitrile, then stirred for 1 h at 100 °C. The solution was cooled in an ice-bath to precipitate the product, which was filtered, washed with small amount of cold ether and dried under vacuum. $PdCl_2(NCPh)_2$ was achieved as a brown powder (2.7 g, 63% yield).

$PdCl_2(PPh_3)_2$[29]

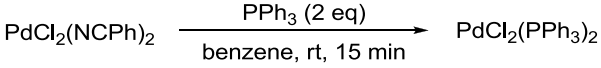

To a solution of $PdCl_2(NCPh)_2$ (0.96 g, 2.5 mmol) in 25 ml benzene, PPh_3 (1.31 g, 5.0 mmol) was added and then stirred for 15 min at ambient temperature. The reaction mixture was filtered and washed with cold ether. After dry under vacuum, the product was obtained as a yellow powder (1.73 g, 98% yield).

PEPPSI-IPr[6]

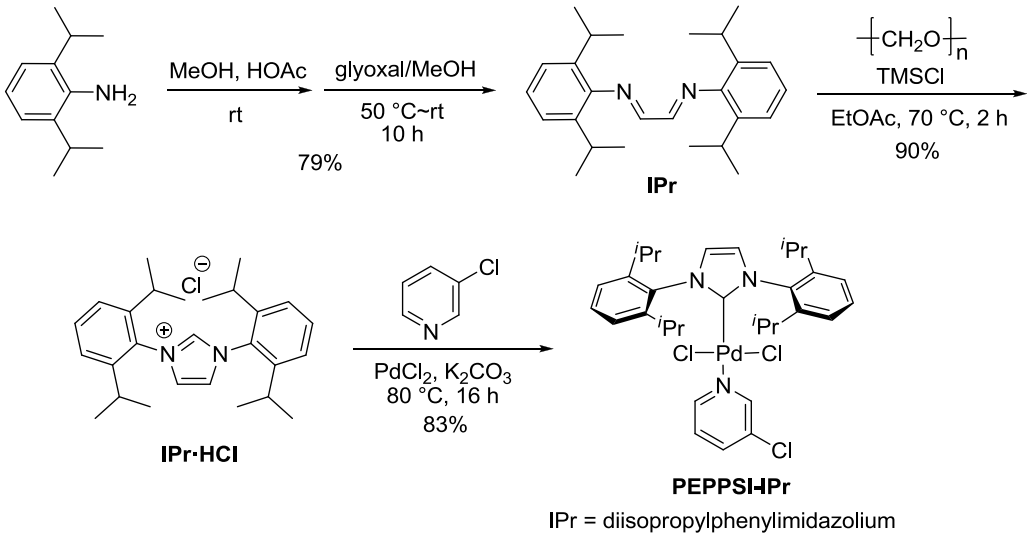

Synthesis of **IPr**:[30] A solution of glyoxal (2.23 mL, 40% in water, 20 mmol) in MeOH (20 mL) was added with vigorous stirring to a warmed (50 °C) solution of 2,6-diisopropylaniline (7.6 mL, 40 mmol) and HOAc (0.2 mL) in MeOH (10 mL). A slightly exothermic reaction commenced and the product started to crystallize after 15 min. The mixture was stirred for 10 h at ambient temperature, after which the resulting suspension was filtered and the solid product washed with MeOH, until the washing phase remained bright yellow. The product was pre-dried by suction over the filter, and then dried to constant weight in high vacuum. The filtrates were collected, evaporated and set aside for a second crystallization. Finally, 5.9 g (79% yield) of bright yellow crystals was obtained.

Synthesis of **IPr·HCl**:[30] 200 mL two necks round bottom flask containing EtOAc (150 mL) was heated to 70 °C in an oil bath. Diazadiene **IPr** (5.89 g, 15.6 mmol) and paraformaldehyde (0.48 g, 16 mmol) were added and the walls washed with EtOAc (2 mL). A solution of TMSCl (2.0 mL, 15.6 mmol) in EtOAc (2.5 mL) was added dropwise over 10

min with vigorous stirring, and the resulting yellow suspension stirred for 2 h at 70 °C. After cooling to 10 °C (ice-bath) with stirring, the suspension was filtered and the solid washed with EtOAc. The solid was dried to constant weight under vacuum, giving 6.02 g (90% yield) of product as colorless microcrystalline powder.

Synthesis of **PEPPSI-IPr**: In argon atmosphere, a 50 mL Schlenk tube was charged with $PdCl_2$ (1.61 g, 9.1 mmol), **IPr·HCl** (4.25 g, 10 mmol), K_2CO_3 (6.28 g, 45.5 mmol) and 3-Chloropyridine (25 g, 220 mmol). The Schlenk tube was heated with vigorous stirring for 16 h at 80 °C. After cooling to ambient temperature, the reaction mixture was diluted with CH_2Cl_2 and passed through a short pad of silica gel covered with a pad of Celite eluting with CH_2Cl_2 until the product was completely recovered. Most of the CH_2Cl_2 was removed by rotary evaporator, and the 3-chloropyridine was then vacuum-distilled (1.6 Torr/50 °C) and saved for reuse. After triturating with hexane, decanting of the supernatant and drying in high vacuum, the pure complex (5.13 g, 83% yield) was isolated as an off-white solid.

^{1}H NMR ($CDCl_3$, 300 MHz, rt): δ 1.12 (d, J = 6.9 Hz, 12H), 1.48 (d, J = 6.9 Hz, 12H), 3.11-3.20 (m, 4H), 7.04-7.09 (m, 1H), 7.14 (s, 2H), 7.35 (d, J = 7.8 Hz, 4H), 7.47-7.56 (m, 3H), 8.52 (d, J = 5.7 Hz, 1H), 8.59 (d, J = 2.4 Hz, 1H).

Synthesis of 1,4-dichloro-2,3-diiodobenzene (1-Cl).[31]

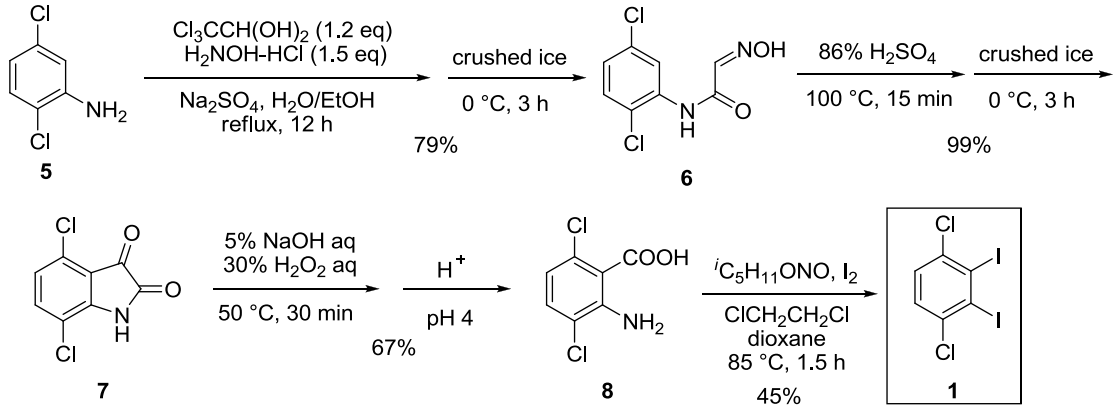

The first two steps followed a general procedure.[32] A commercially available 2,5-dichloroaniline (**5**) (4.86 g, 30 mmol), chloral hydrate (5.95 g, 36 mmol), hydroxylamine

hydrochloride (3.13 g, 45 mmol), and Na_2SO_4 (30.0 g) were suspended in a mixture of H_2O (100 mL) and EtOH (100 mL). The mixture was stirred and kept at reflux temperature (80 °C) for 12 h and then concentrated by evaporation and poured into crushed ice, which caused precipitation of white solid. After being kept at 0 °C for 3 h, the suspension was filtered, and the white solid was dried in air to yield a crude 2,5-dichloroisonitroso-acetanilide (**6**) in 79% yield (5.52 g). Compound **6** was then heated in 86% H_2SO_4 (80 mL) at 100 °C for 15 min. The resulting dark red suspension was poured into crushed ice to yield 3,6-dichloroisatine (**7**) (5.07 g, 99% yield) as bright orange crystals, which were subsequently subjected to basic hydrolysis in aq H_2O_2 to yield off-white crystals of 3,6-dichloroanthranilic acid (**8**) (3.24 g, 67% yield).[33] Finally, compound **8** was converted into 1,4-dichloro-2,3-diiodobenzene (**1-Cl**) by employing the aprotic diazotization procedure.[34] After column chromatography on silica gel (hexanes as eluent) and bulb to bulb distillation (160 ºC/1.4 Torr), the desired product **1** was obtained as white crystals (2.83 g, 45% yield). ^{1}H NMR ($CDCl_3$, 300 MHz, rt): δ 7.41 (s, 2H).

A general procedure for (*Z*)-alkenylboronates 2 by hydroboration:

Synthesis of 4,4,5,5-tetramethyl-2-[(1*Z*)-2-phenylethenyl]-1,3,2-dioxaborolane (2a).

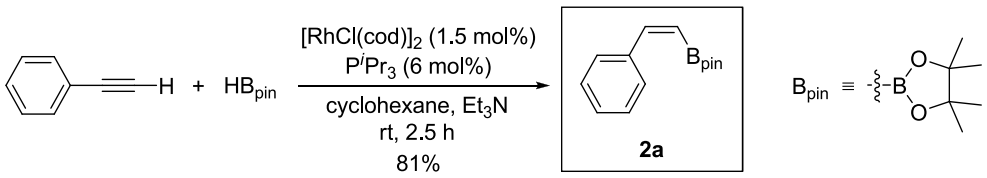

A 50 mL Schlenk tube, equipped with a magnetic stir bar, was charged with $[RhCl(cod)]_2$ (37 mg, 0.075 mmol, 1.5 mol %) and then flushed with argon. Anhydrous cyclohexane (15 mL), P^iPr_3 (0.057 mL, 0.3 mmol, 6 mol %), Et_3N (5 mL), and HB_{pin} (0.725 mL, 5 mmol) were successively added. After being stirred at room temperature for 30 min, phenylacetylene (1.1 mL, 10 mmol) was added in one-portion and the mixture was stirred at room temperature for 2 h before quenching by MeOH. Filtration and evaporation afforded brown oil, which was purified by bulb to bulb distillation (130 °C/1.3 Torr) to obtain product **2a** as colorless liquid (0.93 g, 81% yield).

^{1}H NMR ($CDCl_3$, 300 MHz, rt) δ 1.30 (s, 12H), 5.60 (d, J = 14.7 Hz, 1H), 7.23 (d, J = 14.7 Hz, 1H), 7.26-7.31 (m, 3H), 7.54 (d, J = 7.9 Hz, 2H).

Synthesis of 4,4,5,5-tetramethyl-2-[(1*Z*)-2-(3-trimethylsilane-phenylethenyl]-1,3,2-dioxaborolane (2b).

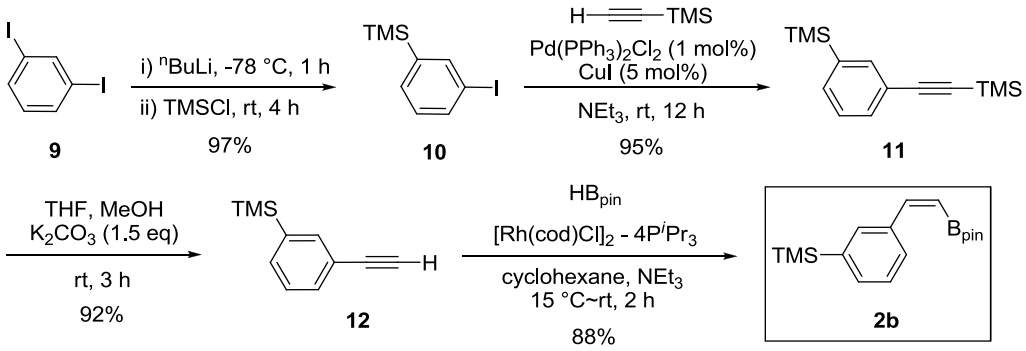

To a stirring solution of 1,3-diiodobenzene (**9**, 6.6 g, 20 mmol) in diethyl ether (50 mL) was cooled to −78 °C. Addition of n-BuLi (12.3 mL, 20 mmol, 1.63 M in hexane) over 10 min resulted in an off-white solution. After stirring for 1 h at this temperature and then quenched with chlorotrimtheylsilane (2.39 g, 22 mmol). The solution was allowed to warm to room temperature for 4 h. Water (10 mL) was added to the above solution. The organic layer was extracted with diethyl ether and washed with brine, dried ($MgSO_4$), and concentrated under vacuum. The crude material **10** (5.38 g, 97% yield) was obtained as brown oil directly for next step.

^{1}H NMR ($CDCl_3$, 300 MHz, rt): δ 0.28 (s, 9H), 7.11 (t, J = 7.7 Hz, 1H), 7.47 (dt, J = 7.2 Hz, 1H), 7.70 (dt, J = 7.8 Hz, 1H), 7.83 (s, 1H).

A 200 mL two necks round bottom flask equipped with a magnetic stir bar was charged with **10** (5.25 g, 19 mmol), $PdCl_2(PPh_3)_2$ (133 mg, 0.19 mmol, 1 mol %), CuI (181 mg, 0.95 mmol, 5 mol %), triethylamine (75 mL) and trimethylsilylacetylene (3.22 mL, 22.8 mmol) under argon atmosphere. The reaction mixture was stirred overnight at room temperature. After evaporation to remove Et_3N, the residue was filtrated with diethyl ether. The solvent was removed under reduced pressure and the desired compound **11** (4.45 g, 95% yield) was afford as a brown oil.

^{1}H NMR ($CDCl_3$, 300 MHz, rt): δ 0.28 (s, 18H), 7.30 (d, J = 7.9 Hz, 1H), 7.46 (d, J = 6.0 Hz, 2H), 7.63 (s, 1H).

To a solution of **11** (4.27 g, 17.3 mmol) in THF (50 mL) and MeOH (30 mL) was added K_2CO_3 (3.58 g, 26 mmol) and H_2O (1.2 mL). The solution was stirred at rt for 4.5 h before pouring the solution into saturated aq. NH_4Cl (50 mL). The mixture was extracted with diethyl ether. The organic layer was washed with 5% aq. NH_4Cl and brine, dried ($MgSO_4$) and the solvent was removed in vacuum. This crude product was purified via Florisil and afforded **12** (2.77 g, 92% yield) as a brown oil.

^{1}H NMR ($CDCl_3$, 300 MHz, rt): δ 0.28 (s, 9H), 3.09 (s, 1H), 7.30 (t, J = 7.8 Hz, 1H), 7.35-7.52 (m, 2H), 7.66 (s, 1H).

4,4,5,5-Tetramethyl-2-[(1*Z*)-2-(3-trimethylsilane-phenylethenyl]-1,3,2-dioxaborolane (**2b**) was obtained as a yellow liquid (2.11 g, 88% yield) via stereoselective hydroboration of **12**[35] with similar experimental procedure of **2a**.

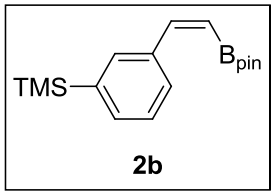

2b

FT-IR (neat, cm^{-1}): 2978 (m), 2359 (m), 1620 (m), 1337 (m), 1250 (s), 1144 (s), 870 (m), 837 (s), 752 (m).

^{1}H NMR ($CDCl_3$, 300 MHz, rt): δ 0.31 (s, 9H), 1.31 (s, 12H), 5.61 (d, J = 14.7 Hz, 1H), 7.23 (d, J = 14.7 Hz, 1H), 7.26-7.35 (m, 1H), 7.45 (d, J = 9.6 Hz, 1H), 7.56 (d, J = 10.5 Hz, 1H), 7.82 (s, 1H).

^{13}C{^{1}H} NMR ($CDCl_3$, 75 MHz, rt) δ −1.1, 24.8, 83.4, 127.3, 129.3, 133.1, 133.8, 137.5, 140.0, 149.0. The carbon signal adjacent to B was not observed due to low intensity.

MS (EI, m/z (relative intensity)): 302 (M^+, 41), 287 (100), 286 (25), 187 (35), 146 (15), 145 (98), 143 (16), 73 (39).

Anal. Calcd for $C_{17}H_{27}BO_2Si$: C, 67.54; H, 9.00%. Found: C, 67.15; H, 8.83%.

Synthesis of 4,4,5,5-tetramethyl-2-[(1*Z*)-2-(3-decyl-phenylethenyl]-1,3,2-dioxaborolane (2c).

Compound **2c** was synthesized by the same procedure as that for compound **2b**. Decyl bromide was used as an alkylation reagent.

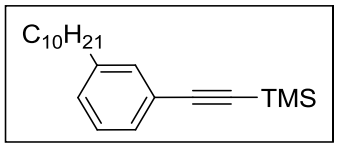

1-(Trimethylsilyl)-3-(2-decylethynyl)benzene. Colorless liquid, 90% yield.

FT-IR (neat, cm^{-1}): 2956 (s), 2926 (s), 2854 (s), 2152 (m), 1601 (w), 1481 (m), 1466 (m), 1250 (s), 854 (s), 843 (s), 793 (w), 760 (m), 694 (m), 648 (w).

^1H NMR ($CDCl_3$, 300 MHz, rt): δ 0.25 (s, 9H), 0.89 (t, J = 6.8 Hz, 3H), 1.26-1.30 (m, 16H), 2.56 (t, J = 7.8 Hz, 2H), 7.12 (d, J = 7.6 Hz, 1H), 7.20 (t, J = 7.5 Hz, 1H), 7.29 (d, J = 9.5 Hz, 2H).

$^{13}C\{^1H\}$ NMR ($CDCl_3$, 75 MHz, rt) δ −0.0, 14.1, 22.7, 29.2, 29.3, 29.5, 29.6, 29.6, 31.3, 31.9, 35.7, 93.5, 105.5, 122.8, 128.1, 128.8, 129.2, 131.9, 142.9.

MS (EI, m/z (relative intensity)): 314 (M^+, 26), 300 (29), 299 (100), 173 (56), 172 (23), 73 (80).

Anal. Calcd for $C_{21}H_{34}Si$: C, 80.18; H, 10.89%. Found: C, 80.43; H, 11.07%.

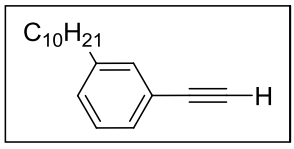

1-Ethynyl-3-decylbenzene. Colorless liquid, 65% yield.

FT-IR (neat, cm^{-1}): 3312 (m), 2955 (s), 2855 (s), 1560 (w), 1481 (m), 1466 (m), 793 (m), 694 (m), 606 (m).

^1H NMR ($CDCl_3$, 300 MHz, rt): δ 0.89 (t, J = 7.2 Hz, 3H), 1.27-1.31 (m, 16H), 2.58 (t, J = 7.8 Hz, 2H), 3.05 (s, 1H), 7.17 (d, J = 7.5 Hz, 1H), 7.23 (t, J = 7.3 Hz, 1H), 7.32 (d, J = 7.2 Hz, 2H).

$^{13}C\{^{1}H\}$ NMR ($CDCl_3$, 75 MHz, rt) δ 14.5, 23.0, 29.6, 29.7, 29.7, 29.8, 29.9, 30.0, 31.6, 32.2, 36.0, 84.3, 122.2, 128.5, 129.4, 129.7, 132.4, 143.4.

MS (EI, m/z (relative intensity)): 242 (M^+, 4), 157 (17), 131 (19), 130 (21), 129 (27), 128 (25), 118 (21), 117 (30), 116 (67), 115 (100).

HRMS (EI) Calcd for $C_{18}H_{26}$: 242.2035. Found: 242.2055.

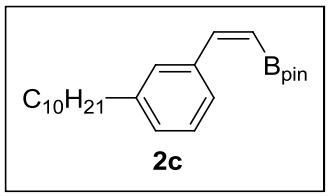

2c

4,4,5,5-tetramethyl-2-[(1*Z*)-2-(3-decyl-phenylethenyl]-1,3,2-dioxaborolane (2c). Colorless liquid, 60% yield.

FT-IR (neat, cm^{-1}): 2955 (s), 2855 (s), 1620 (s), 1427 (m), 1371 (m), 1258 (s), 1144 (s), 968 (m), 873 (w), 808 (m), 698 (m).

^{1}H NMR ($CDCl_3$, 300 MHz, rt): δ 0.86-0.90 (m, 3H), 1.22-1.34 (m, 24H), 1.61 (q, J = 7.6 Hz, 6.8 Hz, 2H), 2.58 (t, J = 7.8 Hz, 2H), 5.56 (d, J = 14.8 Hz, 1H), 7.08 (d, J = 7.6 Hz, 1H), 7.17-7.23 (m, 2H), 7.32 (d, J = 8.0 Hz, 1H), 7.45 (s, 1H).

$^{13}C\{^{1}H\}$ NMR ($CDCl_3$, 75 MHz, rt) δ 14.1, 22.7, 24.8, 29.3, 29.5, 29.5, 29.6, 29.6, 31.5, 31.9, 36.0, 83.4, 126.2, 127.8, 128.2, 128.5, 138.3, 142.5, 148.5. The carbon signal adjacent to B was not observed due to low intensity.

MS (EI, m/z (relative intensity)): 370 (M^+, 28), 313 (28), 285 (28), 242 (22), 157 (25), 144 (39), 143 (100), 129 (26), 117 (23), 85 (42), 84 (93).

Anal. Calcd for $C_{24}H_{39}BO_2$: C, 77.83; H, 10.61%. Found: C,77.51; H, 10.41%.

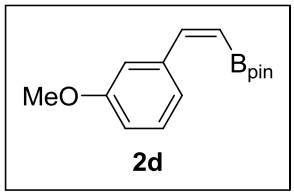

2d

4,4,5,5-Tetramethyl-2-[(1*Z*)-2-(3-methoxylphenylethenyl]-1,3,2-dioxaborolane (2d) was obtained in 68% yield as a yellow liquid via stereoselective hydroboration of the corresponding alkyne.[36]

FT-IR (neat, cm^{-1}): 2978 (m), 2359 (m), 1618 (m), 1582 (m), 1371 (m), 1258 (s), 1144 (s), 872 (m), 799 (m).

^1H NMR ($CDCl_3$, 300 MHz, rt): δ 1.30 (s, 12H), 3.83 (s, 3H), 5.60 (d, J = 15.3 Hz, 1H), 6.84 (d, J = 9.0 Hz, 1H), 7.06 (d, J = 7.5 Hz, 1H), 7.16-7.25 (m, 2H), 7.34 (t, J = 3.9 Hz, 1H).

$^{13}C\{^1H\}$ NMR ($CDCl_3$, 75 MHz, rt) δ 24.7, 55.1, 83.4, 113.1, 114.4, 121.7, 128.8, 139.7, 148.2, 159.3. The carbon signal adjacent to B was not observed due to low intensity.

MS (EI, m/z (relative intensity)): 260 (M^+, 60), 161 (24), 160 (38), 159 (65), 144 (100), 130 (20), 129 (26), 117 (22), 77(22).

Anal. Calcd for $C_{15}H_{21}BO_3$: C, 69.26; H, 8.14%. Found: C, 69.29; H, 8.27%.

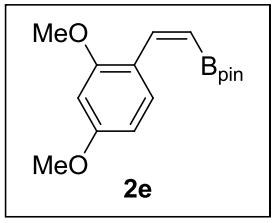

2e

4,4,5,5-Tetramethyl-2-[(1*Z*)-2-(2,4-dimethoxyl-phenylethenyl]-1,3,2-dioxaborolane (2e) was obtained in 74% yield as a yellow liquid via stereoselective hydroboration of the corresponding alkyne.[37]

FT-IR (neat, cm^{-1}): 2974 (m), 1607 (s), 1429 (s), 1333 (m), 1283 (s), 1248 (s), 1161 (m), 1105 (w), 831 (m).

^1H NMR ($CDCl_3$, 300 MHz, rt): δ 1.27 (s, 12H), 3.80 (s, 3H), 3.82 (s, 3H), 5.48 (d, J = 14.7 Hz, 1H), 6.40-6.44 (m, 2H), 7.43 (d, J = 12.0 Hz, 1H), 7.56 (d, J = 8.1 Hz, 1H).

$^{13}C\{^1H\}$ NMR ($CDCl_3$, 75 MHz, rt) δ 24.7, 55.2, 55.3, 83.0, 97.7, 103.8, 120.6, 130.4, 143.4, 158.2, 161.0. The carbon signal adjacent to B was not observed due to low intensity.

MS (EI, m/z (relative intensity)): 290 (M^+, 59), 289 (15), 217 (100), 216 (27), 189 (10), 176 (15), 149 (37), 121 (11).

Anal. Calcd for $C_{16}H_{23}BO_4$: C, 66.23; H, 7.99%. Found: C, 66.31; H, 8.08%.

Synthesis of (*Z*)-4,4,5,5-tetramethyl-2-(2-phenyl-1-buten-1-yl)-1,3,2-dioxaborolane (2f)

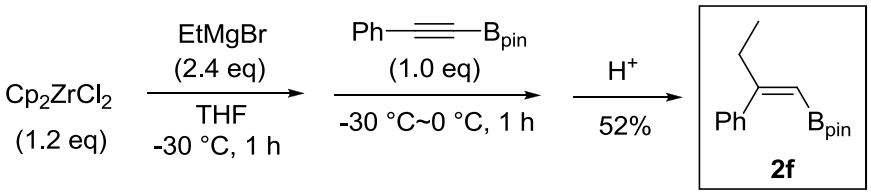

To a solution of zirconocene dichloride (1.75 g, 6 mmol) in THF (25 mL) was added dropwise EtMgBr (12.2 mL, 12 mmol, 0.98 M THF solution) at −78 °C. The reaction mixture was stirred for 1 h at −30 °C and then 4,4,5,5-tetramethyl-2-(phenylethynyl)-1,3,2-dioxaborolane was added. The reaction mixture was stirred for 1 h at 0 °C, quenched with 1 M HCl, and extracted with ethyl acetate. The combined organic layers were washed with brine, and dried over $MgSO_4$. Filtration and concentration under vacuum, followed by purification with bulb to bulb distillation (140 ºC/1.4 Torr) gave product **2f** as colorless liquid. (0.68 g, 52% yield). ^{1}H NMR ($CDCl_3$, 300 MHz, rt): δ 1.05 (t, J = 7.5 Hz, 3H), 1.13 (s, 12H), 2.49 (q, J = 7.5 Hz, 2H), 5.46 (s, 1H), 7.24-7.28 (m, 5H).

A general procedure for Suzuki-Miyaura coupling of 1,4-dichloro-2,3-diiodobenzene with (*Z*)-alkenylboronates: formation of 3.

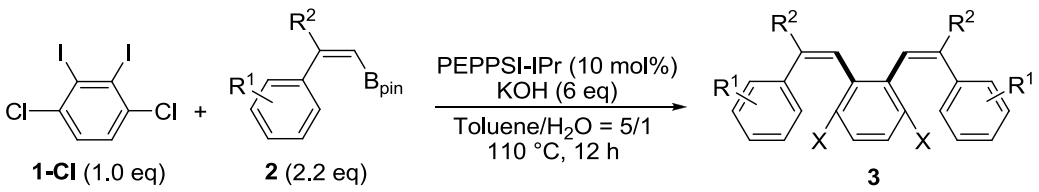

A 20 mL Schlenk tube, equipped with a magnetic stirrer bar, 1,4-dichloro-2,3-diiodobenzene (**1-Cl**, 199 mg, 0.5 mmol), (*Z*)-alkenylboranate **2** (1.1 mmol, 2.2 eq), PEPPSI-IPr (34 mg, 0.05 mmol, 10 mol %), and KOH solid (168 mg, 3 mmol) were

successively added. Then, 1 mL of toluene and 0.2 mL of H_2O were added in one-portion and the reaction mixture was stirred at 110 °C. After react for 12 h, the reaction mixture was quenched with 1 M HCl, and extracted with diethyl ether (3 × 10 mL). The combined ethereal layer was washed with brine and dried over anhydrous magnesium sulfate. Filtration and evaporation afforded brown oil, which was purified by column chromatography (hexanes as eluent) to obtain product **3.**

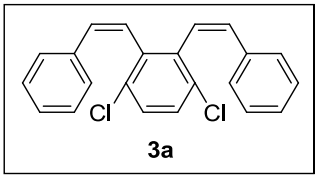

3a

3a, yellow solid, 57% yield.

FT-IR (neat, cm^{-1}): 3049 (w), 1493 (m), 1435 (s), 1121 (s), 870 (m), 810 (s), 773 (s), 745 (m), 691 (s).

^1H NMR ($CDCl_3$, 300 MHz, rt) δ 6.06 (d, J = 12 Hz, 2H), 6.54 (d, J = 12 Hz, 2H), 6.93-7.01(m, 2H), 7.14-7.18 (m, 6H), 7.27-7.33 (m, 4H).

$^{13}C\{^1H\}$ NMR ($CDCl_3$, 75 MHz, rt) δ 126.5, 128.6, 129.1, 129.2, 129.3, 129.6, 130.2, 133.2, 133.5, 137.9, 138.3.

MS (EI, m/z (relative intensity)): 351 (M^+, 5), 350 (17), 272 (15), 261 (32), 259 (49), 202 (28), 167 (56), 91 (100).

Anal. Calcd for $C_{22}H_{16}Cl_2$: C, 75.22; H, 4.59%. Found: C, 74.93; H, 4.56%.

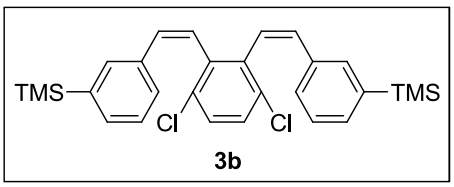

3b

3b, pale yellow oil, 68% yield.

FT-IR (neat, cm^{-1}): 2953 (s), 1435 (m), 1248 (s), 1132 (w), 1113 (m), 837 (s), 800 (m), 754 (m), 691 (w).

^{1}H NMR ($CDCl_3$, 300 MHz, rt) δ 0.14 (s, 18H), 6.03 (d, J = 12.0 Hz, 2H), 6.53 (d, J = 12.3 Hz, 2H), 7.02 (s, 2H), 7.11 (s, 2H), 7.21-7.25 (m, 2H), 7.32-7.35 (m, 4H).

^{13}C{^{1}H} NMR ($CDCl_3$, 75 MHz, rt) δ –1.4, 125.5, 127.7, 128.9, 129.1, 132.3, 132.3, 132.8, 135.9, 137.5, 140.2.

MS (EI, m/z (relative intensity)): 495 (M^+, 1.18), 311 (22), 278 (10), 163 (34), 93 (20), 73 (100).

Anal. Calcd for $C_{28}H_{32}Cl_2Si_2$: C, 67.85; H, 6.51%. Found: C, 68.15; H, 6.48%.

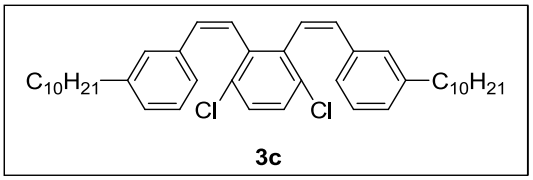

3c

3c, yellow oil, 75% yield.

FT-IR (neat, cm^{-1}): 2924 (s), 2853 (s), 2357 (w), 1600 (w), 1456 (m), 1435 (m), 1128 (m), 903 (w), 804 (s), 696 (s).

^{1}H NMR ($CDCl_3$, 300 MHz, rt) δ 0.87-0.91 (m, 6H), 1.26-1.31 (m, 32H), 2.43 (t, J = 7.7 Hz, 4H), 6.00 (d, J = 12.0 Hz, 2H), 6.49 (d, J = 12.0 Hz, 2H), 6.77 (d, J = 12.0 Hz, 4H), 6.96 (d, J = 7.5 Hz, 2H), 7.07 (t, J = 7.5 Hz, 2), 7.29 (s, 2H).

^{13}C{^{1}H} NMR ($CDCl_3$, 75 MHz, rt) δ 14.1, 22.7, 29.2, 29.4, 29.5, 29.6, 29.7, 31.2, 31.9, 35.7, 125.3, 125.4, 125.7, 128.0, 128.1, 128.1, 129.0, 132.2, 136.7, 137.5, 142.7.

Anal. Calcd for $C_{42}H_{56}Cl_2$: C, 79.84; H, 8.93%. Found: C, 79.52; H, 8.71%.

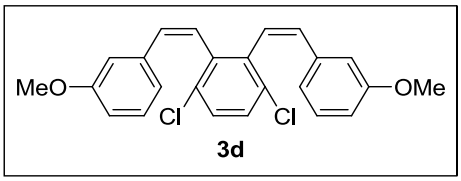

3d

3d, yellow oil, 67% yield.

FT-IR (neat, cm^{-1}): 2938 (w), 1597 (s), 1578 (s), 1489 (s), 1435 (s), 1260 (s), 1153 (m), 1042 (s), 860 (w), 795 (s), 689 (m).

^{1}H NMR ($CDCl_3$, 300 MHz, rt) δ 3.60 (s, 6H), 6.10 (d, J = 12 Hz, 2H), 6.49 (d, J = 3.9 Hz, 3H), 6.55 (t, J = 6.6 Hz, 3H), 6.68-6.75 (m, 2H), 7.05-7.10 (m, 2H), 7.31 (s, 2H).

^{13}C{^{1}H} NMR ($CDCl_3$, 75 MHz, rt) δ 54.9, 112.9, 113.6, 119.3, 124.0, 125.6, 128.7, 129.1, 129.2, 132.2, 133.2, 136.0, 137.4, 138.0.

MS (EI, m/z (relative intensity)): 411 (M^+, 5), 410 (19), 302 (16), 289 (27), 227 (79), 121 (100), 91 (14).

Anal. Calcd for $C_{24}H_{20}Cl_2O_2$: C, 70.08; H, 4.90%. Found: C, 69.93; H, 4.78%.

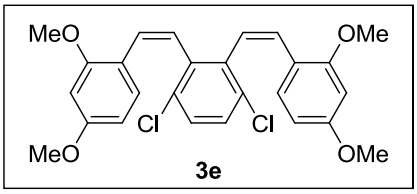

3e

3e, yellow oil, 38% yield.

FT-IR (neat, cm^{-1}): 2938 (w), 1608 (s), 1503 (s), 1464 (w), 1292 (s), 1290 (s), 1159, (s), 823 (w).

^{1}H NMR ($CDCl_3$, 300 MHz, rt) δ 3.76 (s, 6H), 3.80 (s, 6H), 6.17 (q, J = 8.7 Hz, 2H), 6.36 (s, 2H), 6.57 (q, J = 7.5 Hz, 2H), 6.78 (d, J = 12 Hz, 2H), 7.23 (s, 2H), 7.29 (s, 2H).

^{13}C{^{1}H} NMR ($CDCl_3$, 75 MHz, rt) δ 55.0, 55.4, 98.1, 104.1, 119.0, 123.5, 128.5, 128.9, 131.9, 137.9, 157.9, 160.3.

MS (EI, m/z (relative intensity)): 471 (M^+, 7), 470 (26), 332 (12), 151 (100), 121 (16).

HRMS (EI) Calcd for $C_{26}H_{24}Cl_2O_4$: 470.1052. Found: 470.1043.

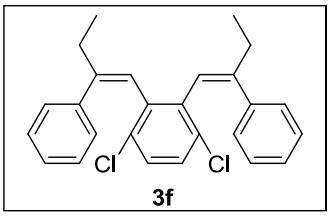

3f

3f, yellow oil, 67% yield.

FT-IR (neat, cm^{-1}): 2965 (s), 2929 (s), 2359 (s), 1427 (m), 1150 (m), 806 (w), 772 (m), 698 (s).

^{1}H NMR ($CDCl_3$, 600 MHz, rt) δ 1.04 (t, J = 7.2 Hz, 6H), 2.48-2.54 (m, 4H), 5.46 (s, 2H), 6.91-6.97 (m, 4H), 7.06 (s, 2H), 7.10-7.18 (m, 6H).

^{13}C{^{1}H} NMR ($CDCl_3$, 150 MHz, rt) δ 13.1, 31.1, 122.0, 126.9, 127.6, 127.7, 127.7, 127.8, 127.8, 132.5, 137.9, 140.5.

MS (EI, m/z (relative intensity)): 407 (M^+, 7), 406 (24), 377 (26), 289 (24), 252 (23), 119 (43), 117 (40), 105 (39), 91(100).

HRMS (EI) Calcd for $C_{26}H_{24}Cl_2$: 406.1255. Found: 406.1263.

A general procedure for synthesis of picene derivatives via the Pd-catalyzed intramolecular double cyclization.

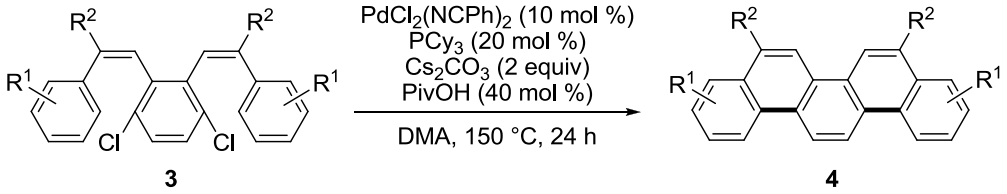

3 **4**

A 20 mL Schlenk tube equipped with a magnetic stirring bar was charged with PCy_3 (11.5 mg, 0.04 mmol, 20 mol %), $PdCl_2(NCPh)_2$ (7.6 mg, 0.02 mmol, 10 mol %), and DMA (1 mL) under argon atmosphere. After stirring for 10 min, Cs_2CO_3 (130 mg, 0.4 mmol, 2.0 equiv), PivOH (8.3 mg, 0.08 mmol, 40 mol %), and substrate (**3**, 0.2 mmol, 1.0 eq) were added into reaction mixture at room temperature. The tube was put into a preheated hot box at 150 °C for 24 h. The reaction mixture was cooled to room temperature, quenched with 1 M HCl (3 mL), and extracted with chloroform (3 × 10 mL). The combined organic extracts were washed adequately by water and dried over anhydrous magnesium sulfate, filtered with enough amount of $CHCl_3$, and concentrated in vacuo. Due to the poor solubility of picene, the crude residue was purified via simple extraction and washing instead of column chromatography.

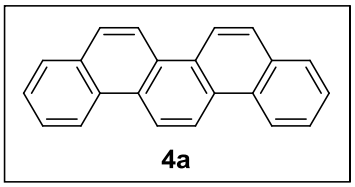

4a

4a, picene[5a], 23 % yield as off-white solid.

^{1}H NMR ($CDCl_3$, 300 MHz, rt) δ 7.68 (q, J = 9.0 Hz, 2H), 7.74 (q, J = 9.0 Hz, 2H), 8.00-8.06 (m, 4H), 8.80 (d, J = 9.3 Hz, 2H), 8.87 (d, J = 8.1 Hz, 2H), 8.97 (s, 2H).

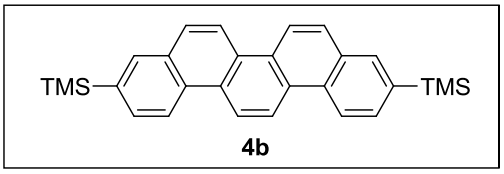

4b

4b, white solid. Isolated yield was 47%.

Mp. > 300 °C.

FT-IR (KBr, cm^{-1}): 2953 (w), 1248 (m), 1109 (m), 910 (m), 845 (s), 808 (s), 759 (m), 689 (w), 637 (w).

^{1}H NMR ($CDCl_3$, 300 MHz, rt) δ 0.42 (s, 18H), 7.87 (d, J = 8.1 Hz, 2H), 8.04 (d, J = 9.0 Hz, 2H), 8.16 (s, 2H), 8.81 (q, J = 9.0 Hz, 4H), 8.96 (s, 2H).

^{13}C{^{1}H} NMR ($CDCl_3$, 75 MHz, rt) δ 0.81, 121.82, 122.37, 127.81, 128.72, 128.89, 128.99, 130.95, 131.32, 131.44, 134.41, 138.96.

MS (EI, m/z (relative intensity)): 422 (M^+, 100), 409 (13), 408 (36), 407 (85), 196 (49), 73 (62).

Anal. Calcd for $C_{28}H_{30}Si_2$: C, 79.56; H, 7.15%. Found: C, 79.66; H, 7.06%.

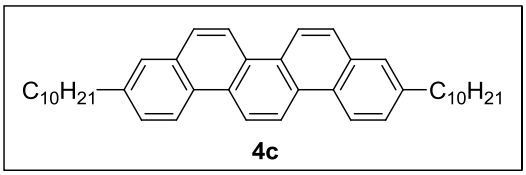

4c

4c, white solid. Isolated yield was 20%.

Mp. > 300 °C.

FT-IR (KBr, cm^{-1}): 1713 (w), 1466 (w), 1263 (w), 1096 (m), 785 (m), 507 (m).

^{1}H NMR ($CDCl_3$, 600 MHz, rt) δ 0.86-0.89 (m, 6H), 1.25-1.44 (m, 28H), 1.75-1.80 (m, 4H), 2.86 (t, 4H), 7,58 (q, J = 6 Hz, 2H), 7.78 (s, 2H), 7.97 (d, J = 9.0 Hz, 2H), 8.75 (q, J = 12 Hz, 4H), 8.90 (s, 2H).

$^{13}C\{^{1}H\}$ NMR ($CDCl_3$, 150 MHz, rt) δ 14.1, 22.7, 29.3, 29.4, 29.6, 29.6, 29.6, 31.5, 31.9, 35.9, 121.5, 121.6, 123.0, 127.2, 127.3, 128.0, 128.2, 128.5, 128.7, 132.0, 141.3.

HRMS (EI) Calcd for $C_{42}H_{54}$: 558.4226. Found: 558.4240.

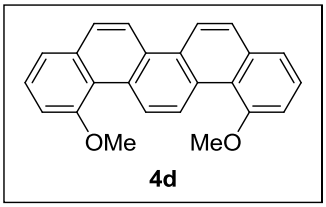

4d

4d, white solid. Isolated yield was 24%.

Mp. > 300 °C.

FT-IR (KBr, cm^{-1}): 2930 (w), 1522 (m), 1450 (s), 1427 (s), 1269 (s), 1238 (s), 1140 (s), 1059 (s), 841 (s), 820 (s), 748 (s), 704 (w).

^{1}H NMR ($CDCl_3$, 600 MHz, rt) δ 4.21 (s, 6H), 7.21 (q, J = 12 Hz, 2H), 7.58-7.64 (m, 4H), 7.96 (d, J = 9.6 Hz, 2H), 8.83 (d, J = 9.0 Hz, 2H), 9.92 (s, 2H).

$^{13}C\{^{1}H\}$ NMR ($CDCl_3$, 150 MHz, rt) δ 55.9, 108.2, 121.1, 121.4, 122.5, 126.5, 126.6, 127.1, 128.5, 128.8, 134.3, 158.9.

Anal. Calcd for $C_{24}H_{18}O_2$: C, 85.18; H, 5.36%. Found: C, 85.52; H, 5.16%.

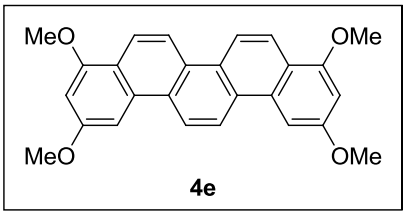

4e

4e, white solid. Isolated yield was 31%.

Mp. > 300 °C.

FT-IR (KBr, cm^{-1}): 2999 (w), 1618 (s), 1454 (m), 1416 (m), 1383 (m), 1261 (s), 1148 (s), 1047 (s), 808 (m), 644 (w).

^{1}H NMR ($CDCl_3$, 600 MHz, rt) δ 4.06 (s, 6H), 4.08 (s, 6H), 6.70 (d, J = 2.4 Hz, 2H), 7.73 (d, J = 1.8 Hz, 2H), 8.37 (d, J = 9.6 Hz, 2H), 8.64 (d, J = 9.0 Hz, 2H), 8.74 (s, 2H).

$^{13}C\{^{1}H\}$ NMR ($CDCl_3$, 150 MHz, rt) δ 55.7, 56.0, 95.5, 97.9, 118.9, 119.2, 121.1, 121.6, 127.9, 129.8, 132.6, 157.3, 159.3.

HRMS (EI) Calcd for $C_{26}H_{22}O_4$: 398.1518. Found: 398.1502.

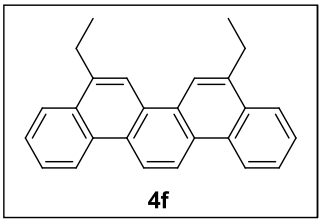

4f

4f, white solid. Isolated yield was 30%.

Mp. > 300 °C.

FT-IR (KBr, cm^{-1}): 2926 (m), 1452 (w), 1248 (w),1042 (w), 876 (m), 746 (s).

^{1}H NMR ($CDCl_3$, 300 MHz, rt) δ 1.57 (t, J = 8.1 Hz, 6H), 3.35 (q, J = 18 Hz, 4H), 7.66-7.76 (m, 4H), 8.23 (q, J = 6.0 Hz, 2H), 8.65 (s, 2H), 8.87 (s, 2H), 8.91 (q, J = 9.0 Hz, 2H).

$^{13}C\{^{1}H\}$ NMR ($CDCl_3$, 75 MHz, rt) δ 15.2, 27.1, 120.2, 120.8, 123.7, 124.3, 126.2, 126.4, 127.9, 128.1, 130.9, 131.0, 138.9.

HRMS (EI) Calcd for $C_{26}H_{22}$: 334.1722. Found: 334.1700.

2-5-3 Copies of ^{1}H and $^{13}C\{^{1}H\}$ NMR charts for the new compounds

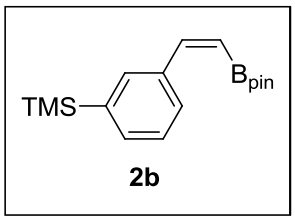

2b

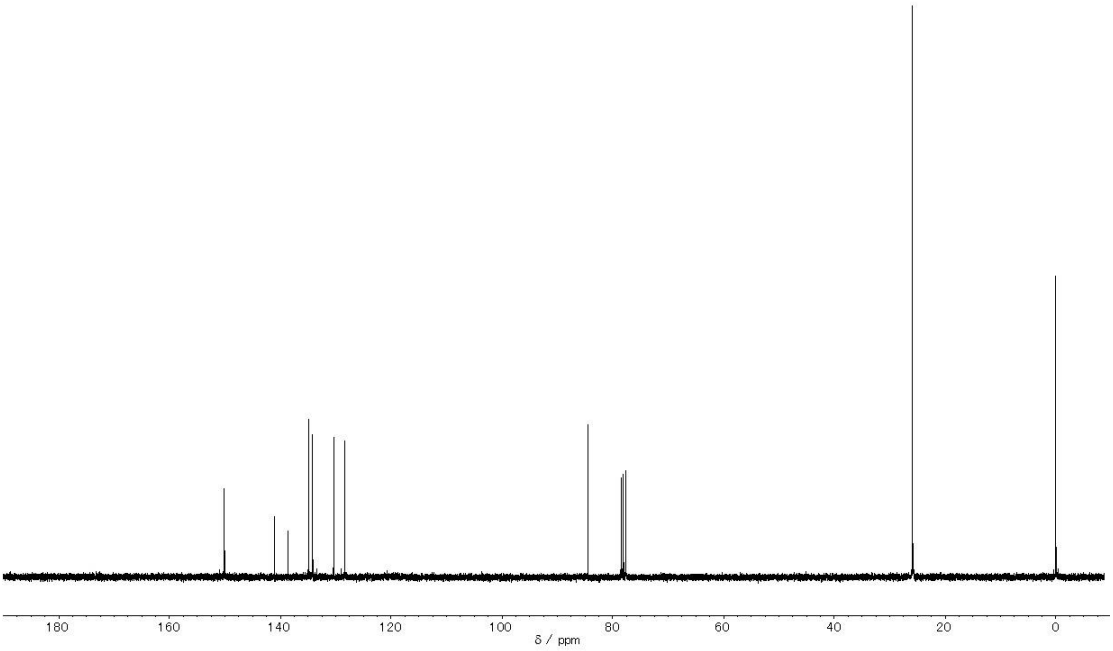

^{1}H (300 MHz) and $^{13}C\{^{1}H\}$ NMR (75 MHz) spectra of **2b** (rt, $CDCl_3$).

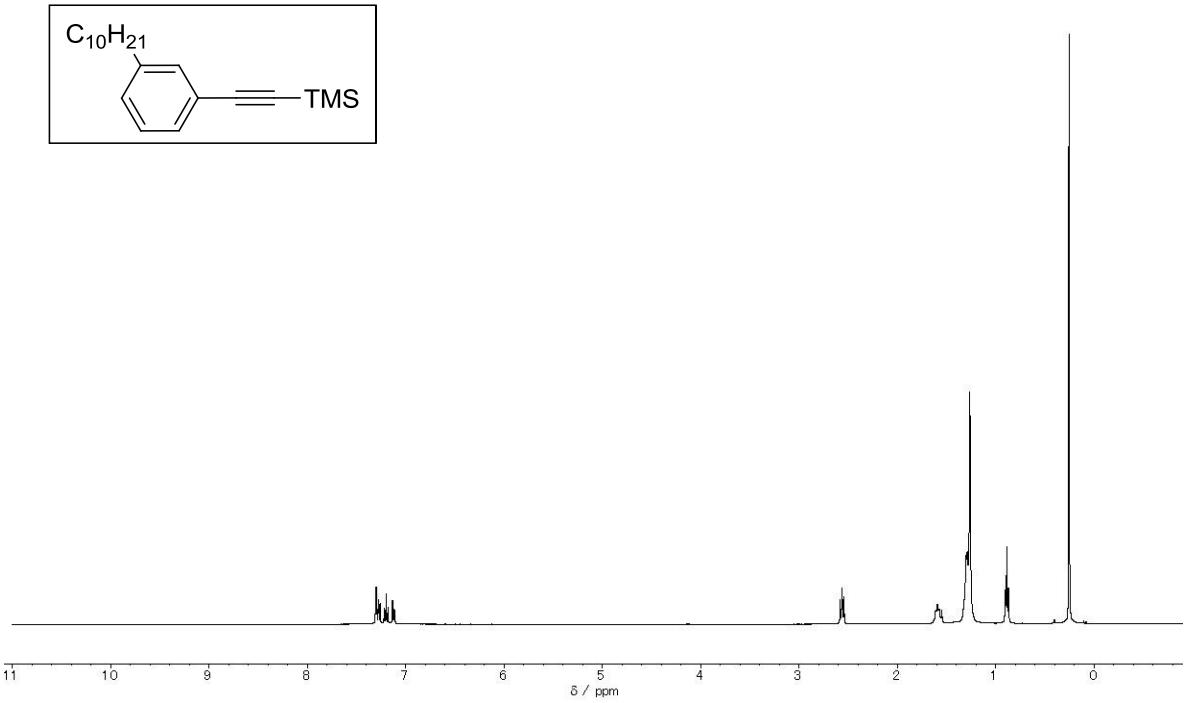

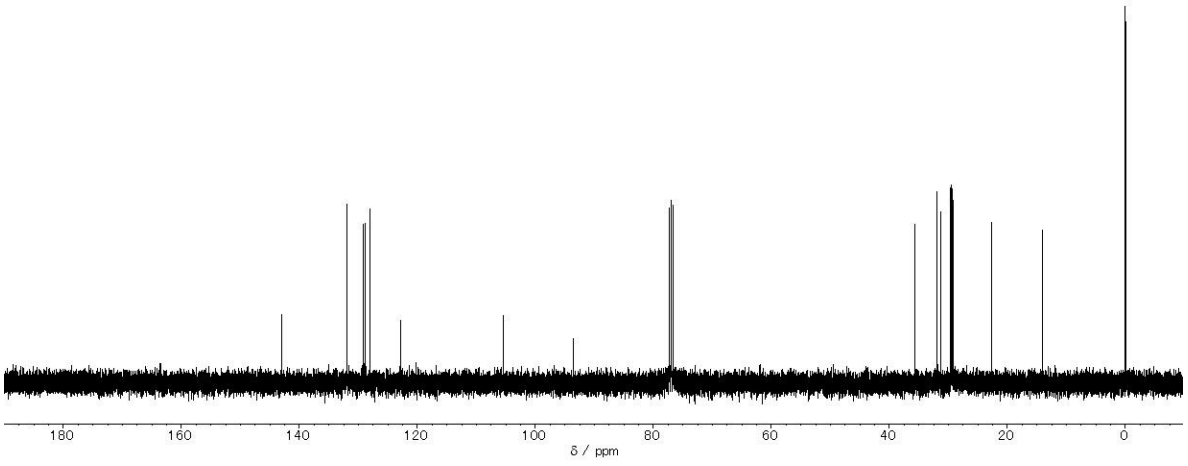

^{1}H (300 MHz) and $^{13}C\{^{1}H\}$ NMR (75 MHz) spectra of 1-(trimethylsilyl)-3-[2-(decyl)ethynyl]-benzene (rt, $CDCl_3$).

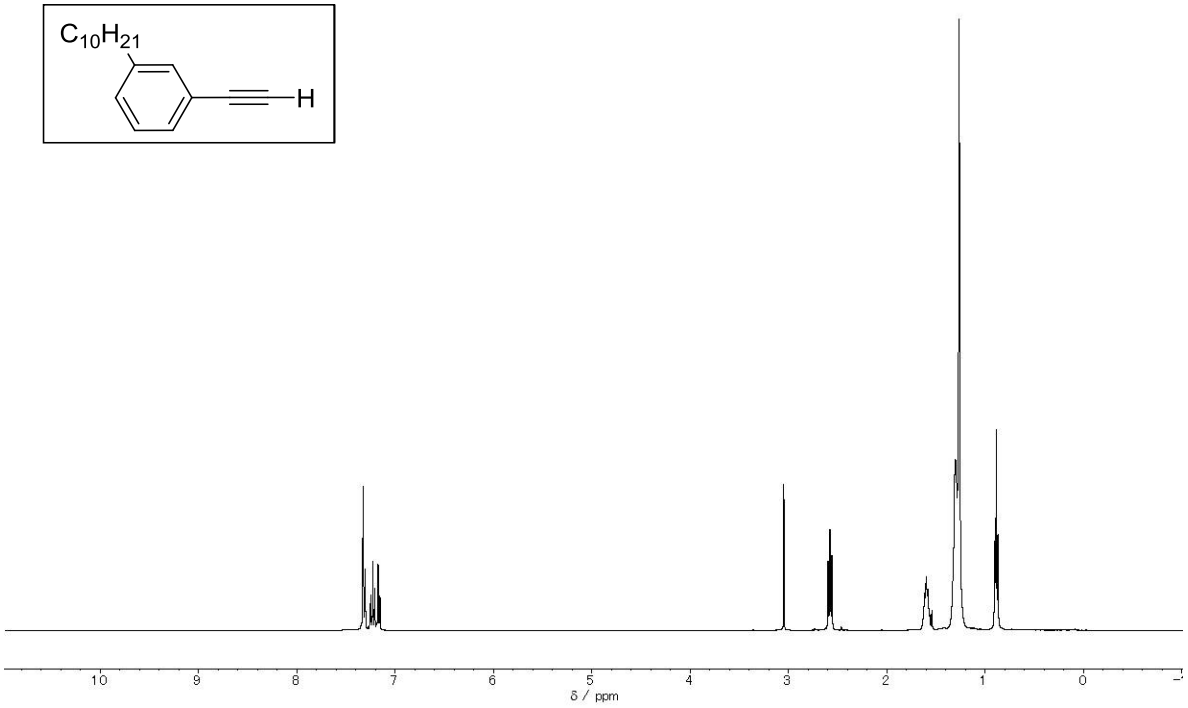

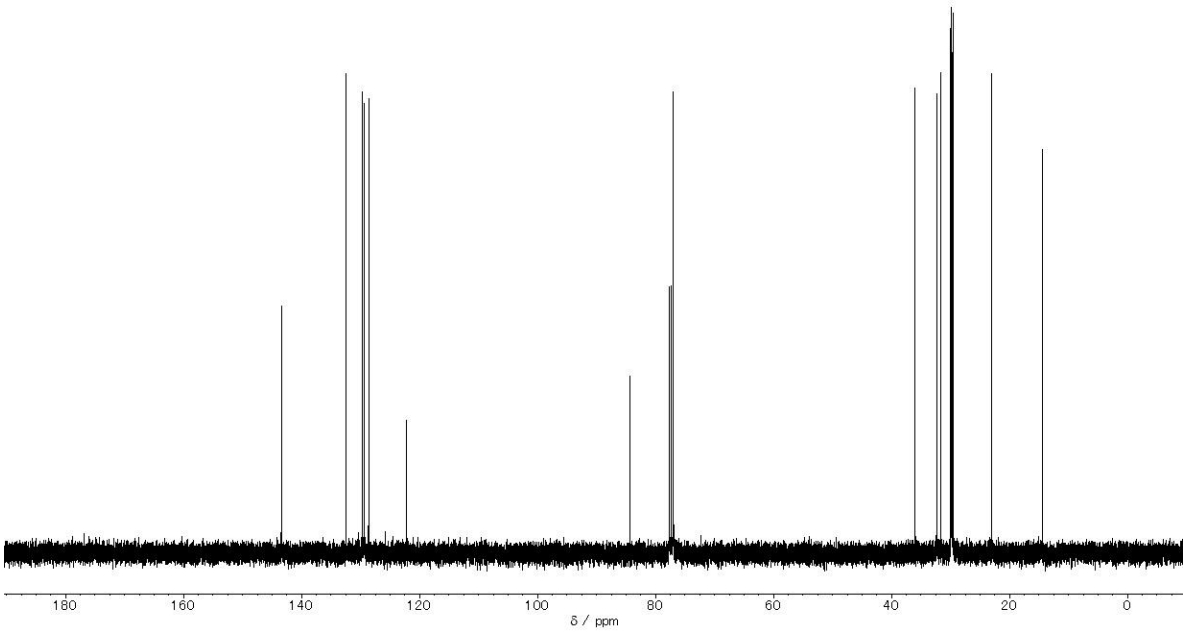

^{1}H (300 MHz) and $^{13}C\{^{1}H\}$ NMR (75 MHz) spectra of 1-ethynyl-3-decyl-benzene (rt, $CDCl_3$).

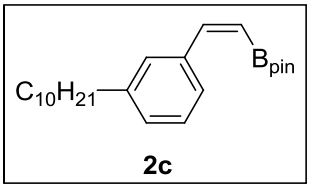

2c

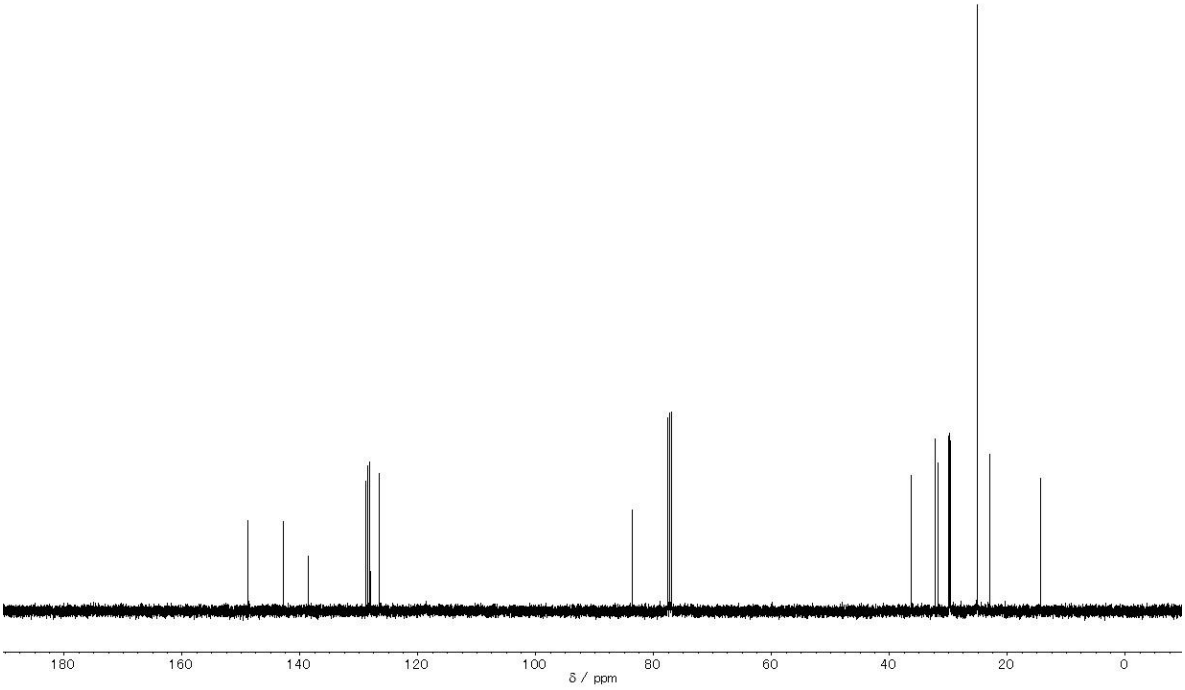

^{1}H (300 MHz) and $^{13}C\{^{1}H\}$ NMR (75 MHz) spectra of **2c** (rt, $CDCl_3$).

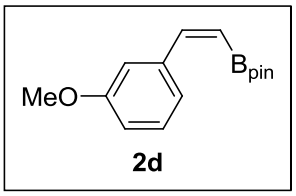

2d

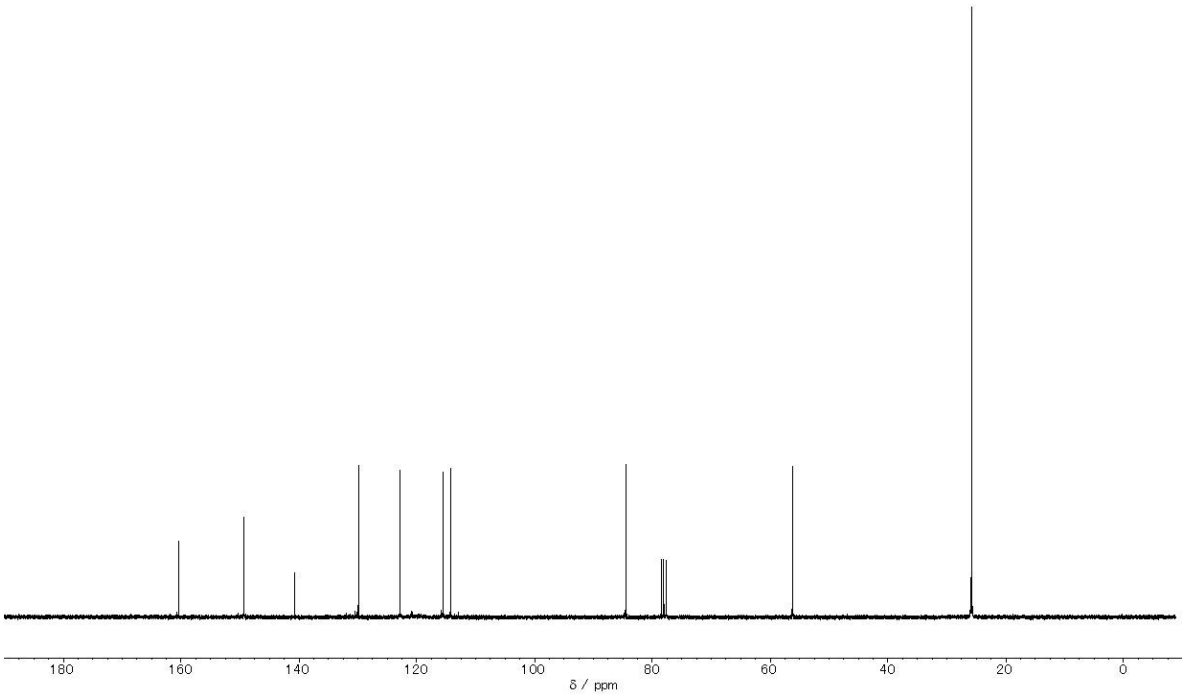

^{1}H (300 MHz) and ^{13}C{^{1}H} NMR (75 MHz) spectra of **2d** (rt, $CDCl_3$).

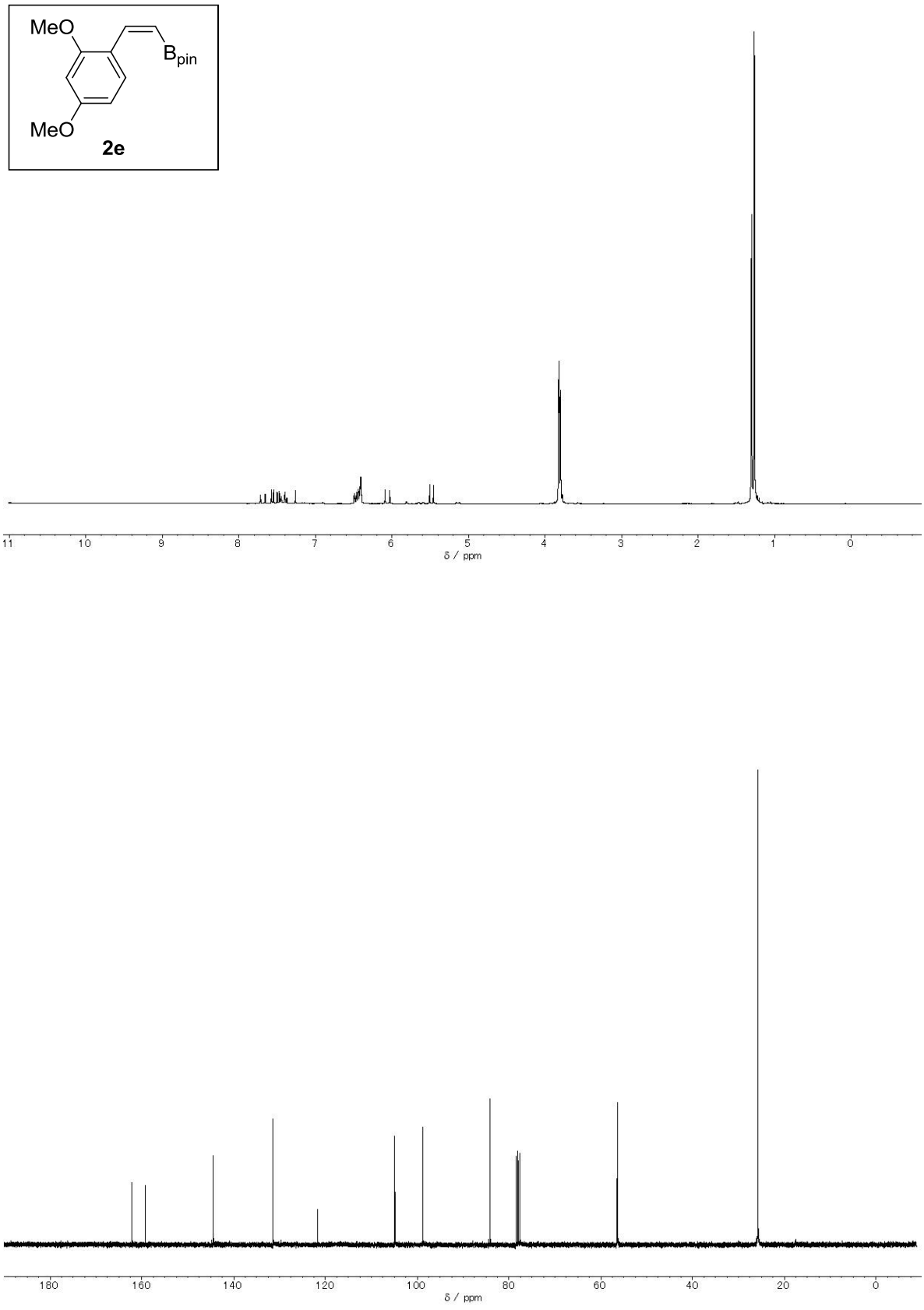

^{1}H (300 MHz) and $^{13}C\{^{1}H\}$ NMR (75 MHz) spectra of **2e** (rt, $CDCl_3$).

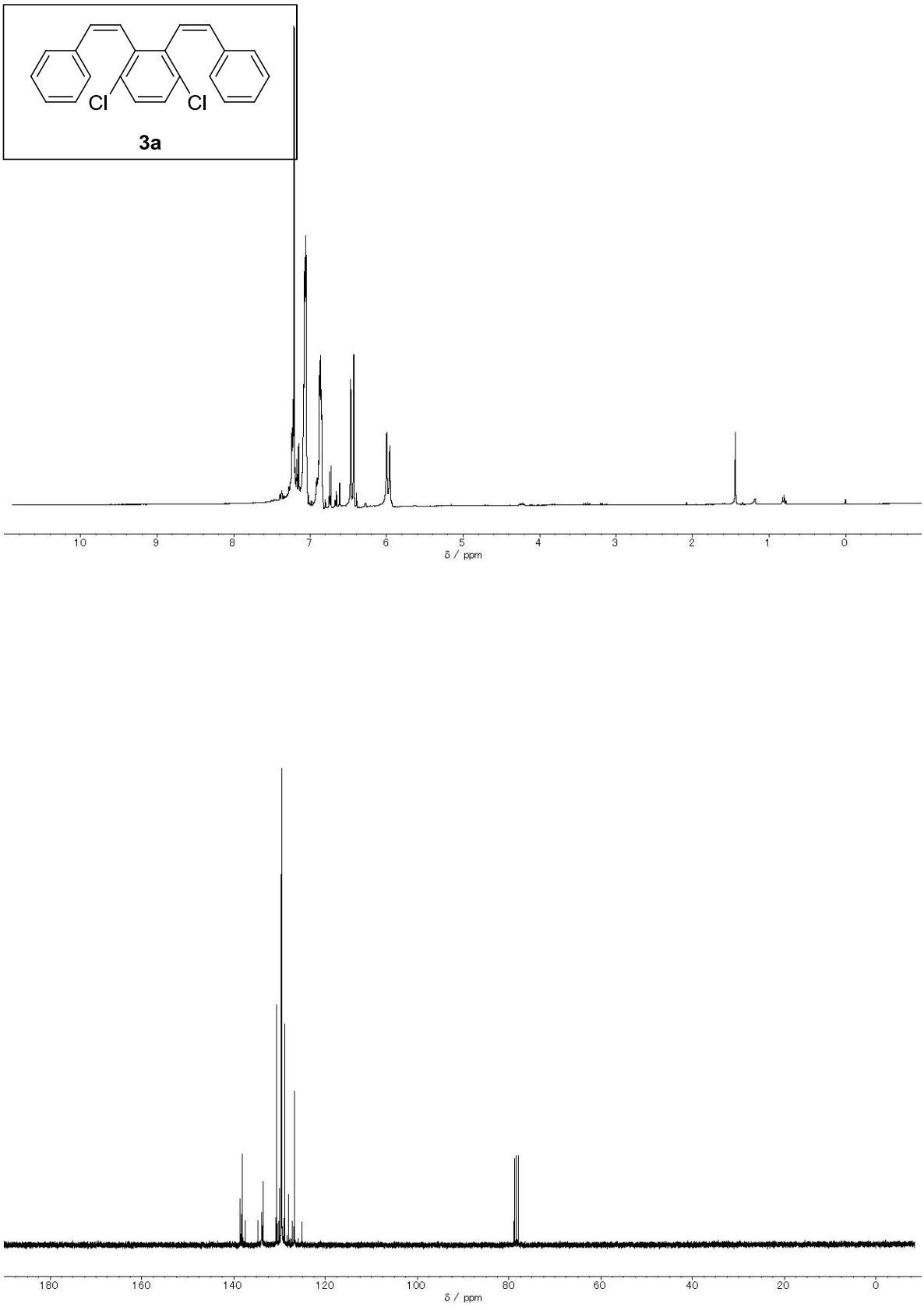

^{1}H (300 MHz) and $^{13}C\{^{1}H\}$ NMR (75 MHz) spectra of **3a** (rt, $CDCl_3$).

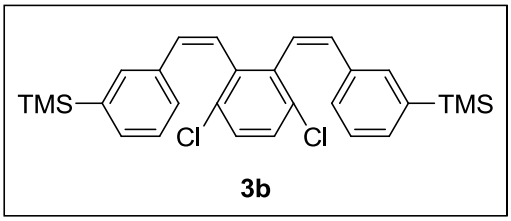

3b

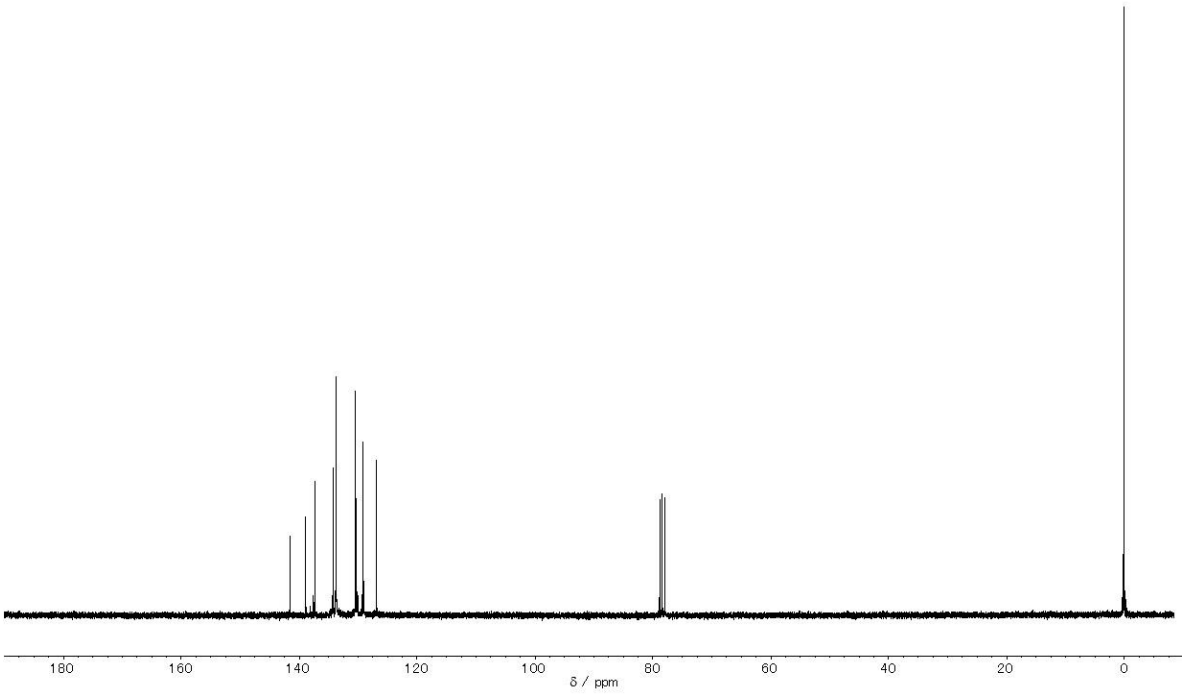

^{1}H (300 MHz) and $^{13}C\{^{1}H\}$ NMR (75 MHz) spectra of **3b** (rt, $CDCl_3$).

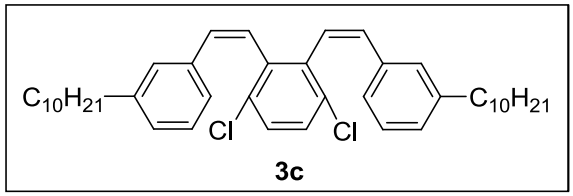

3c

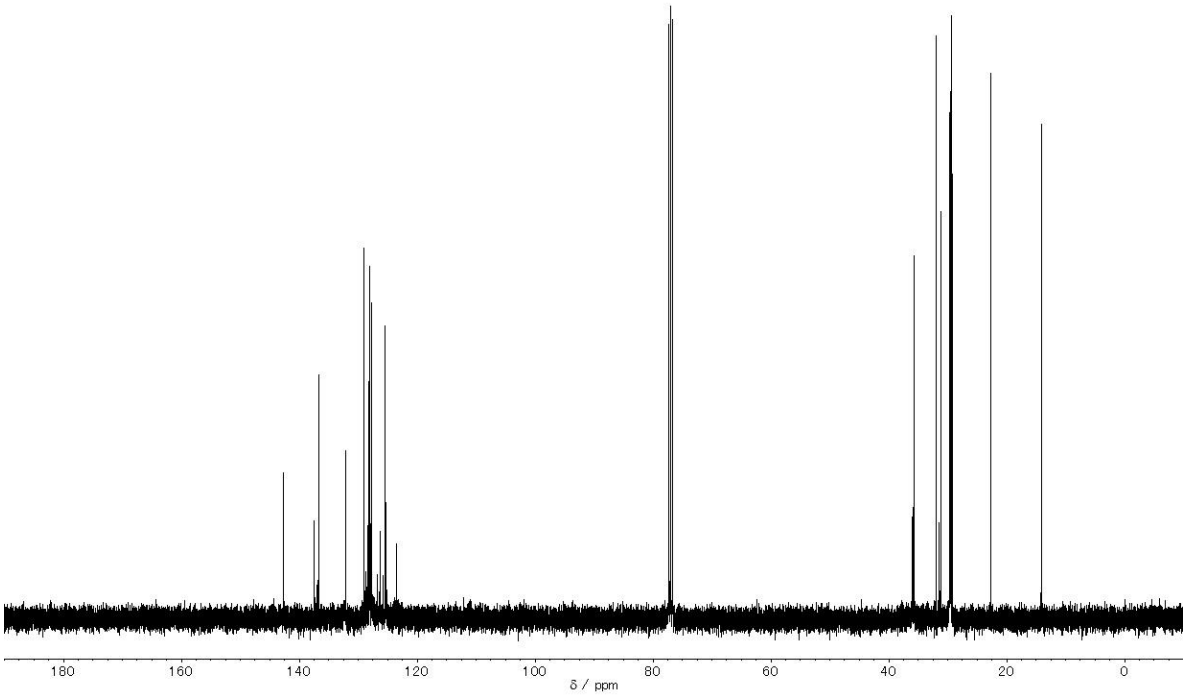

^{1}H (300 MHz) and $^{13}C\{^{1}H\}$ NMR (75 MHz) spectra of **3c** (rt, $CDCl_3$).

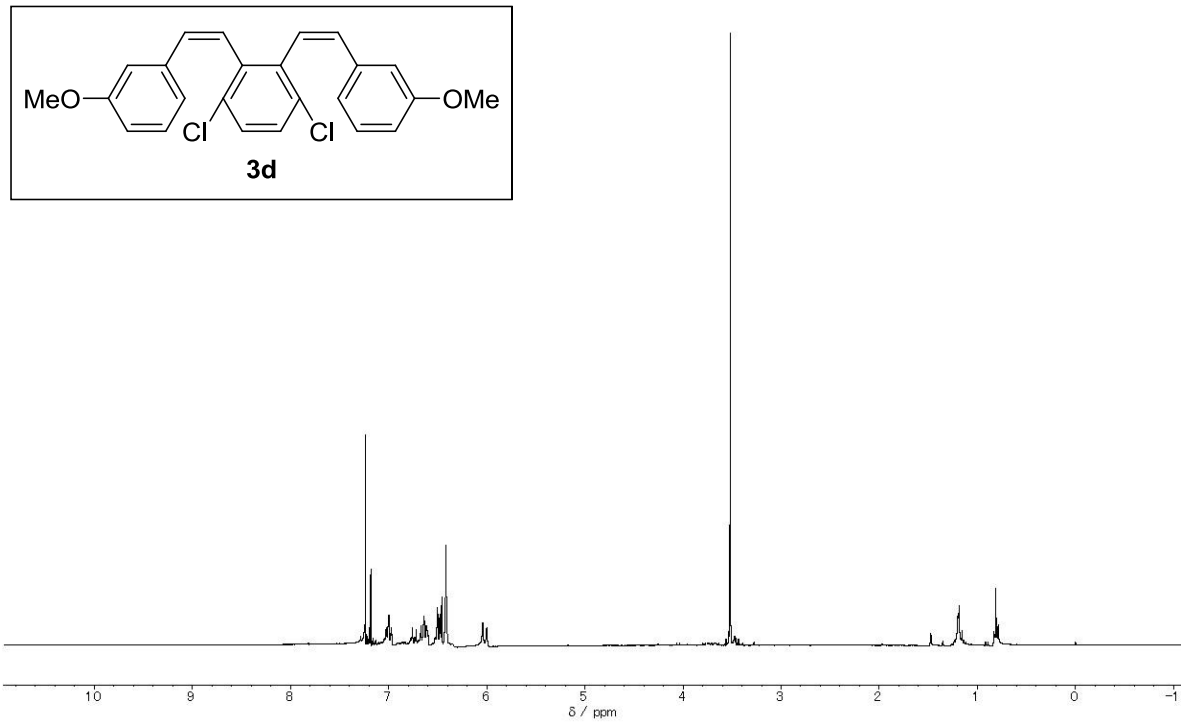

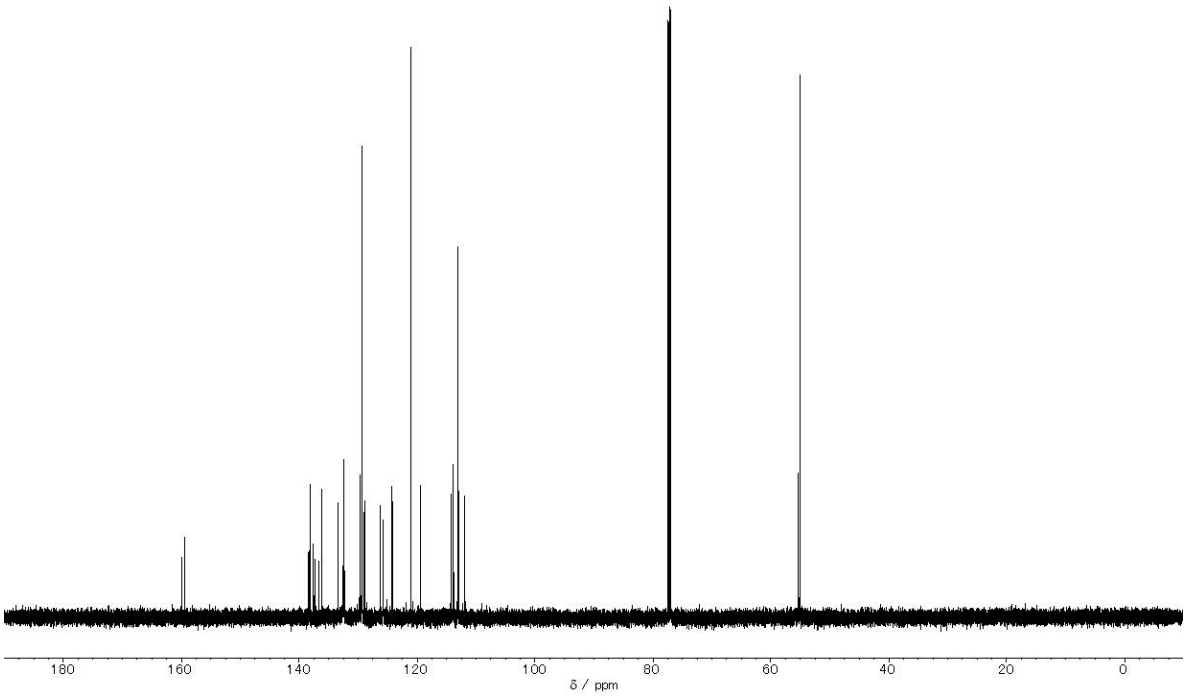

^{1}H (300 MHz) and $^{13}C\{^{1}H\}$ NMR (75 MHz) spectra of **3d** (rt, $CDCl_3$).

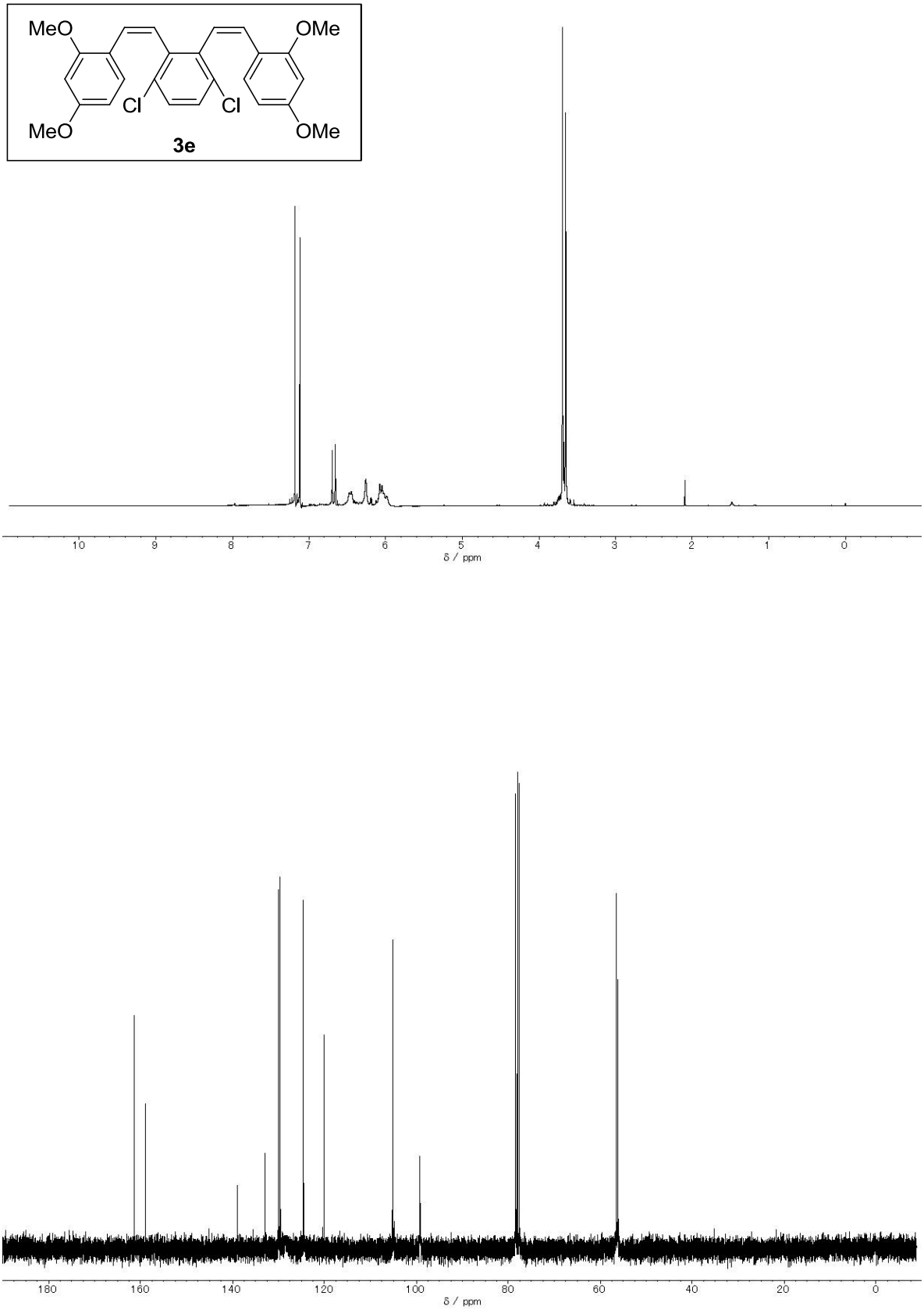

^{1}H (300 MHz) and $^{13}C\{^{1}H\}$ NMR (75 MHz) spectra of **3e** (rt, $CDCl_3$).

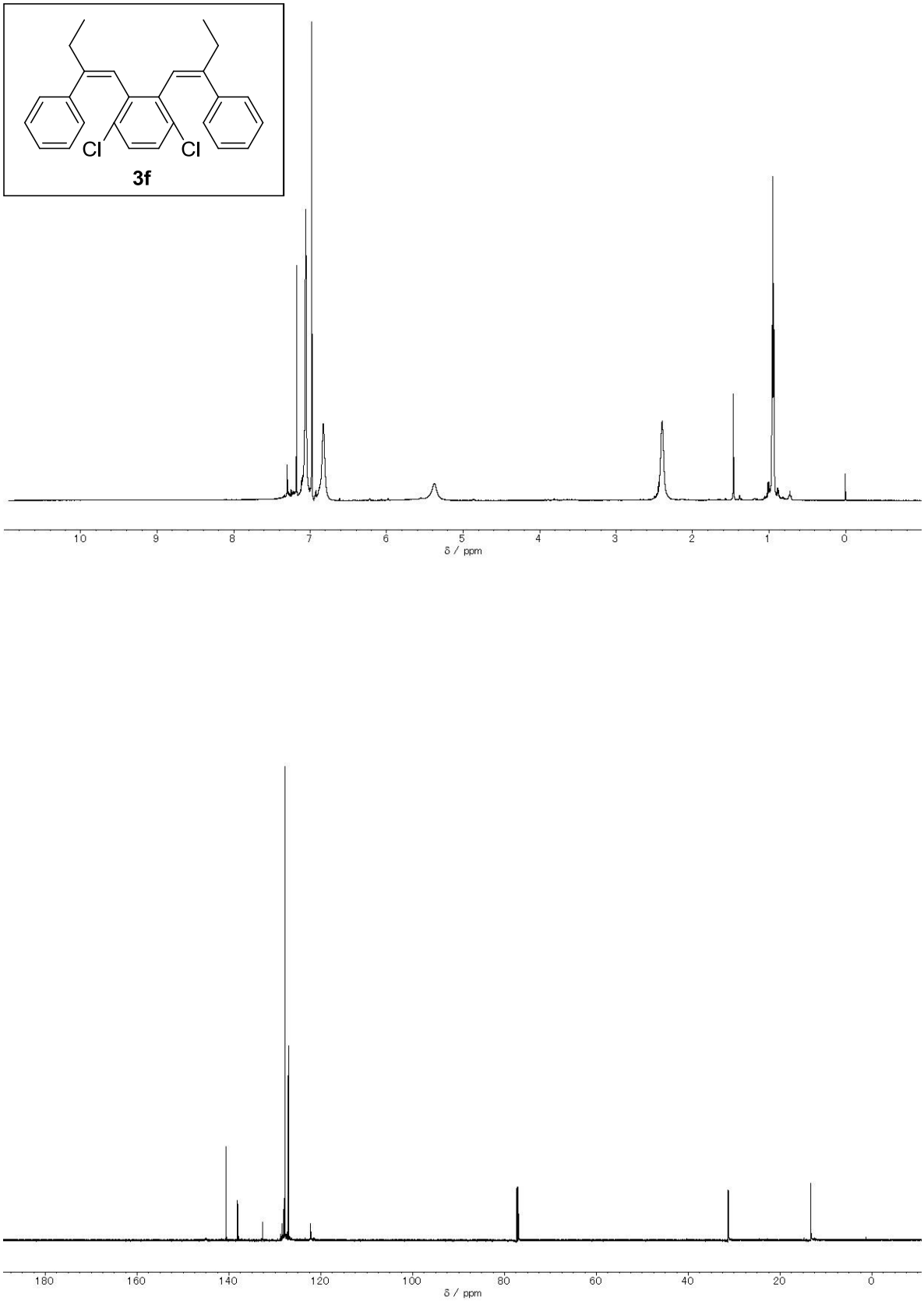

^{1}H (600 MHz) and $^{13}C\{^{1}H\}$ NMR (150 MHz) spectra of **3f** (rt, $CDCl_3$).

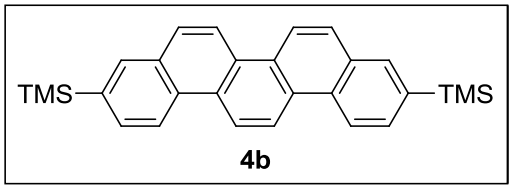

4b

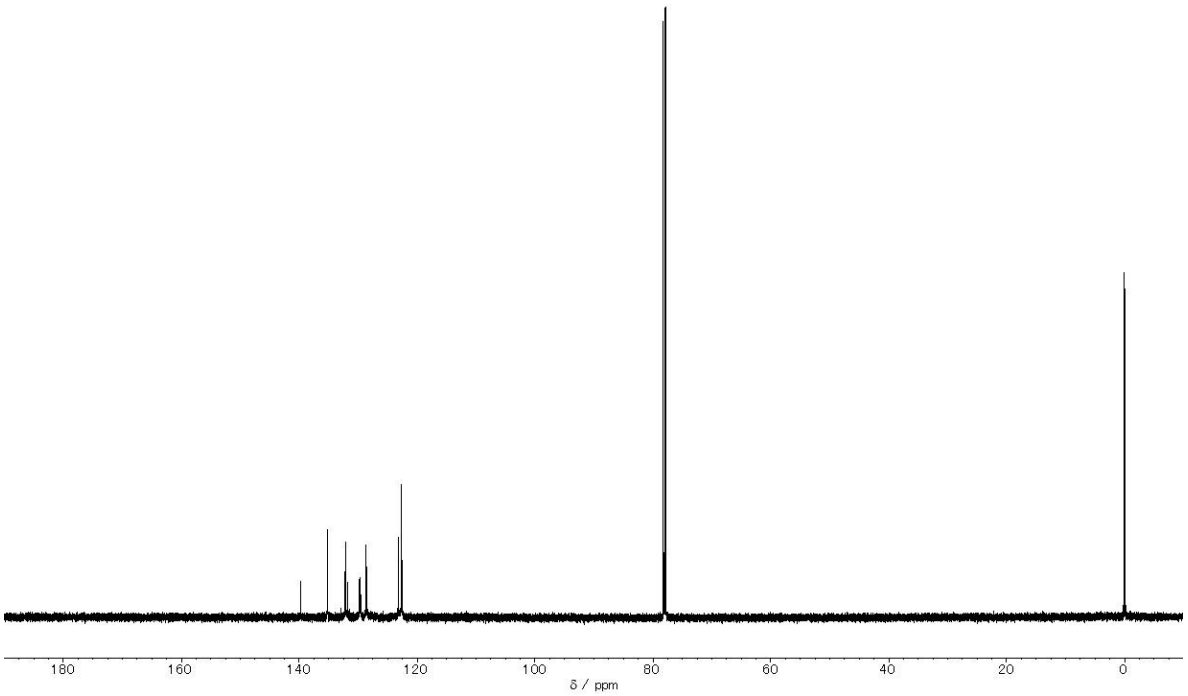

^{1}H (300 MHz) and $^{13}C\{^{1}H\}$ NMR (75 MHz) spectra of **4b** (rt, $CDCl_3$).

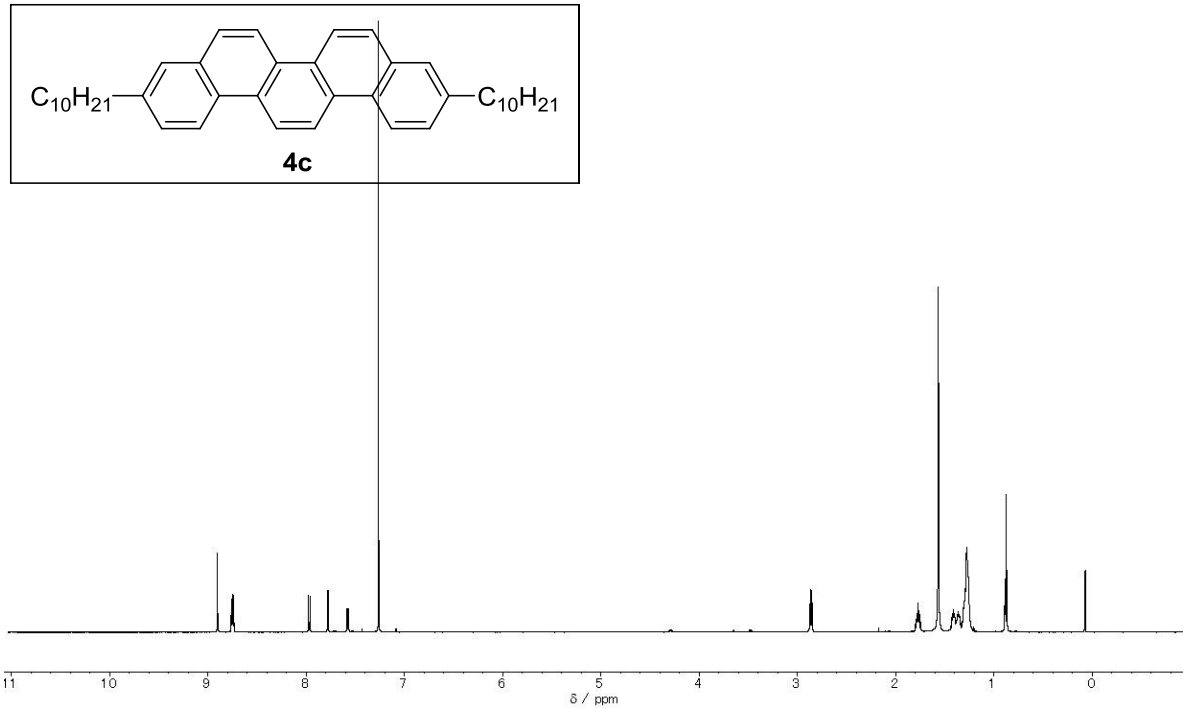

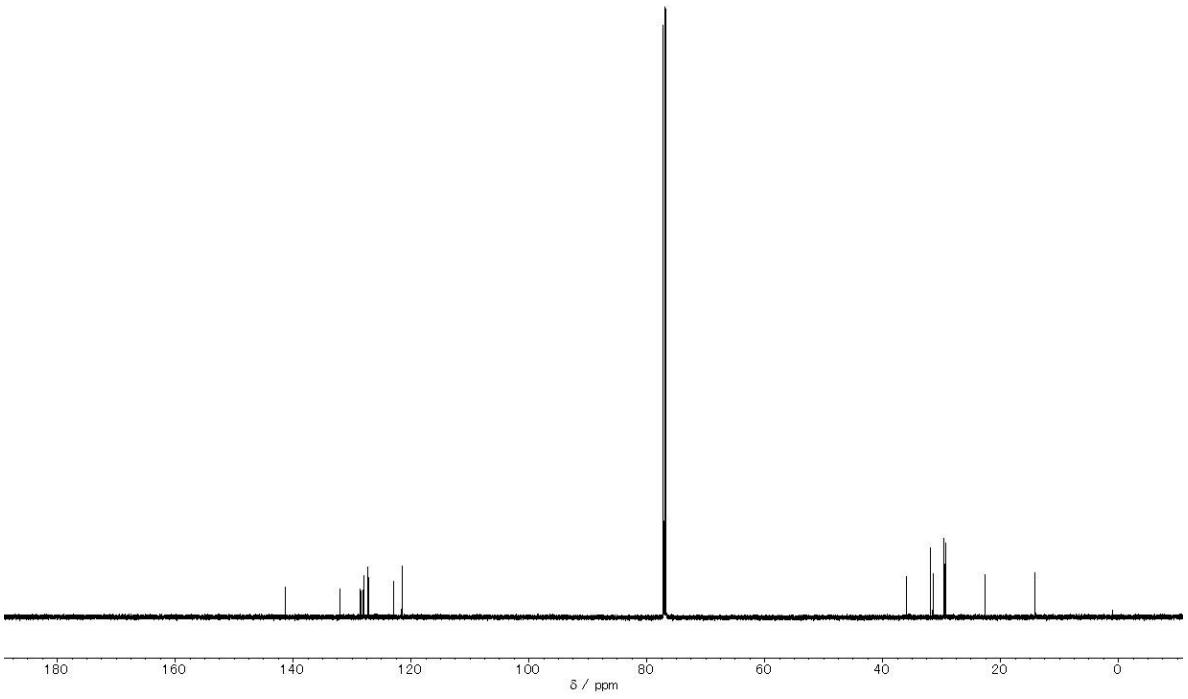

^{1}H (600 MHz) and $^{13}C\{^{1}H\}$ NMR (150 MHz) spectra of **4c** (rt, $CDCl_3$).

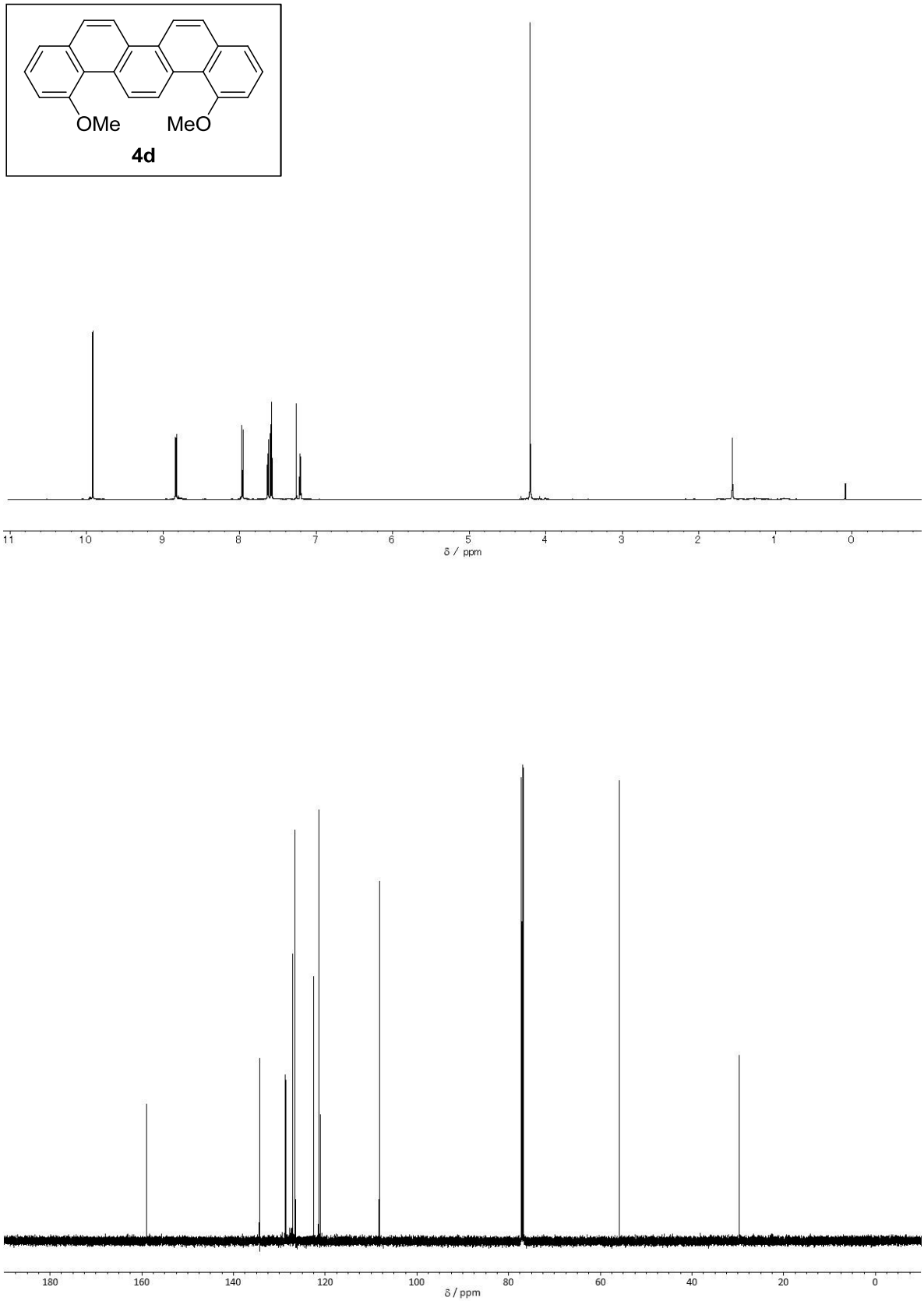

^{1}H (600 MHz) and $^{13}C\{^{1}H\}$ NMR (150 MHz) spectra of **4d** (rt, $CDCl_3$).

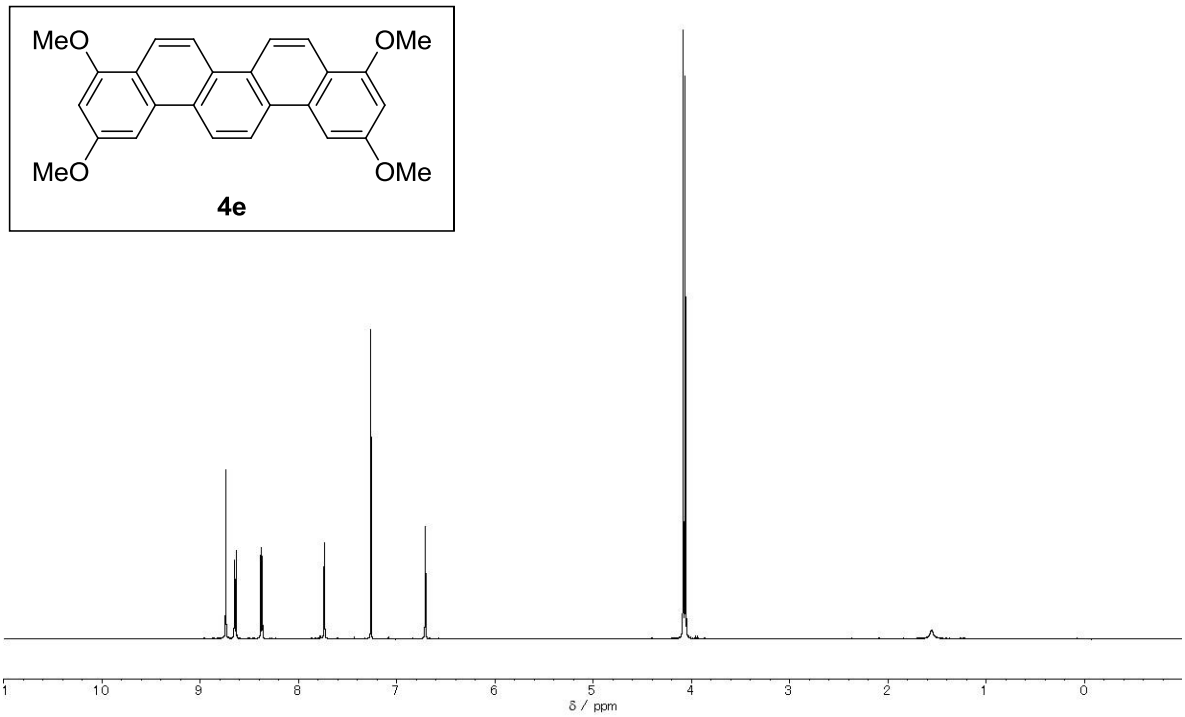

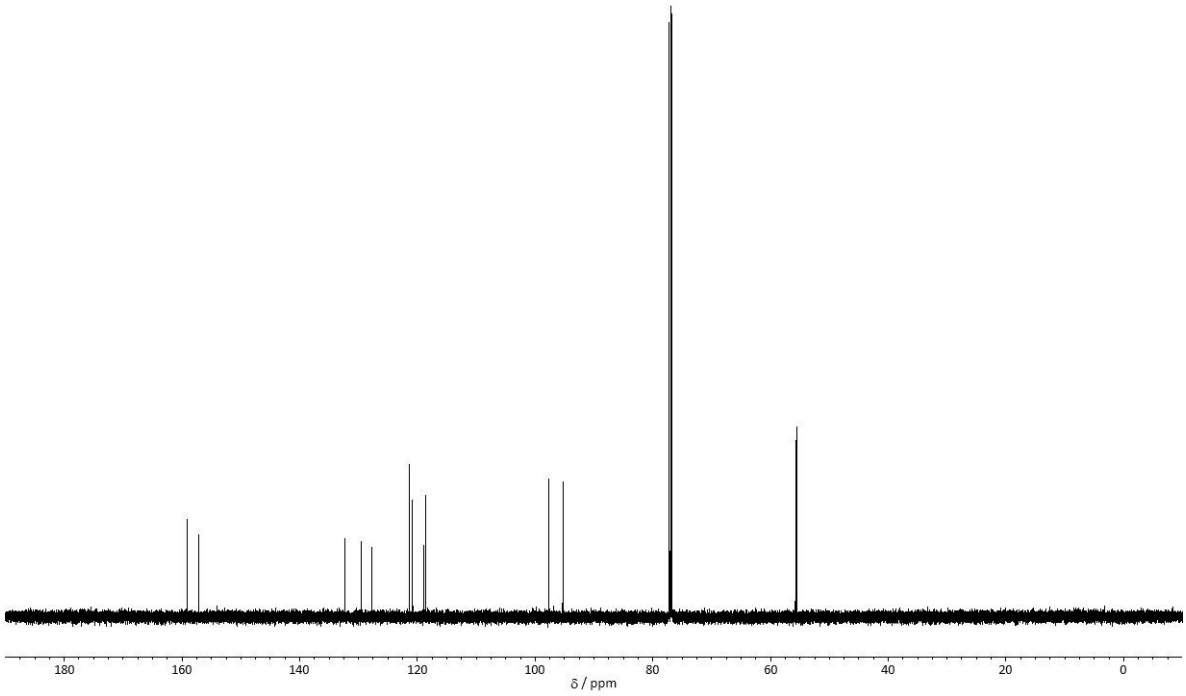

^{1}H (600 MHz) and ^{13}C{^{1}H} NMR (150 MHz) spectra of **4e** (rt, $CDCl_3$).

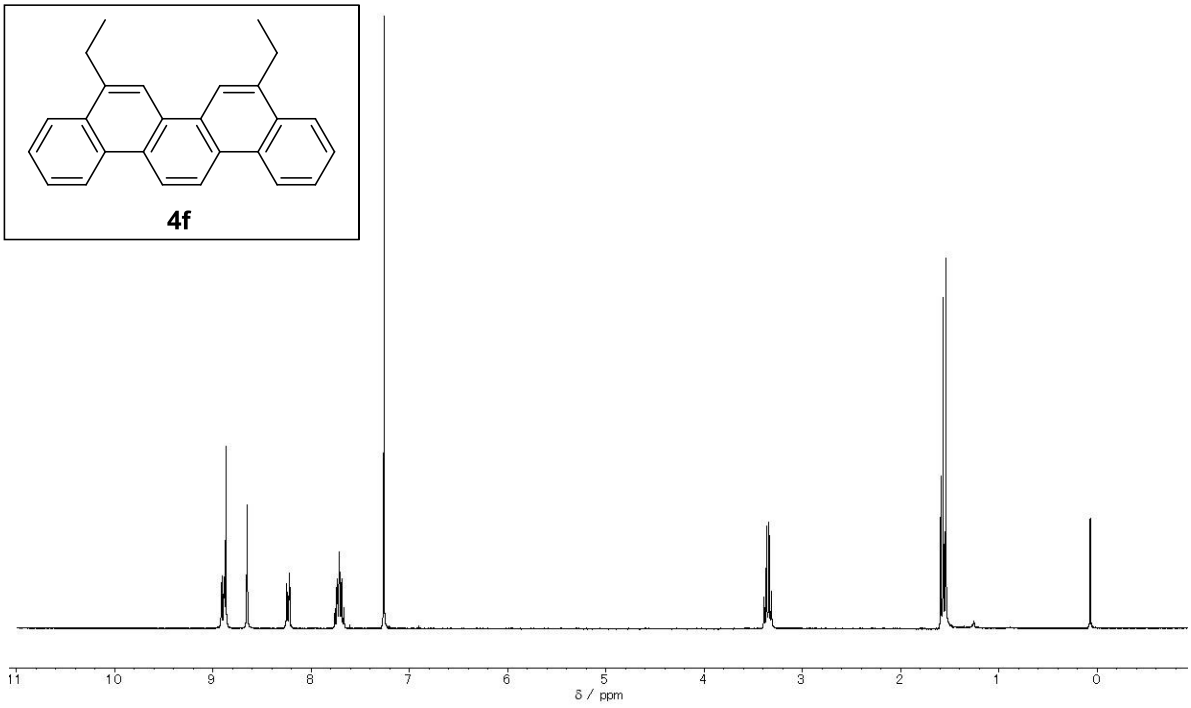

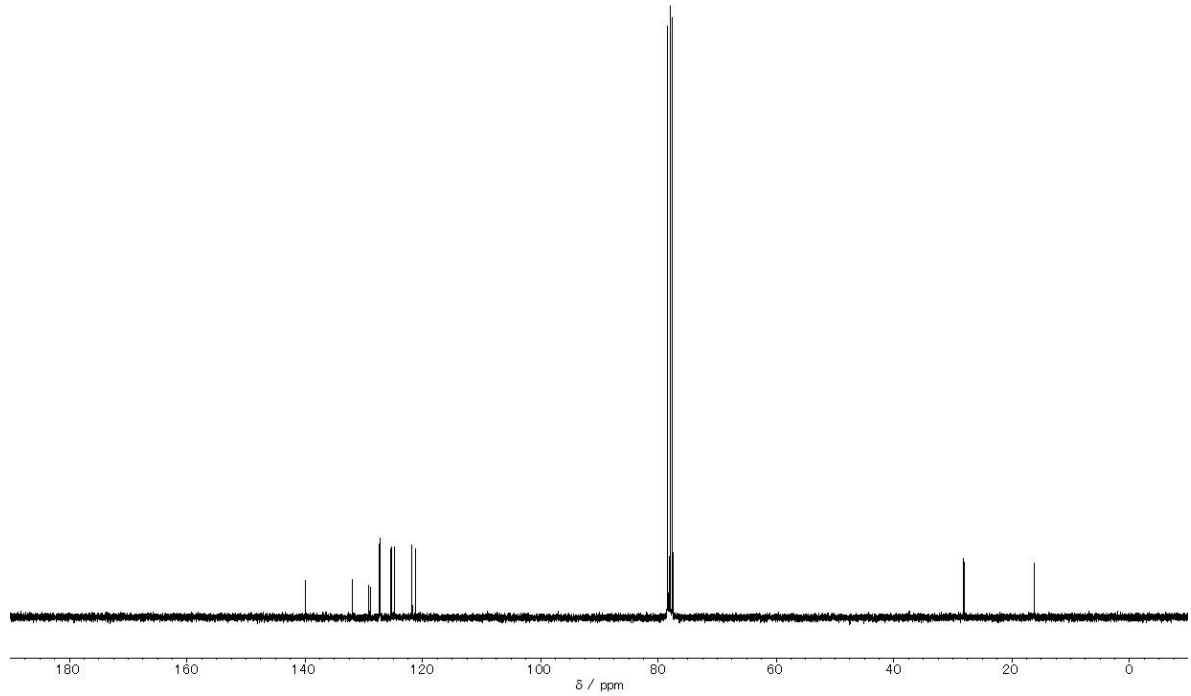

^{1}H (300 MHz) and $^{13}C\{^{1}H\}$ NMR (75 MHz) spectra of **4f** (rt, $CDCl_3$).

2-6 References and Notes

[1] Special issue on Organic Electronics and Optoelectronics: Forrest, S. R.; Thompson, M. E. *Chem. Rev*. **2007**, *107*, 923. (b) Wu, J.; Pisula, W.; Müllen, K. *Chem. Rev.* **2007**, *107*, 718. (c) Watson, M. D.; Fechtenkötter, A.; Müllen, K. *Chem. Rev.* **2001**, *101*, 1267. (d) Harvey, R. G. Polycyclic Aromatic Hydrocarbons, Wiley-VCH, New York, 1996.

[2] (a) Sugawara, Y.; Kaji, Y.; Ogawa, K.; Eguchi, R.; Oikawa, S.; Gohda, H.; Fujiwara, A.; Kubozono, Y. *Appl. Phys. Lett.* **2011**, *98*, 013303. (b) Komura, N.; Goto, H.; He, X.; Mitamura, H.; Eguchi, R.; Kaji, Y.; Okamoto, H.; Sugawara, Y.; Gohda, S.; Sato, K.; Kubozono, Y. *Appl. Phys. Lett.* **2012**, *101*, 083301.

[3] (a) Okamoto, H.; Kawasaki, N.; Kaji, Y.; Kubozono, Y.; Fujiwara, A.; Yamaji, M. *J. Am. Chem. Soc.* **2008**, *130*, 10470. (b) Kawasaki, N.; Kubozono, Y.; Okamoto, H.; Fujiwara, A.; Yamaji, M. *Appl. Phys. Lett.* **2009**, *94*, 043310. (c) Mitsuhashi, R.; Suzuki, Y.; Yamanari, Y.; Mitamura, H.; Kambe, T.; Ikeda, N.; Okamoto, H.; Fujiwara, A.; Yamaji, M.; Kawasaki, N.; Maniwa, Y.; Kubozono, Y. *Nature* **2010**, *464*, 76. (d) Wang, Y.; Motta, S. D.; Negri, F.; Friedlein, R. *J. Am. Chem. Soc.* **2011**, *133*, 10054. (e) Kawai, N.; Eguchi, R.; Goto, H.; Akaike, K.; Kaji, Y.; Kambe, T.; Fujiwara, A.; Kubozono, Y. *J. Phys. Chem. C* **2012**, *116*, 7983.

[4] For examples of the pentacene synthesis, see: (a) Takahashi, T.; Kitamura, M.; Shen, B.; Nakajima, K. *J. Am. Chem. Soc.* **2000**, *122*, 12876. (b) Payne, M. M.; Parkin, S. R.; Anthony, J. E.; Kuo, C-C.; Jackson, T. N. *J. Am. Chem. Soc.* **2005**, *127*, 4986.

[5] (a) Okamoto, H.; Yamaji, M.; Gohda, S.; Kubozono, Y.; Komura, N.; Sato, K.; Sugino, H.; Satake, K. *Org. Lett.* **2011**, *13*, 2758. (b) Kitazawa, K.; Kochi, T.; Nitani, M.; Ie, Y.; Aso, Y.; Kakiuchi, F. *Chem. Lett.* **2011**, *40*, 300. (c) Xia, Y.; Liu, Z.; Xiao, Q.; Qu, P.; Ge, R.; Zhang, Y.; Wang, J. *Angew. Chem., Int. Ed*. **2012**, *51*, 5714. (d) Mallory, F. B.; Mallory, C. W.; Regan, C. K.; Aspden, R. J.; Ricks, A. B.; Racowski,

J. M.; Nash, A. I.; Gibbons, A. V.; Carroll, P. J.; Bohen, J. M. *J. Org. Chem.* **2013**, *78*, 2040.

[6] O'Brien, C. J.; Kantchev, E. A. B.; Valente, C.; Hadei, N.; Chass, G. A.; Lough, A.; Hopkinson, A. C.; Organ, M. G. *Chem. Eur. J.* **2006**, *12*, 4743.

[7] (a) Klumpp, D. A.; Baek, D. N.; Prakash, G. K. S.; Olah, G. A. *J. Org. Chem*. **1997**, *62*, 6666. (b) King, B. T.; Kroulík, J.; Robertson, C. R.; Rempala, P.; Hilton, C. L.; Korinek, J. D.; Gortari, L. M. *J. Org. Chem.* **2007**, *72*, 2279. (c) Sarhan, A. A. O.; Bolm, C. *Chem. Soc. Rev*. **2009**, *38*, 2730. (d) Navale, T. S.; Thakur, K.; Rathore, R. *Org. Lett.* **2011**, *13*, 1634. (e) Hackeloer, K.; Schnakenburg, G.; Waldvogel, S. R. *Org. Lett*. **2011**, *13*, 916.

[8] (a) Tang, X.-Q.; Harvey, R. G. *J. Org. Chem*, **1995**, *60*, 3568. (b) Talele, H. R.; Gohil, M. J.; Bedekar, A. V. *Bull. Chem. Soc. Jpn*. **2009,** *82*, 1182.

[9] Miljanić, O. Š.; Vollhardt, K. P. C.; Whitener, G. D. *Synlett* **2003**, 29.

[10] Nishihara, Y.; Miyasaka, M.; Okamoto, M.; Takahashi, H.; Inoue, E.; Tanemura, K.; Takagi. K. *J. Am. Chem. Soc.* **2007**, *129*, 12634.

[11] For reviews, see: (a) Echavarren, A. M.; Gómez-Lor, B.; González, J. J.; Frutos, Ó. D. *Synlett* **2003**, 585. (b) Alberico, D.; Scott, M. E.; Lautens, M. *Chem. Rev*. **2007**, *107*, 174. (c) Lyons, T. W.; Sanford, M. S. *Chem. Rev.* **2010**, *110*, 1147.

[12] (a) Peng, J.-S.; Chen, T.-H.; Chen, C.-X.; Li, B. *J. Org. Chem*. **2011**, *76*, 9507. (b) Wu, T.-C.; Hsin, H.-J.; Kuo, M.-Y.; Li, C.-H.; Wu, Y.-T. *J. Am. Chem. Soc*. **2011**, *133*, 16319.

[13] Ohmura, T.; Yamamoto, Y.; Miyaura, N. *J. Am. Chem. Soc.* **2000**, *122*, 4990.

[14] (a) Takahashi, T.; Seki, T.; Nitto, Yu; Saburi, M.; Rousset, C. J.; Negishi, E. *J. Am. Chem. Soc.* **1991**, *113*, 6266. (b) Nishihara, Y.; Miyasaka, M.; Okamoto, M.; Takahashi, H.; Inoue, E.; Tanemura, K.; Takagi, K. *J. Am. Chem. Soc.* **2007**, *129*, 12634.

[15] Although the picene precursor **3** from a (*Z*)-arylethenylboronate bearing an electron-withdrawing CF_3 group in the 3-position was successfully synthesized, Pd-catalyzed double cyclization resulted in the formation of a mixture of structural isomers in a ratio of 46:54.

[16] The Author screened various bases for the intramolecular cyclization of **3b-Cl** and the results showed the yield of **4b** could be up to 60% when Na_2CO_3 was used as the base.

[17] Kato, S.; Noguchi, H.; Kobayashi, A.; Yoshihara, T.; Tobita, S.; Nakamura, Y. *J. Org. Chem.* **2012**, *77*, 9120.

[18] Okamoto, H.; Yamaji, M.; Gohda, S.; Sato, K.; Sugino, H.; Satake, K. *Res. Chem. Intermed.* **2013**, *39*, 147.

[19] (a) Fery-Forgues, S.; Lavabre, D. *J. Chem. Educ.* **1999**, *76*, 1260. (b) Suzuki, K.; Kobayashi, A.; Kaneko, S.; Takehira, K.; Yoshihara, T.; Ishida, H.; Shiina, Y.; Oishi, S.; Tobita, S. *Phys. Chem. Chem. Phys*. **2009**, *11*, 9850.

[20] Liu, S.-Y.; Shi, M.-M.; Huang, J.-C.; Jin, Z.-N.; Hu, X.-L.; Pan, J.-Y.; Li, H.-Y.; Jen, A. K.-Y.; Chen, H.-Z. *J. Mater. Chem. A*, **2013**, *1*, 2795.

[21] Li, G.; Wu, Y.; Gao, J.; Wang, C.; Li, J.; Zhang, H.; Zhao, Y.; Zhao, Y.; Zhang, Q. *J. Am. Chem. Soc*. **2012**, *134*, 20298.

[22] (a) Bredas, J.-L.; Beljonne, D.; Coropceanu, V.; Cornil, J. *Chem. Rev.* **2004**, *104*, 4971. (b) Sakanoue, K.; Motoda, M.; Sugimoto, M.; Sakaki, S. *J. Phys. Chem. A* **1999**, *103*, 5551.

[23] The calculations of transfer integrals (*t*) between HOMOs in the semiconducting layer were elucidated by the single crystal X-ray analysis. Calculations of t_{HOMO}s were performed with PW91 functional and Slater-type triple-ε plus polarization (TZP) basis sets using the Amsterdam Density Functional (ADF) program package. See: (a) Senthilkumar, K.; Grozema, F. C.; Bickelhaupt, F. M.; Siebbeles, L. D. A. *J. Chem. Phys.* **2003,** *119*, 9809. (b) Prins, P.; Senthilkumar, K.; Grozema, F. C.; Jonkheijm, P.;

Schenning, A. P. H. J.; Meijer, E. W.; Siebbeles, L. D. A. *J. Phys. Chem. B* **2005,** *109*, 18267.

[24] Takimiya, K.; Shinamura, S.; Osaka, I.; Miyazaki, E. *Adv. Mater.* **2011**, *23*, 4347.

[25] Frisch, M. J.; Trucks, G. W.; Schlegel, H. B.; Scuseria, G. E.; Robb, M. A.; Cheeseman, J. R.; Scalmani, G.; Barone, V.; Mennucci, B.; Petersson, G. A.; Nakatsuji, H.; Caricato, M.; Li, X.; Hratchian, H. P.; Izmaylov, A. F.; Bloino, J.; Zheng, G.; Sonnenberg, J. L.; Hada, M.; Ehara, M.; Toyota, K.; Fukuda, R.; Hasegawa, J.; Ishida, M.; Nakajima, T.; Honda, Y.; Kitao, O.; Nakai, H.; Vreven, T.; Montgomery, Jr., J. A.; Peralta, J. E.; Ogliaro, F.; Bearpark, M.; Heyd, J. J.; Brothers, E.; Kudin, K. N.; Staroverov, V. N.; Kobayashi, R.; Normand, J.; Raghavachari, K.; Rendell, A.; Burant, J. C.; Iyengar, S. S.; Tomasi, J.; Cossi, M.; Rega, N.; Millam, J. M.; Klene, M.; Knox, J. E.; Cross, J. B.; Bakken, V.; Adamo, C.; Jaramillo, J.; Gomperts, R.; Stratmann, R. E.; Yazyev, O.; Austin, A. J.; Cammi, R.; Pomelli, C.; Ochterski, J. W.; Martin, R. L.; Morokuma, K.; Zakrzewski, V. G.; Voth, G. A.; Salvador, P.; Dannenberg, J. J.; Dapprich, S.; Daniels, A. D.; Farkas, Ö.; Foresman, J. B.; Ortiz, J. V.; Cioslowski, J.; Fox, D. J. Gaussian, Inc., Wallingford CT, 2009.

[26] Schenk, T. G.; Downes, J. M.; Milne, C. R. C.; Mackenzie, P. B.; Boucher, H.; Whelan, J.; Bosnich, B. *Inorg. Chem.* **1985**, *24*, 2334.

[27] Fairlamb, I. J. S.; Kapdi, A. R.; Lee, A. F. *Org. Lett.* **2004**, *6*, 4435.

[28] Fan, G.-Z.; Li, T.; Li, G.-X. *Appl. Organometal. Chem*. **2006**, *20*, 656.

[29] Noskowska, M.; Sliwinska, E.; Duczmal, W. *Transition Metal Chem.* **2003**, *28*, 756.

[30] Hintermann, L. *Beilstein J. Org. Chem.* **2007**, *3*, doi:10.1186/1860-5397-3-22.

[31] Jeong, E. J.; Moon, H. S.; Han, K. M. U.S. Pat. Appl. Publ. 2007, US 20070120120 A1 20070531.

[32] Garden, S. J.; Torres, J. C.; Ferreira, A. A.; Silva, R. B.; Pinto, A. C. *Tetrahedron Lett*. **1997**, *38*, 1501.

[33] Lisowski, V.; Robba, M.; Rault, S. *J. Org. Chem.* **2000**, *65*, 4193.

[34] Nakayama, J.; Sakai, A.; Hoshino, M. *J. Org. Chem.* **1984**, *49*, 5084.

[35] Yoshida, H.; Yamaryo, Y.; Ohshita, J.; Kunai, A. *Chem. Commun.* **2003**, 1510.

[36] Nishi, M.; Kuninobu, Y.; Takai, K. *Org. Lett*. **2012**, *14*, 6116.

[37] Mehta, S.; Larock, R. C. *J. Org. Chem.* **2010**, *75*, 1652.

CHAPTER 3

Synthesis of [6]Phenacenes and Their Physicochemical Properties

3-1 Introduction

Organic thin-film transistors (OTFTs) with [n]phenacenes,[1] where n is the number of fused benzene rings with an arm-chaired structure, have attracted much attention owing to their superior FET characteristics.[2] The [5]phenacene (picene, Chart 3-1)-based OTFT has been fabricated[2a] and the field-effect mobility, μ_{FET}, improved as high as 3.2 $cm^2\ V^{-1}\ s^{-1}$ under O_2 atmosphere.[2b] Recently, the OTFT with the expanded [6]phenacene (fulminene, Chart 3-1) has shown the more higher μ_{FET} value of 3.7 $cm^2\ V^{-1}\ s^{-1}$.[3] These results imply that the increased numbers of the benzene rings in [n]phenacene would have potentials to improve the FET characteristics. However, solubilities of the unsubstituted [n]phenacenes dramatically decrease with increasing n. For instance, [5]phenacene is sparingly soluble in $CHCl_3$, whereas the $^{13}C\{^1H\}$ NMR spectrum of [6]phenacene cannot be obtained due to its extreme insolubility. This solubility problem would be solved by incorporating alkyl substituents. Since ideal OFETs are expected to be solution-processed and exhibit high carrier mobility, high solubility of the molecules in common organic solvents are highly desired.

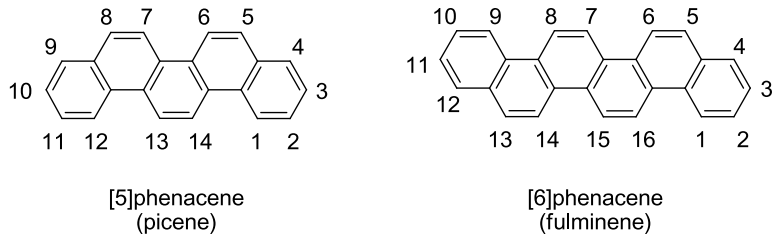

Chart 3-1. Structures of [5]phenacene and [6]phenacene.

From the synthetic point of view, most of the precedent [n]phenacene synthesis by oxidative photocyclizations of (*Z*)-stilbene skeletons[4] are mainly applicable to the synthesis of symmetrical [n]phenacene (i.e. n = 5 and 7). Notably, although the unsubstituted [6]phenacene has been barely synthesized,[1,5,6] to the best of the Author's knowledge, the synthesis of the substituted [6]phenacenes are unprecedented to date.

In this Chapter, a series of unsymmetrically substituted [6]phenacenes are synthesized for the first time by using established synthetic strategy[7] in Chapter 2. Characterization and physicochemical properties of these [6]phenacenes are also investigated.

3-2 Results and Discussion

3-2-1 The order of the reagent addition in the cross-coupling

In order to obtain [6]phenacene as the target molecule through intramolecular double cyclization, there are two pathways to synthesize the precursor of [6]phenacene using a stepwise procedure (Scheme 3-1).

Scheme 3-1. Two pathways to synthesis of the [6]phenacene precursor.

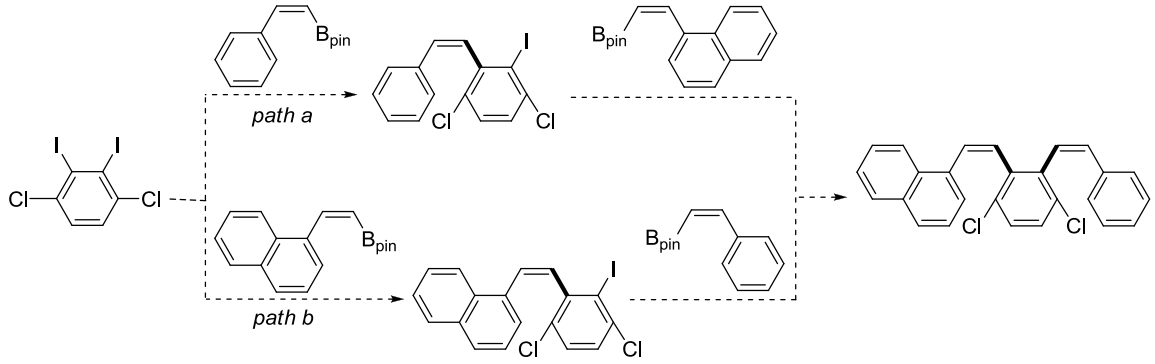

The Author carried out the reaction in paths *a* and *b* to investigate the effect of adding reagents in an opposite order.

In path a, 1,4-dichloro-2,3-diiodobenzene was treated with an equimolar amount of (*Z*)-phenylethenylboronate under Suzuki-Miyaura coupling reaction conditions (eq 3.1). The results showed that a disubstituted product was major. Even though amounts of the catalyst and the base were decreased, the desired product was still minor.

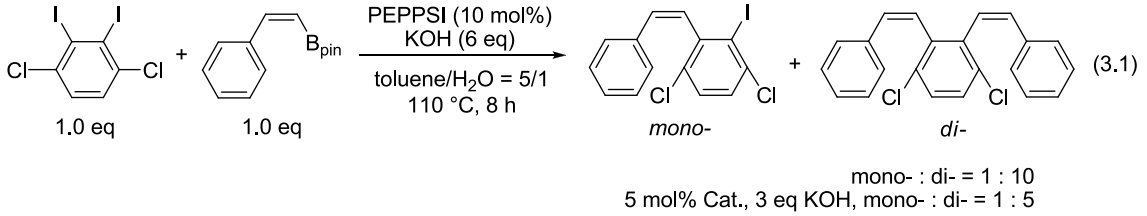

In path b, 1,4-dichloro-2,3-diiodobenzene was reacted first with (*Z*)-naphthylethenyl boronate to give mono-coupled product as a desired product with a considerable amount of a by-product derived from deborylation of (*Z*)-naphthylethenylboronate (eq 3.2). Next, the second coupling with (*Z*)-phenylethenylboronate was performed to synthesize the precursor of [6]phenacene in 65% yield (eq 3.3).

1st: with (Z)-naphthylethenylboronate

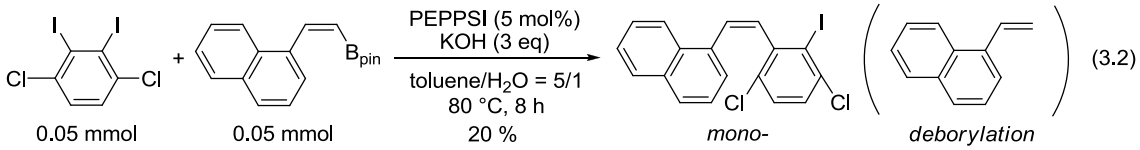

(3.2)

2nd: with (Z)-phenylethenylboronate

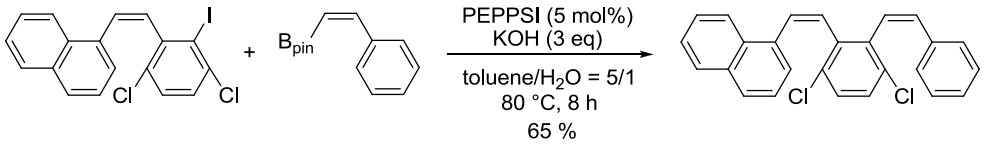

(3.3)

Instead of a stepwise procedure, the one-pot reaction was also carried out (eq 3.4). Equimolar amounts of 1,4-dichloro-2,3-diiodobenzene, (*Z*)-naphthylethenylboronate and (*Z*)-phenylethenylboronate were combined in one portion. Although the desired product was obtained in 12% yield, the GC-MS showed that this reaction gave much more complicated result and that the di-coupled product with (*Z*)-phenylethenylboronate was the major product.

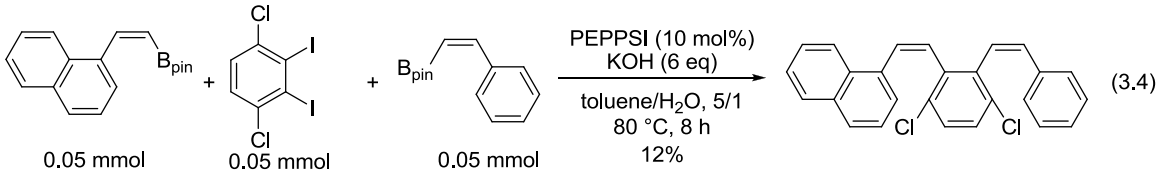

(3.4)

In comparison of procedures above, path b is much more reliable. However, due to the low yield of first coupling, the Author next paid more attention to improve the yield of the first coupled product.

3-2-2 Optimization of first cross-coupling reaction

A set of experiments were performed to examine the reaction conditions of Suzuki-Miyaura coupling of 1,4-dichloro-2,3-diiodobenzene (**1**) with a slightly excess of (*Z*)-naphthylethenylboronate (**2**). The results are summarized in Table 3-1.

Table 3-1. Optimization of conditions in the cross-coupling reaction of **1** with **2**.

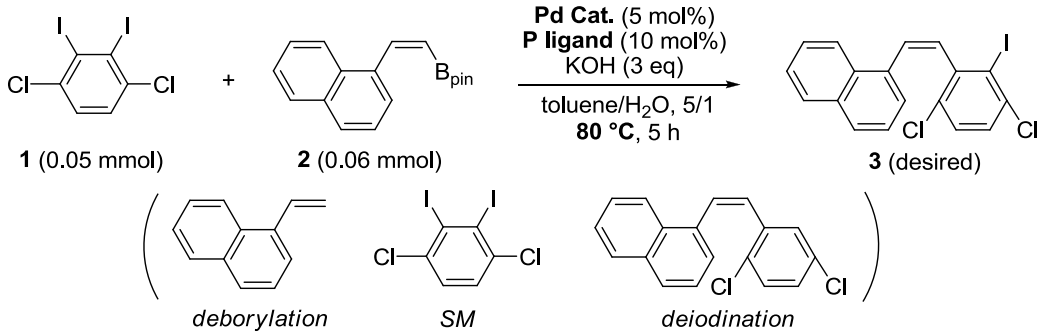

entry	Pd Cat.	P ligand	relative ratio (determined from GC)			
			deborylation	*SM*	*deiodination*	***3***[a]
1	PEPPSI-IPr	-	10	68	-	22 (20)
2	$Pd(OAc)_2$	PCy_3	21	29	7	43
3	$Pd(OAc)_2$	dppe	10	75	5	10
4	$Pd(OAc)_2$	-	20	74	-	6
5[b]	$Pd(OAc)_2$	PCy_3	-	100	-	0
6	$Pd(OAc)_2$	$P[2,4,6\text{-}(OMe)_3C_6H_2]_3$	16	45	5	34
7	$Pd(OAc)_2$	$P[3,5\text{-}(CF_3)_2C_6H_3]_3$	1	20	18	61
8	$PdCl_2(NCPh)_2$	$P[3,5\text{-}(CF_3)_2C_6H_3]_3$	2	30	15	53
9	$Pd(OAc)_2$	RuPhos	1	57	10	32
10	$Pd(OAc)_2$	SPhos	1	27	12	60
11[c]	$PdCl_2$dppp	-	1	22	17	60
12[c]	**$PdCl_2$dppf**	-	**1**	**8**	**17**	**74 (57%)**
13[c]	$Pd(OAc)_2$	$P(3,5\text{-}CF_3C_6H_3)_3$	1	30	34	35
14[d]	$PdCl_2$dppf	-	2	29	11	58
15[e]	$PdCl_2$dppf	-	10	27	63	0
16[f]	$PdCl_2$dppf	-	7	20	73	0
17[g]	$PdCl_2$dppf	-	1	24	71	4

[a] Isolated yields were shown in parentheses. [b] Without H_2O. [c] Aqueous KOH (3 M) as the base and THF as the solvent were employed at 50 °C. [d] rt. [e] DMA solvent. [f] DMF solvent. [g] DMSO solvent.

When PEPPSI-IPr was utilized as the catalyst, which exerted high efficiency in the previous work,[8] the desired product **3** was obtained in only 22% due to a concurrent protodeborylation of **2** (Table 3-1, entry 1). The Author then exploited other palladium catalysts, mainly, with bulky phosphine ligands. The reaction with ligand, such as PCy_3 and $P(2,4,6\text{-}OMeC_6H_2)_3$ gave a slightly higher yield of **3** (Table 3-1, entries 2 and 6). A combination of $Pd(OAc)_2$ with $P(3,5\text{-}CF_3C_6H_3)_3$ gave the desired product **3** in 61% yield with a decrease amount of deborylation (Table 3-1, entry 7). When the reactions were carried out under mild conditions, the conversion of the starting material were improved (Table 3-1, entries 11 and 12). To his delight, when the bidentate ligands were surveyed, $PdCl_2$(dppf) (dppf = 1,1'-bis(diphenylphosphino)ferrocene) gave the best yield of **3** up to 74% (Table 3-1, entry 12). Besides, the reaction using other solvent, such as DMA, DMF, and DMSO were completely inactive (entries 15–17).

3-2-3 Second cross-coupling reaction

With the synthesized **3** in hand, the second cross-coupling were conducted with the synthesized alkenylboronates **4a**–**4d** as the coupling partners. The PEPPSI-IPr catalyst gave rise to the corresponding [6]phenacene precursors **5a**−**5d** in 63−83% yields (Table 3-2).[9]

Finally, the Pd-catalyzed double cyclization of **5a**−**5d** were performed through the C−H activation toward the synthesis of [6]phenacenes **6a**−**6d** (Scheme 3-2).[10] The solubility of [6]phenacene **6b** is so poor that its ^{13}C NMR data were not available, whereas the solubility of **6c** and **6d** was obviously improved by introducing the OMe groups and alkyl chains, thus implying the possibility to fabricate single crystals by solution process.

Table 3-2. Synthesis of **5a**–**5d** by Suzuki-Miyaura coupling of **3** with **4a**–**4d**.[a]

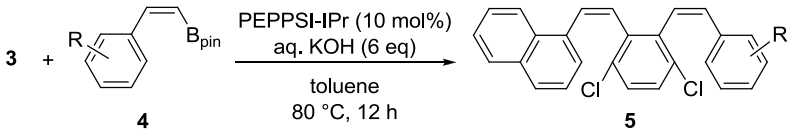

entry	4		product	yield (%)[b]
1	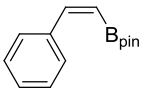	**4a**	**5a**	63
2	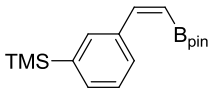	**4b**	**5b**	76
3	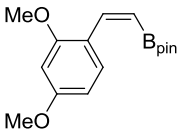	**4c**	**5c**	83
4	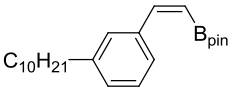	**4d**	**5d**	69

[a] Reaction conditions: **3** (0.2 mmol), **4** (0.24 mmol), PEPPSI-IPr (10 mol%), and KOH (3 M, 1.2 mmol) at 80 °C for 12 h. [b] Isolated yields.

Scheme 3-2. Synthesis of [6]phenacenes **6a**–**6d** by intramolecular double cyclization of **5a**–**5d**.

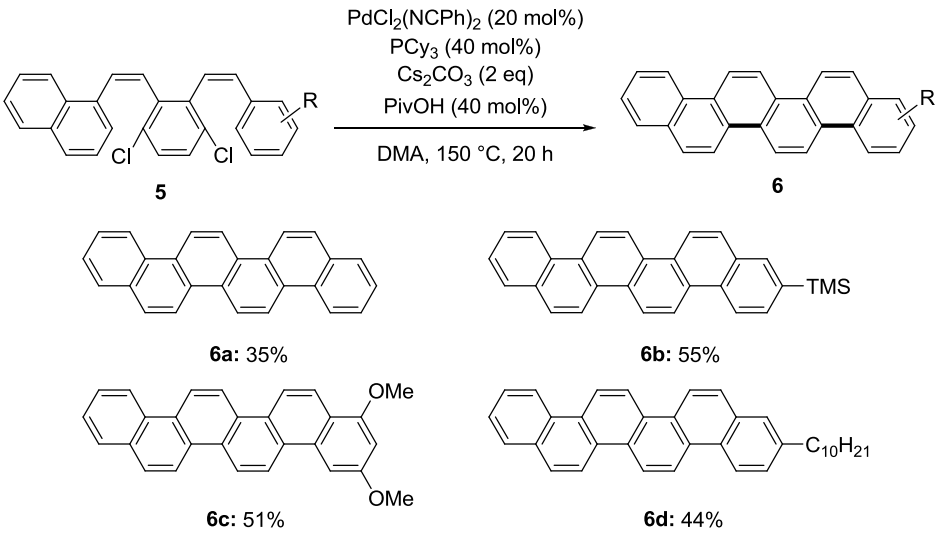

3-3 Physicochemical Properties of [6]Phenacenes

3-3-1 Measurements of UV-vis absorption spectra

In order to further survey the potentials toward organic electronic materials, UV-vis absorption spectroscopy of **6a**−**6d** were measured and the results are listed in Table 3-3. As shown in Figure 3-1(left), the absorption spectra of **6b**−**6d** exhibit main transition around 300 nm (λ_{max}^{abs}) and the other transitions appeared at higher wavelengths, which are similar with the parent **6a**. The [6]phenacene derivatives **6b**−**6d** bearing electron-donating groups on the aromatic ring showed a slightly red-shift absorption maximum compared to that of the parent **6a**. Molar extinction coefficient ε values of substituted [6]phenacenes **6b**−**6d** are available owing to the increased solubility than that of **6a**. Solution/thin-film absorption spectra of the selected [6]phenacene **6d** are shown in Figure 3-2. The thin film was fabricated on the quartz cell by spin-coating from 1 g/L $CHCl_3$ solution at a rate of 500 rpm for 30 sec. The film absorption maxima are red-shifted by approximately 2−10 nm versus the corresponding solution absorption maxima, indicating the existence of the layer by layer structure in the solid state.[11]

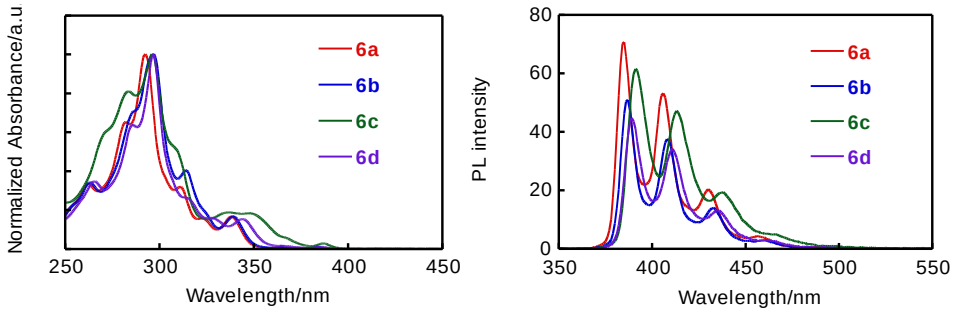

Figure 3-1. UV-vis absorption (left) and fluorescence emission (right) spectra of **6a**−**6d** in CH_2Cl_2.

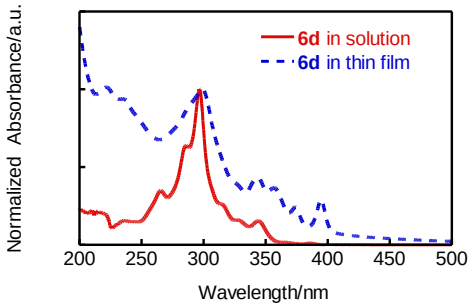

Figure 3-2. UV-vis absorption spectra of **6d** in solution and thin film.

Obviously, these results indicate that an introduction of the substituents into a [6]phenacene framework can affect the physical properties. In particular, a substitution effect of two methoxy groups in the 2,4-position is larger than that of alkyl and TMS groups in the 3-position.

Table 3-3. UV-vis and fluorescence data of [6]phenacenes **6a**–**6d**.

[6]phenacenes	λ_{max}^{abs} /nm[a]	ε /$M^{-1}\cdot cm^{-1}$	λ_{max}^{em} /nm[b]	Stokes shift /cm^{-1}	Φ_f[c]
6a	293	nd[d]	385	204	0.07
6b	297	40000	387	202	0.09
6c	296	45000	391	264	0.17
6d	297	55700	389	200	0.09

[a] Absorption maxima in the CH_2Cl_2 solution (1×10^{-5} M). [b] Emission maxima in CH_2Cl_2 solution (1×10^{-6} M) excited at λ_{max}^{abs}. [c] Fluorescence quantum yield were determined by the relative method using *p*-terphenyl (Φ_f = 0.87 in cyclohexane) as a standard. [d] Molar absorption coefficient of parent [6]phenacene **6a** cannot be determined due to its low solubility (saturated solution was used).

3-3-2 Measurements of fluorescence spectra

Steady-state fluorescence spectra of **6a**–**6d** in diluted CH_2Cl_2 solution (1×10^{-6} M) are shown in Figure 3-1(right) and the results are also summarized in Table 3-3. The Stokes shifts of **6b** and **6d** are ca. 200 cm^{-1}, which are similar to that of the parent **6a**.[6] In contrast, the shift of **6c** is higher than that of **6a**. This can be attributed to the slightly large and flexible molecular geometry of **6c**, which can have access to different geometrical configuration. The relative fluorescence quantum yields (Φ_f) of **6a**–**6d** were estimated with relative method.[12] The Φ_f values of **6c** are more than twice as much as that of **6a**, suggesting that an introduction of two electron-donating methoxy groups increased the Φ_f values due to the *p*-π conjugated effect.

3-3-3 Measurements of cyclic voltammograms

The absorption band-edges (λ_{edge}) of [6]phenacene **6a**–**6d** and the corresponding optical band gaps (E_g^{opt}) are summarized in Table 3-4. The electrochemical properties of **6a**–**6d** were also investigated by cyclic voltammetry (CV) (Figure 3-3) and the electrochemical

data are also listed in Table 3-4. The observed oxidation waves with oxidation onsets at +0.36−0.84 V (vs Ag/Ag^+) and no reduction waves in the CV measurements suggest that all compounds **6a**−**6d** have a potential for p-channel semiconductors in organic electronics. Moreover, **6d** shows quasi-reversible oxidation peaks at +0.76 V (onset, vs Ag/Ag^+). The good reversibility of its voltammograms implies that its oxidized species is electrochemically stable.

Table 3-4. Physicochemical properties of [6]phenacenes **6a**−**6d**.

[6]phenacenes	E_{onset} (V)[a]	E_{HOMO} (eV)[b]	E_{LUMO} (eV)[c]	E_g^{opt}/λ_{edge} [(eV)[d]/nm]	E_{HOMO} (eV)[e]	E_{LUMO} (eV)[e]	E_g (eV)[e]
6a	+0.84	–5.76	–2.57	3.19/389	–5.41	–1.39	4.02
6b	+0.81	–5.73	–2.58	3.15/393	–5.39	–1.39	4.00
6c	+0.36	–5.29	–2.17	3.12/397	–5.02	–1.22	3.80
6d	+0.76	–5.68	–2.56	3.12/397	–5.36	–1.34	4.02

[a] Obtained from cyclic voltammograms in CH_2Cl_2. V vs Ag/Ag^+. [b] All the potentials were calibrated with the Fc/Fc^+ ($E^{1/2}$ = -0.12 V measured under identical conditions). Estimated with a following equation: E_{HOMO} (eV) = –4.92 – E_{onset}. [c] Calculated according to the formula $E_{LUMO} = E_{HOMO} + E_g^{opt}$. [d] Optical band gap calculated from λ_{edge}, $E_g^{opt} = 1240/\lambda_{edge}$. [e] Obtained from theoretical calculations.

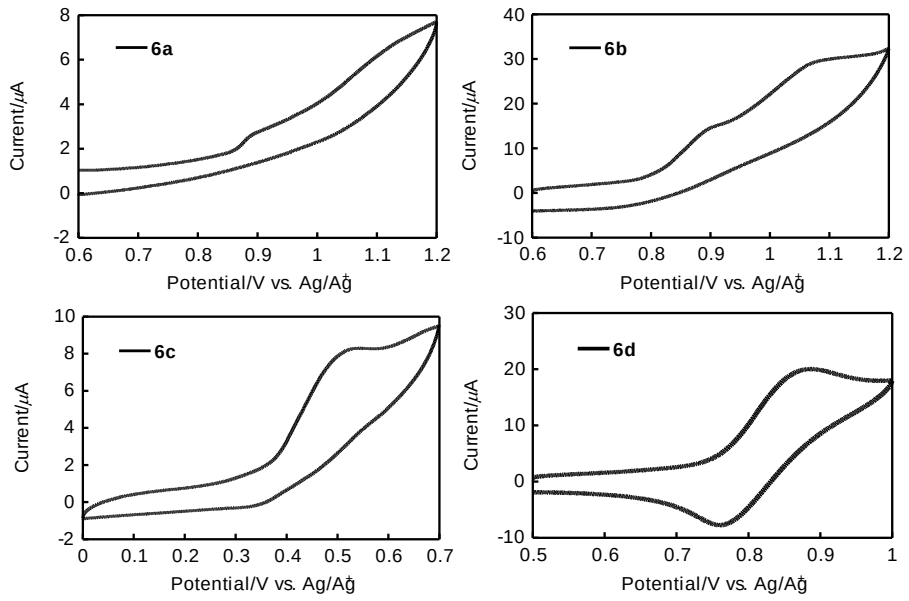

Figure 3-3. Cyclic voltammograms of compounds **6a**−**6d**.

[6]phenacenes **6b** and **6d** bearing the substituents in the 3-position have the similar HOMO energy levels and slightly narrow optical band gaps than that of **6a**. These results

indicate that a substituent effect of the [6]phenacene core in the 3-positions is rather small. In a sharp contrast, the methoxy-substituted [6]phenacene **6c** has almost the same optical energy gaps (~3.12 eV), but the higher HOMO energy level than that of **6a**.

3-3-4 Density functional theory (DFT) calculation

In order to understand the difference of the electronic structure, the molecular geometries of **6a**–**6d** were optimized using density functional theory (DFT) at the B3LYP/6-31G(d) level using Gaussian 09, Revision A. 02. The results are also listed in Table 3-4. The frontier molecular orbitals of the optimized molecules were also calculated (Figure 3-4). All the HOMOs and LUMOs of [6]phenacenes except **6c** are evenly delocalized over the entire molecular π-frameworks. The HOMO coefficient of [6]phenacene in the 3-position is relatively small, implying the small inductive effect of alkyl and TMS groups. On the other hand, the HOMO coefficient is strongly located in the 2,4-positions of a [6]phenacene core of **6c**. In fact, the HOMOs of **6c** partially delocalized to the peripheral groups, whilst the LUMOs were mainly localized on the core. These results are clearly consistent with the similarity/difference of the energy levels of the frontier orbitals as well as the molecular electronic structures among **6a**–**6d**, as evident from their physicochemical properties.

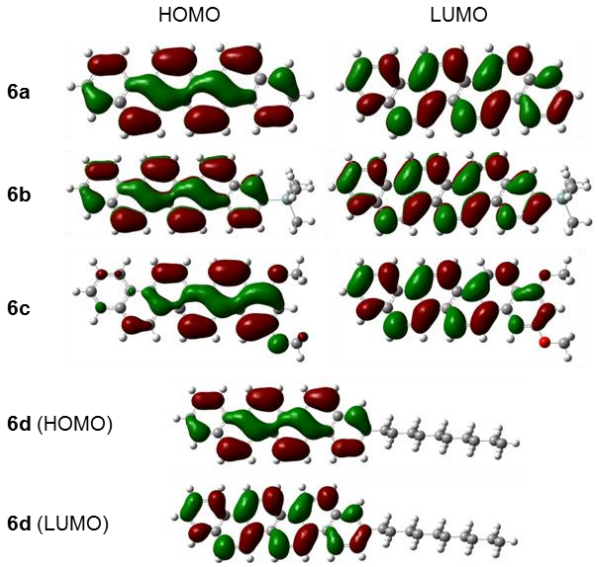

Figure 3-4. Wave functions for the HOMO and LUMO of **6a**–**6d**.

3-4 Summary

A new family of the unsymmetrically substituted [6]phenacenes were synthesized through Suzuki-Miyaura coupling and intramolecular double cyclization utilizing polyhalobenzene and two alkenylboronates. An introduction of methoxy and alkyl groups into the [6]phenacene framework increased the solubility of [6]phenacenes. This methodology addresses a straightforward route to [6]phenacenes, which are a promising material for practical high-performance organic field-effect transistors (OFETs). Physicochemical properties of four [6]phenacenes were evaluated by UV-vis and fluorescence spectra as well as cyclic voltammetry (CV). Obviously, these characteristic data indicated that an introduction of the substituents into a [6]phenacene framework can affect the physicochemical properties. In particular, a substitution effect of two methoxy groups at the 2,4-position was larger than that of alkyl and TMS groups at the 3-position. A further elucidation of physical properties, in particular, FET characteristics of the obtained [6]phenacenes is currently in progress.

3-5 Experimental Section

3-5-1 General

All the reactions were carried out under an Ar atmosphere using standard Schlenk techniques. Glassware was dried in an oven (130 °C) and heated under reduced pressure before use. Dehydrated toluene, dichloromethane, hexane, and diethyl ether were purchased from Kanto Chemicals Co., Ltd. For thin layer chromatography (TLC) analyses throughout this work, Merck precoated TLC plates (silica gel 60 GF254, 0.25 mm) were used. Silica gel column chromatography was carried out using Silica gel 60 N (spherical, neutral, 40-100 μm) from Kanto Chemicals Co., Ltd. NMR spectra (^{1}H, ^{13}C{^{1}H}) were recorded on Varian INOVA-600 (600 MHz) or Mercury-300 (300 MHz) spectrometers. Infrared spectra were recorded on a Shimadzu IRPrestige-21 spectrophotometer. GC analyses were performed on a Shimadzu GC-14A equipped with a flame ionization detector using Shimadzu Capillary Column (CBP1-M25-025) and Shimadzu C-R6A-Chromatopac integrator. Melting Points were measured on a Yanagimoto micromelting point apparatus and are uncorrected. The GC yields were determined using suitable hydrocarbon internal standards. GC/MS analyses were carried out on a SHIMADZU GC-17A equipped with a SHIMADZU QP-5050 GC-MS system. Elemental analyses were carried out with a Perkin-Elmer 2400 CHN elemental analyzer.

3-5-2 Experimental procedures

Synthesis of (*Z*)-naphthylethenylboronate 2.

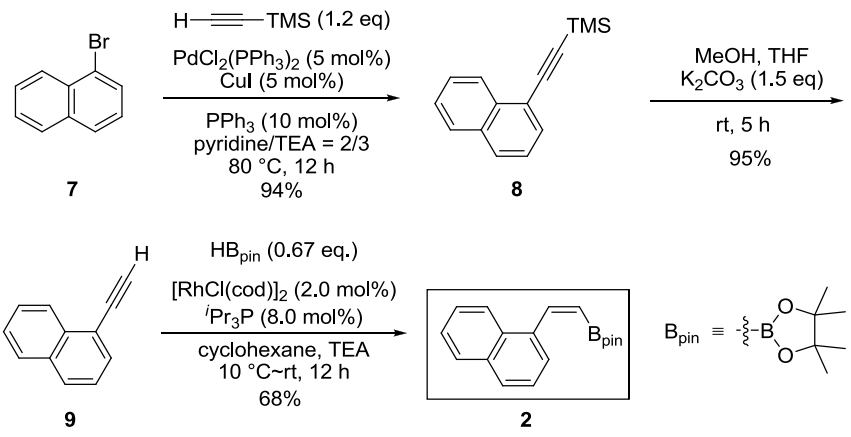

A 300 mL two-necked round bottom flask equipped with a magnetic stir bar was charged with **7** (10.35 g, 7.0 mL, 50.0 mmol), $PdCl_2(PPh_3)_2$ (1.75 g, 2.5 mmol, 5 mol %), CuI (0.48 g, 2.5 mmol, 5 mol %), PPh_3 (1.32 g, 5.0 mmol, 10 mol %), triethylamine (TEA, 75 mL), pyridine (50 mL), and trimethylsilylacetylene (8.48 mL, 60.0 mmol, 1.2 eq) under an argon atmosphere. After being stirred for 12 h at 80 °C, the reaction mixture was filtrated and washed with diethyl ether. The solvent was removed under reduced pressure and the crude product was purified by bulb to bulb distillation (150 °C/1.4 Torr) to obtain desired product **8**[13] as white crystals (10.55 g, 94%).

^{1}H NMR ($CDCl_3$, 300 MHz, rt) δ 0.36 (s, 12H), 7.42 (t, J = 7.6 Hz, 1H), 7.52-7.60 (m, 2H), 7.72 (d, J = 6.0 Hz, 1H), 7.84 (t, J = 7.2 Hz, 2H), 8.36 (d, J = 8.4 Hz, 1H).

To a solution of **8** (10.55 g, 47.0 mmol) in THF (90 mL) and MeOH (45 mL) was added K_2CO_3 (9.74 g, 70.5 mmol) and H_2O (4.0 mL). The solution was stirred at room temperature for 5 h before pouring the solution into saturated aq. NH_4Cl (50 mL). The mixture was extracted with diethyl ether and organic layer was washed with 5% aq. NH_4Cl and brine, dried with $MgSO_4$, and the solvent was removed in vacuum. This crude product was purified via Florisil to afford **9**[14] (6.80 g, 95%) as a colorless liquid.

^{1}H NMR ($CDCl_3$, 300 MHz, rt): δ 3.50 (s, 1H), 7.44 (t, J = 8.1 Hz, 1H), 7.53-7.56 (m, 1H), 7.61 (t, J = 4.8 Hz, 1H), 7.76 (d, J = 6.6 Hz, 1H), 7.87 (d, J = 8.4 Hz, 2H), 8.39 (d, J = 8.4 Hz, 1H).

A 100 mL two-necked round bottom flask equipped with a magnetic stir bar was charged with $[RhCl(cod)]_2$ (0.16 g, 0.32 mmol, 2 mol %) and then flushed with argon. Cyclohexane (40 mL), ^{i}Pr$_3$P (0.24 mL, 1.28 mmol, 8 mol %), Et_3N (15 mL), and HB_{pin} (2.04g, 2.3 mL, 16.0 mmol, 1 eq) were successively added. After being stirred at 10 °C for 30 min, **9** (3.64 g, 24.0 mmol, 1.5 eq) was added in one-portion and the mixture was stirred at 10-15 °C for 12 h before quenching by MeOH. Filtration with Celite and evaporation under vacuum afforded brown oil, which was purified by bulb to bulb distillation (145 °C/1.1 Torr) to obtain product **2** as colorless viscous liquid (3.1 g, 68%).

FT-IR (neat, cm^{-1}): 2978 (s), 1612 (s), 1422 (m), 1329 (m), 1258 (s), 1143 (s), 966 (w), 851 (w), 783 (m).

^1H NMR ($CDCl_3$, 600 MHz, rt) δ 1.12 (s, 12H), 5.90 (d, J = 14.0 Hz, 1H), 7.42 (t, J = 7.8 Hz, 1H), 7.48-7.51 (m, 2H), 7.56 (d, J = 7.2 Hz, 1H), 7.80 (d, J = 8.4 Hz, 1H), 7.85-7.90 (m, 2H), 8.05 (d, J = 8.4 Hz, 1H).

$^{13}C\{^1H\}$ NMR ($CDCl_3$, 150 MHz, rt) δ 24.6, 83.2, 124.6, 125.0, 125.6, 125.9, 126.4, 128.2, 128.3, 131.5, 133.3, 136.3, 146.2. The carbon signal adjacent to B was not observed due to low intensity.

MS (EI, m/z (relative intensity)): 280 (M^+, 39), 180 (27), 179 (43), 164 (39), 163 (36), 153 (43), 152 (100), 84 (94).

Anal. Calcd for $C_{18}H_{21}BO_2$: C, 77.17; H, 7.55%. Found: C, 77.18; H, 7.76%.

Synthesis of 3 by Suzuki-Miyaura cross-coupling reaction of 1 with 2.

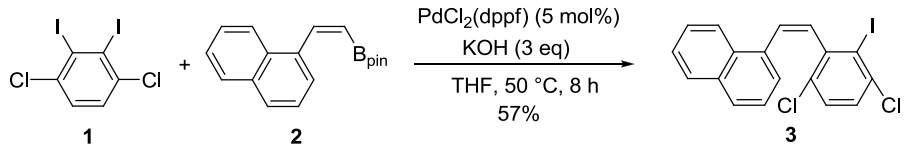

To a 50 mL Schlenk tube equipped with a magnetic stirrer bar, were successively added 1,4-dichloro-2,3-diiodobenzene (**1**, 0.40 g, 1.0 mmol), (*Z*)-alkenylboronate **2** (0.35 g, 1.2 mmol), $PdCl_2$(dppf) (36.6 mg, 0.05 mmol, 5 mol %), THF (20 mL) and KOH (3M, 1 mL, 3 mmol). After being stirred at 50 °C for 12 h, the reaction mixture was quenched with 1 M HCl, and extracted with diethyl ether (3 × 10 mL). The combined ethereal layers were washed with brine and dried over anhydrous magnesium sulfate. Filtration and evaporation afforded brown oil, which was purified by chromatography on silica gel (hexanes as eluent) to obtain product **3** as white solid (0.24 g, 57% yield).

Mp: 110-112°C.

FT-IR (neat, cm^{-1}): 1503 (w), 1423 (s), 1341 (m), 1157 (s), 814 (m), 791 (s), 766 (s), 738 (w).

^{1}H NMR ($CDCl_3$, 600 MHz, rt) δ 6.64 (d, J = 11.4 Hz, 1H), 6.97 (d, J = 7.8 Hz, 1H), 7.18 (t, J = 8.4 Hz, 2H), 7.24 (d, J = 8.4 Hz, 1H), 7.37 (d, J = 11.4 Hz, 1H), 7.48-7.55 (m, 2H), 7.71 (d, J = 7.8 Hz, 1H), 7.83 (d, J = 9.0 Hz), 8.14 (d, J = 9.0 Hz, 1H).

^{13}C{^{1}H} NMR ($CDCl_3$, 150 MHz, rt) δ 105.4, 124.5, 125.3, 125.8, 126.0, 126.3, 128.1, 128.4, 128.7, 130.3, 131.2, 131.5, 131.8, 132.7, 133.4, 133.7, 137.9, 143.3.

MS (EI, m/z (relative intensity)): 426 (M^+, 36), 424 (85), 298 (25), 264 (24), 263 (56), 226 (100), 224 (39), 113 (69).

Anal. Calcd for $C_{18}H_{11}Cl_2I$: C, 50.86; H, 2.61%. Found: C, 51.01; H, 2.42%.

A general procedure for the synthesis of 5 by the reaction of 3 with alkenylboronates 4.

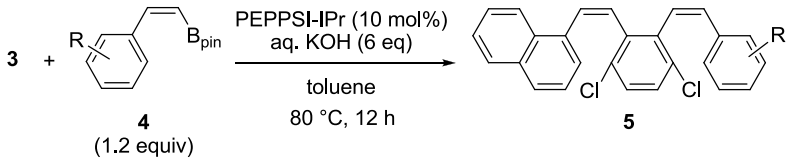

To a 20 mL of Schlenk tube equipped with a magnetic stirrer bar, were successively added **3** (85 mg, 0.2 mmol), (*Z*)-alkenylboranate **4** (0.24 mmol, 1.2 eq), PEPPSI-IPr (13.6 mg, 0.02 mmol, 10 mol %), toluene (2 mL), and KOH (3 M, 0.4 mL, 1.2 mmol, 6 eq). After being stirred at 80 °C for 12 h, the reaction mixture was quenched with 1 M HCl, and extracted with diethyl ether (3 × 10 mL). The combined ethereal layers were washed with brine and dried over anhydrous magnesium sulfate. Filtration and evaporation afforded crude product, which was purified by chromatography on silica gel (hexanes as the eluent) to afford compound **5**.

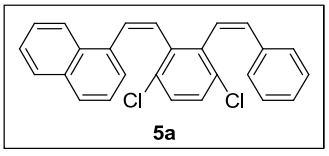

Colorless oil (50.5 mg, 63% yield).

FT-IR (neat, cm^{-1}): 1493 (w), 1431 (m), 1130 (m), 964 (w), 903 (w), 808 (s), 795 (s), 775 (s), 694 (m).

^{1}H NMR ($CDCl_3$, 600 MHz, rt) δ 5.62 (br.s, 1H), 6.23 (d, J = 12.6 Hz, 1H), 6.32 (d, J = 12.0 Hz, 1H), 6.86-6.89 (m, 3H), 7.13-7.17 (m, 5H), 7.19-7.25 (m, 2H), 7.48 (t, J = 7.2 Hz, 1H), 7.54 (d, J = 7.2 Hz, 1H), 7.64 (d, J = 7.8 Hz, 1H), 7.78 (d, J = 7.8 Hz, 1H), 8.00 (d, J = 8.4 Hz, 1H).

$^{13}C\{^{1}H\}$ NMR ($CDCl_3$, 150 MHz, rt) δ 124.3, 125.2, 125.4, 125.6, 125.7, 125.9, 126.0, 127.4, 127.4, 128.0, 128.0, 128.2, 128.5, 128.6, 128.9, 128.9, 131.2, 131.9, 132.1, 132.6, 133.4, 133.5, 133.9, 136.7, 136.9, 137.2.

MS (EI, m/z (relative intensity)): 401 (M^+, 11), 400 (35), 252 (20), 239 (26), 217 (87), 141 (100), 91(30).

HRMS (FAB) Calcd for $C_{26}H_{18}Cl_2$: 400.0782. Found: 400.0777.

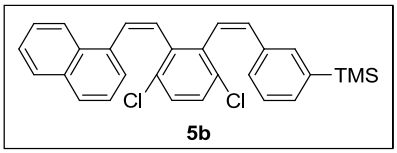

5b

Pale yellow oil (72.2 mg, 76% yield).

FT-IR (neat, cm^{-1}): 2955 (s), 1433 (m), 1400 (w), 1250 (s), 1130 (s), 916 (m), 860 (s), 837 (s), 802 (s), 773 (s), 691 (w).

^{1}H NMR ($CDCl_3$, 600 MHz, rt) δ 0.14 (s, 9H), 5.62 (d, J = 11.7 Hz, 1H), 6.26 (d, J = 12.3 Hz, 1H), 6.31 (s, 1H), 6.86 (d, J = 7.2 Hz, 1H), 6.97 (d, J = 7.2 Hz, 1H), 7.03 (s, 1H), 7.12-7.24 (m, 4H), 7.32-7.38 (m, 2H), 7.48-7.59 (m, 2H), 7.65 (d, J = 8.4 Hz, 1H), 7.81 (d, J = 8.1 Hz, 1H), 8.02 (d, J = 8.1 Hz, 1H).

$^{13}C\{^{1}H\}$ NMR ($CDCl_3$, 150 MHz, rt) δ –1.2, 124.5, 125.4, 125.7, 125.9, 126.1, 126.2, 127.6, 127.9, 128.1, 128.7, 129.1, 129.1, 131.1, 131.4, 132.1, 132.4, 132.5, 132.9, 133.0, 133.7, 134.1, 136.1, 136.7, 137.0, 137.6, 140.3.

MS (EI, m/z (relative intensity)): 473 (M^+, 16), 401 (20), 239 (31), 208 (28), 207 (46), 141 (51), 73 (100).

HRMS (FAB) Calcd for $C_{29}H_{26}Cl_2Si$: 472.1181. Found: 472.1158.

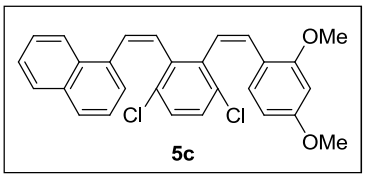

5c

Pale yellow oil (77.4 mg, 83% yield).

FT-IR (neat, cm^{-1}): 2957 (w), 1609 (s), 1574 (m), 1503 (s), 1460 (m), 1292 (s), 1159 (m), 1125 (s), 912 (s), 808 (m), 754 (w).

^1H NMR ($CDCl_3$, 600 MHz, rt) δ 3.76 (s, 3H), 3.84 (s, 3H), 5.65 (br.s, 1H), 6.17 (d, J = 8.4 Hz, 1H), 6.22 (d, J = 13.8 Hz, 1H), 6.39 (s, 1H), 6.52 (d, J = 12.0 Hz, 2H), 6.82 (s, 1H), 7.01-7.15 (m, 2H), 7.18 (s, 2H), 7.47-7.54 (m, 2H), 7.65 (d, J = 7.8 Hz, 1H), 7.79 (d, J = 8.4 Hz, 1H), 8.10 (d, J = 8.4 Hz, 1H).

$^{13}C\{^1H\}$ NMR ($CDCl_3$, 150 MHz, rt) δ 55.0, 55.2, 97.9, 103.9, 118.7, 123.4, 124.5, 124.9, 125.4, 125.5, 125.7, 127.1, 127.5, 128.1, 128.2, 128.4, 128.9, 130.4, 131.0, 132.0, 132.1, 133.2, 133.9, 136.7, 136.9, 137.6, 157.7, 160.1.

HRMS (FAB) Calcd for $C_{28}H_{22}Cl_2O_2$: 460.0997. Found: 460.1017.

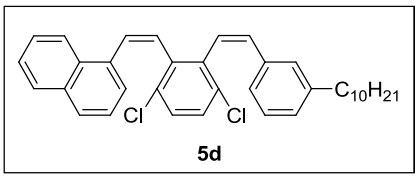

5d

Pale yellow oil (74.7 mg, 69% yield).

FT-IR (neat, cm^{-1}): 2953 (m), 2924 (s), 2853 (m), 1464 (w), 1435 (w), 1130 (w), 804 (m), 777 (m).

^1H NMR ($CDCl_3$, 600 MHz, rt) δ 0.88 (t, J = 7.8 Hz, 5H), 1.26-1.33 (m, 11H), 1.42 (t, J = 7.2 Hz, 2H), 2.43 (t, J = 7.8 Hz, 2H), 2.52 (t, J = 8.4 Hz, 1H), 5.60 (br.s, 1H), 6.22 (d, J = 12.0 Hz, 1H), 6.28 (d, J = 11.4 Hz, 1H), 6.87 (d, J = 6.0 Hz, 1H), 6.97 (d, J = 7.2 Hz, 1H), 7.07 (t, J = 7.2 Hz, 1H), 7.11-7.15 (m, 2H), 7.17-7.25 (m, 4H), 7.48 (t, J = 7.2 Hz, 1H),

7.54 (t, J = 7.2 Hz, 1H), 7.64 (d, J = 7.8 Hz, 1H), 7.78 (t, J = 7.8 Hz, 1H), 8.00 (d, J = 8.4 Hz, 1H).

$^{13}C\{^{1}H\}$ NMR ($CDCl_3$, 150 MHz, rt) δ 14.1, 22.7, 29.2, 29.3, 29.5, 29.7, 31.2, 31.5, 31.9, 35.7, 123.5, 124.3, 125.1, 125.2, 125.7, 126.0, 127.7, 128.0, 128.2, 128.8, 129.2, 131.1, 131.4, 132.0, 132.1, 132.6, 133.5, 133.5, 134.0, 136.2, 136.6, 136.8, 136.9, 137.4, 142.6, 143.0.

Anal. Calcd for $C_{36}H_{38}Cl_2$: C, 79.84; H, 7.07%. Found: C, 79.50; H, 7.07%.

A general procedure for synthesis of [6]phenacenes 6a–6d.

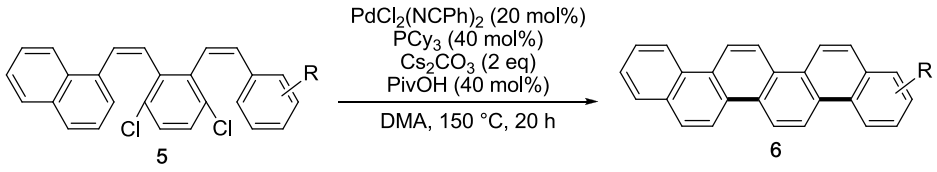

A 20 mL Schlenk tube equipped with a magnetic stirring bar was charged with PCy_3 (18.2 mg, 0.065 mmol, 40 mol %), $PdCl_2(NCPh)_2$ (12.3 mg, 0.032 mmol, 20 mol %), and DMA (1 mL) under an argon atmosphere. After being stirred for 10 min, Cs_2CO_3 (104.2 mg, 0.32 mmol, 2 eq), PivOH (6.67 mg, 0.065 mmol, 40 mol %), substrate **5** (0.16 mmol, 1 eq), and additional 2 mL of DMA were added into reaction mixture at room temperature. The tube was put into a preheated hot box at 150 °C for 20 h. The reaction mixture was cooled to room temperature, quenched with 1 M HCl (3 mL), and filtered directly with water to remove DMA. The residue was washed very carefully with a little amount of $CHCl_3$, the insoluble residue was purified by Soxhlet extractor to afford desired product **6**.

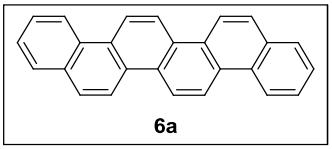

[6]Phenacene (6a).[6]

White solid (18.4 mg, 35% yield). Mp > 300 °C (Mp 467 ºC).[15]

^{1}H NMR (600 MHz, CDCl3,) δ 9.05 (d, 2H, J = 9.1 Hz, $H_{8,16}$), 9.00 (d, 2H, J = 9.1 Hz, $H_{7,15}$), 8.89 (d, 2H, J = 7.6 Hz, $H_{1,9}$), 8.88 (d, 2H, J = 9.1 Hz, $H_{6,14}$), 8.08 (d, 2H, J = 9.1 Hz,

$H_{5,13}$), 8.04 (d, 2H, J = 7.6 Hz, $H_{4,12}$), 7.77 (t, 2H, J = 7.6 Hz, $H_{2,10}$), 7.69 (t, 2H, J = 7.6 Hz, $H_{3,11}$).

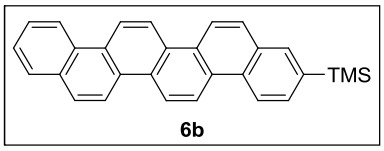

6b

3-Trimethylsilyl-[6]phenacene (6b).

Colorless plates (35 mg, 55% yield). Mp > 300 °C.

FT-IR (neat, cm^{-1}): 2951 (w), 1277 (m), 1246 (m), 1111 (w), 1047 (w), 910 (w), 808 (s), 762 (s), 745 (m);

^1H NMR ($CDCl_3$, 600 MHz, rt) δ 0.07 (s, 9H), 7.40 (t, J = 7.2 Hz, 1H), 7.48 (t, J = 7.2 Hz, 2H), 7.53 (t, J = 9.0 Hz, 2H), 7.68 (d, J = 7.2 Hz, 1H), 7.77 (q, J = 19.2 Hz, 1H), 7.85 (d, J = 7.8 Hz, 1H), 7.88 (s, 1H), 8.04 (s, 1H), 8.08 (d, J = 8.4 Hz, 1H), 8.82 (t, J = 9.0 Hz, 2H), 9.02 (d, J = 19.2 Hz, 2H).

$^{13}C\{^1H\}$ NMR ($CDCl_3$, 150 MHz, rt) spectrum was not obtained due to the extreme insolubility.

HRMS (EI) Calcd for $C_{29}H_{24}Si$: 400.1647. Found: 400.1637.

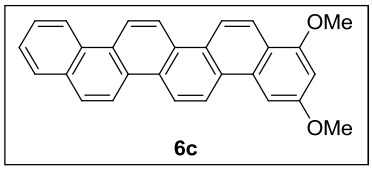

6c

2,4-Dimethoxy-[6]phenacene (6c).

Colorless plates (32 mg, 51% yield). Mp > 300 °C.

FT-IR (neat, cm^{-1}): 2358 (w), 1610 (s), 1456 (m), 1406 (m), 1278 (m), 1203 (m), 1144 (s), 1049 (s), 934 (w), 810 (s), 752 (m).

^1H NMR ($CDCl_3$, 600 MHz, rt) δ 4.08 (s, 3H), 4.10 (s, 3H), 6.73 (s, 1H), 7.68 (t, J = 7.2 Hz, 1H), 7.76 (t, J = 7.2 Hz, 2H), 8.03 (d, J = 7.8 Hz, 1H), 8.07 (d, J = 9.0 Hz, 1H), 8.43 (d, J = 9.6 Hz, 1H), 8.72 (d, J = 9.6 Hz, 1H), 8.84-8.89 (m, 3H), 8.96 (q, J = 9.0 Hz, 2H), 9.04 (d, J = 9.0 Hz, 1H).

$^{13}C\{^{1}H\}$ NMR ($CDCl_3$, 150 MHz, rt) δ 55.5, 55.8, 95.3, 97.8, 118.4, 119.1, 119.2, 121.2, 121.4, 121.6, 121.7, 122.3, 122.4, 123.2, 126.6, 126.8, 127.4, 127.5, 128.5, 128.5, 128.5, 129.0, 129.5, 130.5, 132.0, 132.4, 157.2, 159.2.

HRMS (FAB) Calcd for $C_{28}H_{20}O_2$: 388.1463. Found: 388.1449.

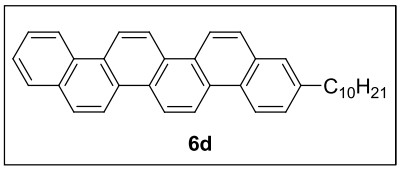

6d

3-Decyl-[6]phenacene (6d).

Colorless plates (33 mg, 44% yield). Mp > 300 °C.

FT-IR (neat, cm^{-1}): 2920 (m), 2851 (m), 2360 (w), 1468 (w), 1277 (w), 1032 (w), 810 (s), 756 (m), 743 (m).

^{1}H NMR ($CDCl_3$, 600 MHz, rt) δ 0.87 (t, J = 7.8 Hz, 4H), 1.25-1.35 (m, 11H), 1.43 (q, J = 15.0 Hz, 2H), 2.00 (t, J = 7.8 Hz, 2H), 3.54 (t, J = 7.8 Hz, 2H), 7.56-7.61 (m, 2H), 7.67 (t, J = 7.2 Hz, 1H), 7.75 (t, J = 7.2 Hz, 1H), 7.87 (d, J = 6.6 Hz, 1H), 8.02 (t, J = 8.4 Hz, 2H), 8.06 (d, J = 9.0 Hz, 1H), 8.82 (d, J = 9.0 Hz, 1H), 8.86-8.88 (m, 2H), 8.91 (d, J = 9.6 Hz, 1H), 8.96 (dd, J = 11.4, 9.6 Hz, 2H), 9.01 (d, J = 9.6 Hz, 1H).

$^{13}C\{^{1}H\}$ NMR ($CDCl_3$, 150 MHz, rt) δ 14.3, 22.9, 29.6, 29.7, 29.9, 29.9, 30.2, 31.5, 32.2, 38.5, 120.6, 121.5, 121.7, 121.9, 122.6, 123.4, 126.3, 126.5, 126.8, 127.0, 127.5, 127.7, 128.4, 128.5, 128.6, 128.8, 129.0, 129.1, 129.3, 130.1, 130.4, 130.7, 130.7, 132.3, 133.9, 140.6.

HRMS (FAB) Calcd for $C_{36}H_{36}$: 468.2817. Found: 468.2844.

3-5-3 Copies of ^{1}H and $^{13}C\{^{1}H\}$ NMR charts for the new compounds

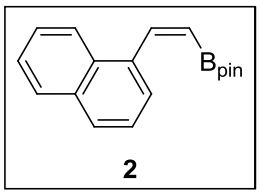

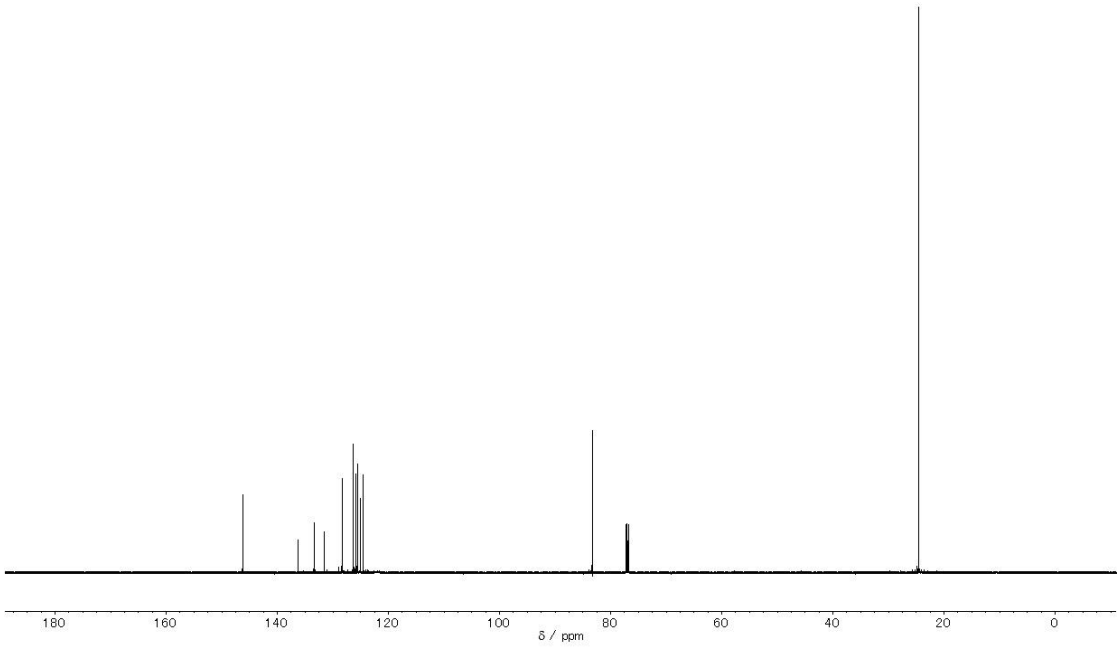

^{1}H (600 MHz) and $^{13}C\{^{1}H\}$ NMR (150 MHz) spectra of **2** (rt, $CDCl_3$).

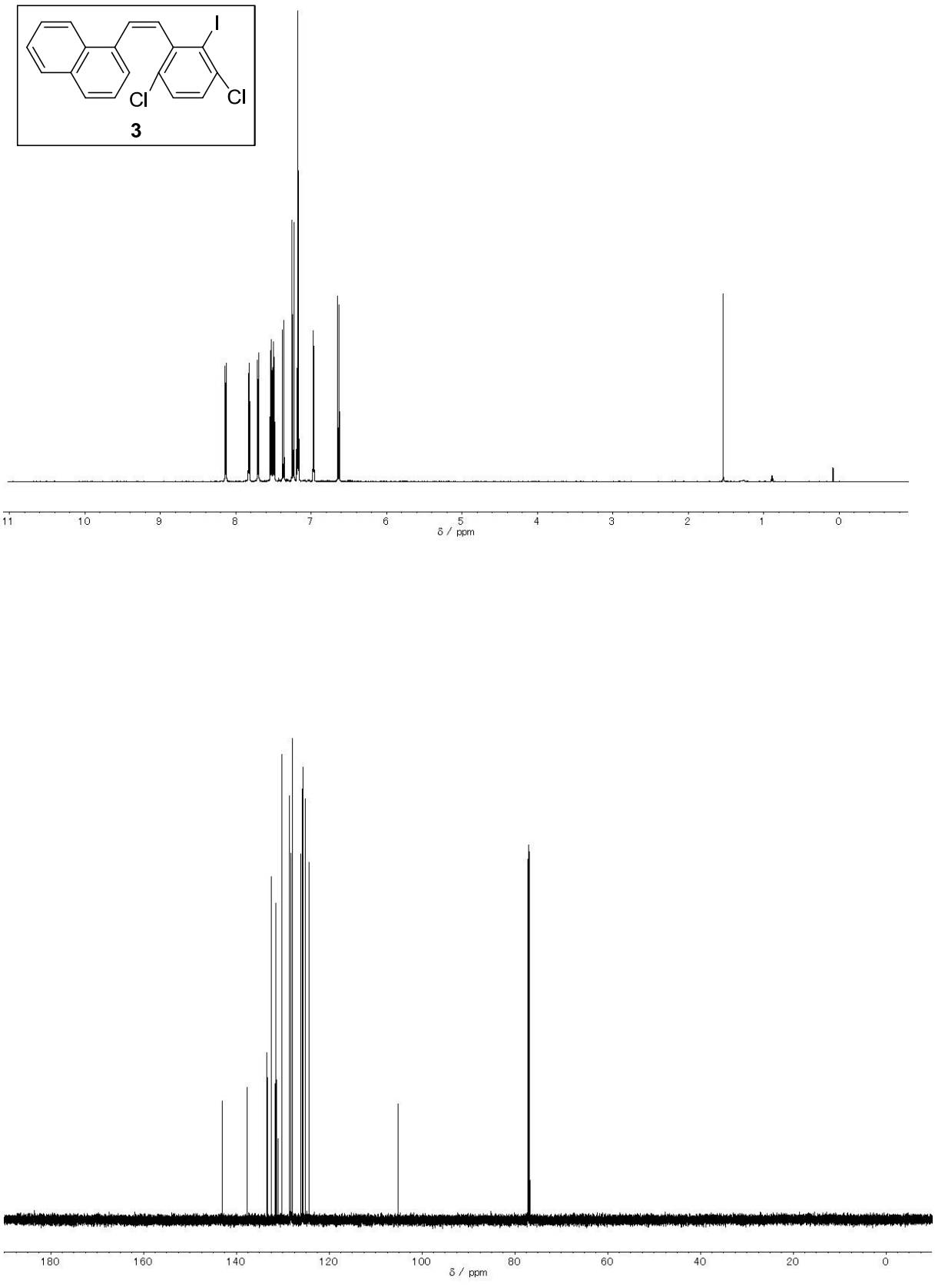

^{1}H (600 MHz) and $^{13}C\{^{1}H\}$ NMR (150 MHz) spectra of **3** (rt, $CDCl_3$).

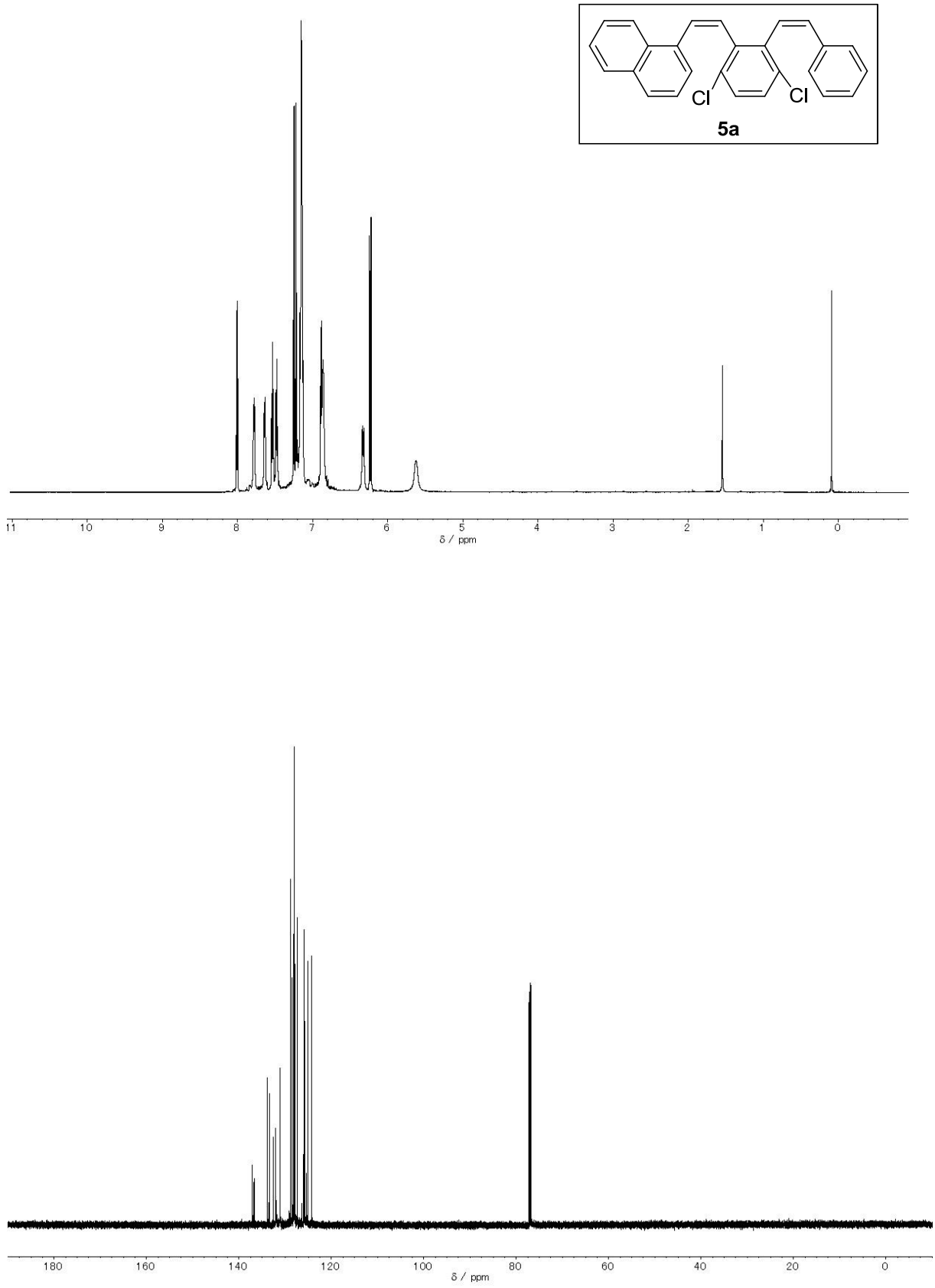

^{1}H (600 MHz) and $^{13}C\{^{1}H\}$ NMR (150 MHz) spectra of **5a** (rt, $CDCl_3$).

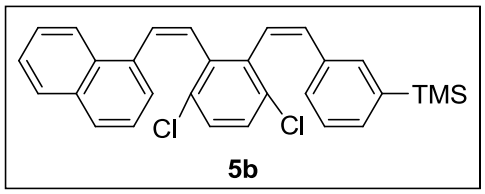

5b

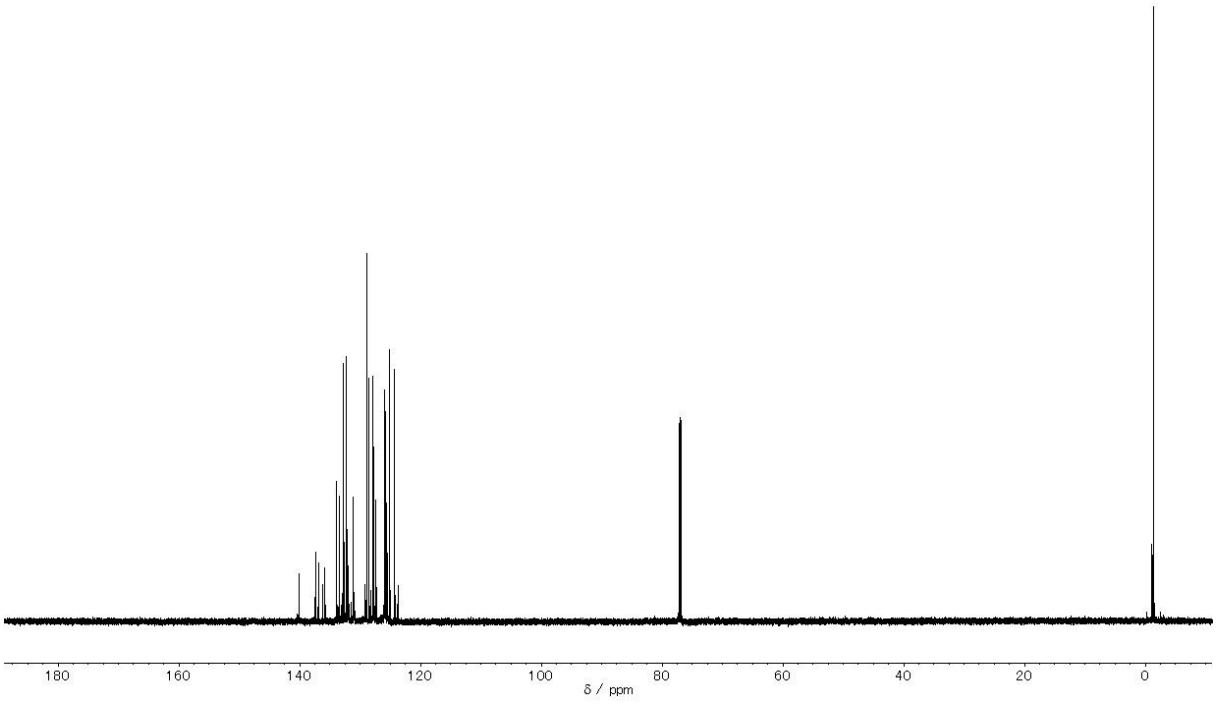

^{1}H (600 MHz) and $^{13}C\{^{1}H\}$ NMR (150 MHz) spectra of **5b** (rt, $CDCl_3$).

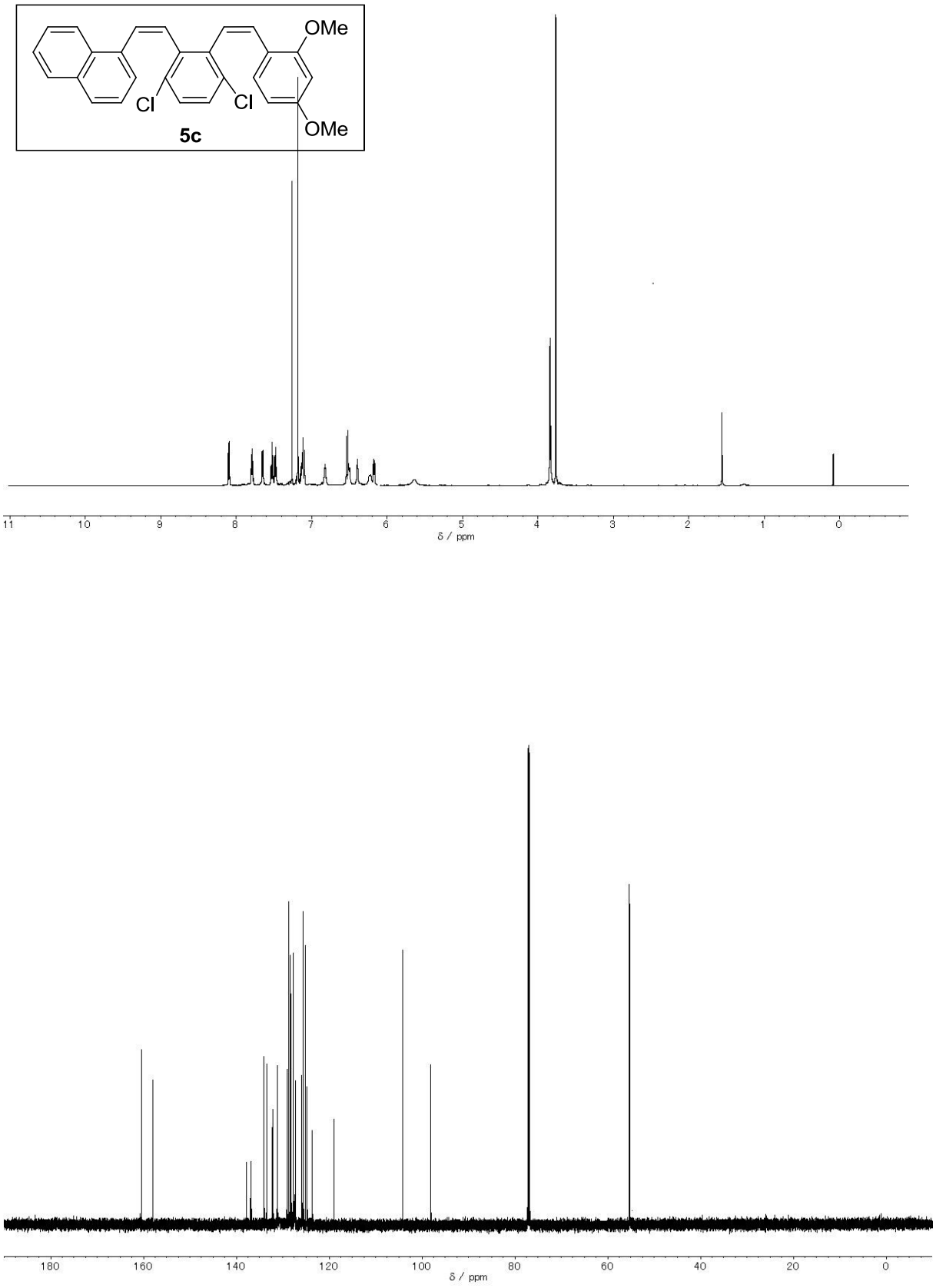

^{1}H (600 MHz) and $^{13}C\{^{1}H\}$ NMR (150 MHz) spectra of **5c** (rt, $CDCl_3$).

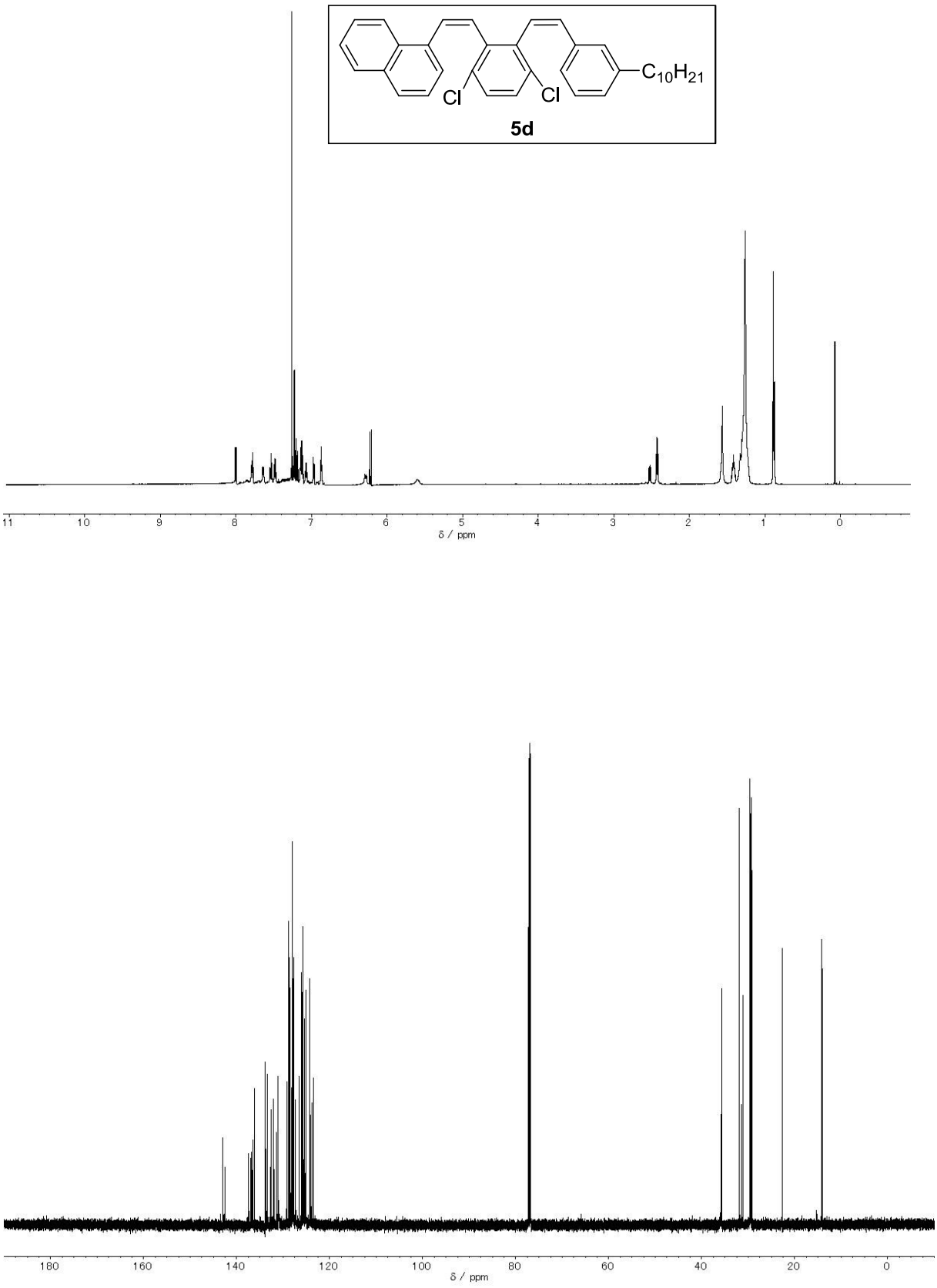

^{1}H (600 MHz) and $^{13}C\{^{1}H\}$ NMR (150 MHz) spectra of **5d** (rt, $CDCl_3$).

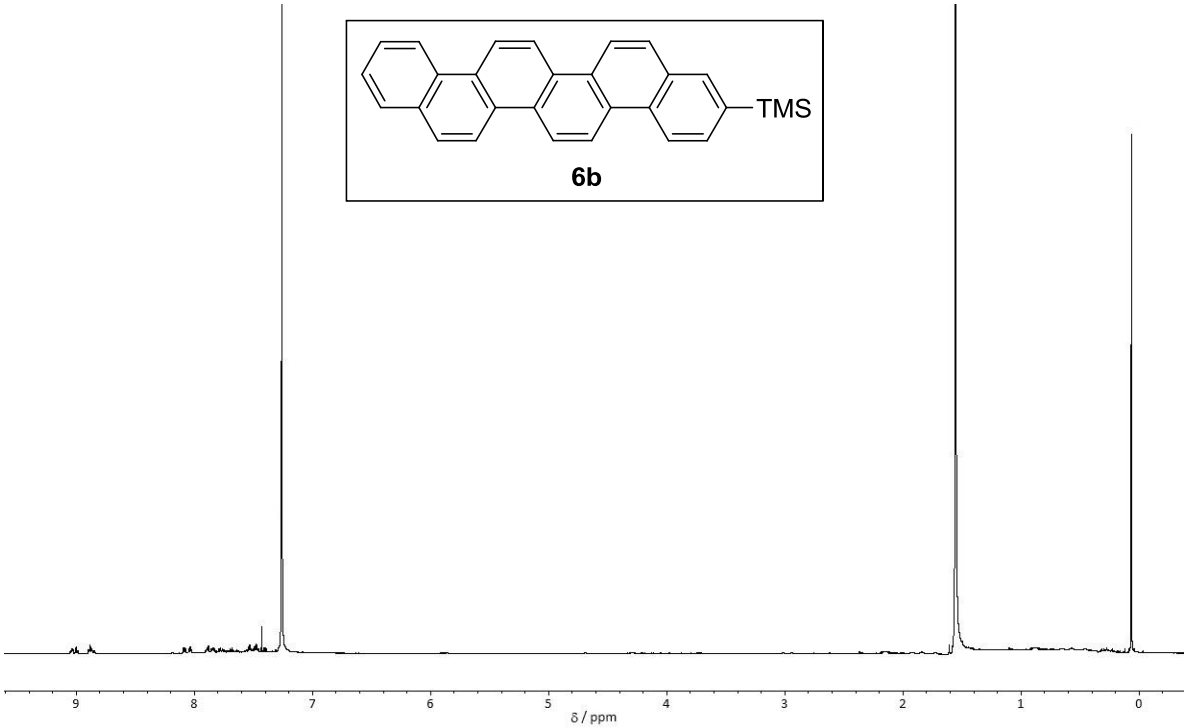

^{1}H NMR (600 MHz) spectrum of **6b** (rt, $CDCl_3$).

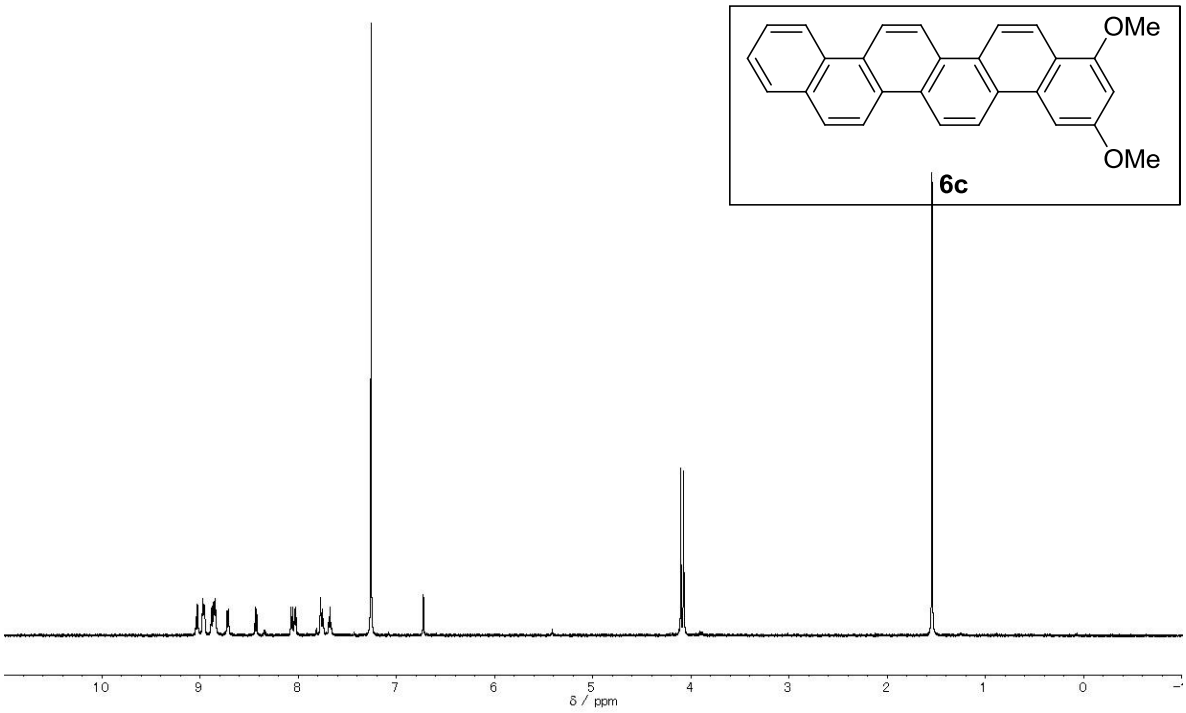

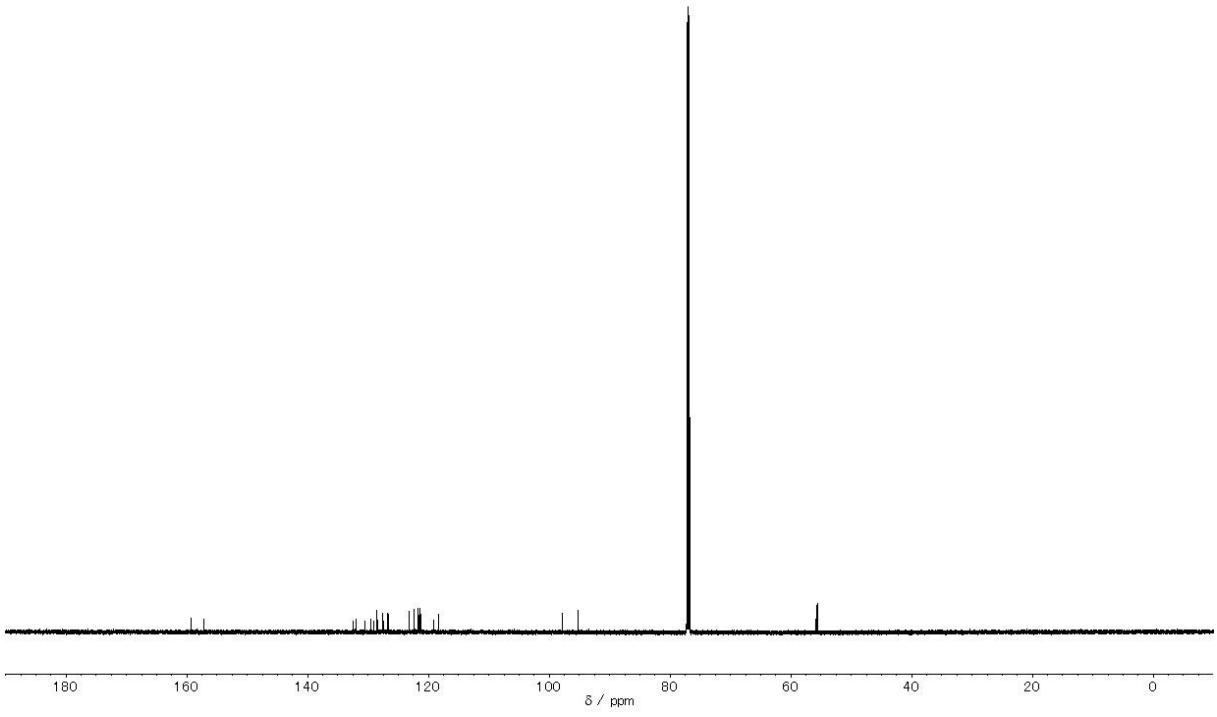

^{1}H (600 MHz) and $^{13}C\{^{1}H\}$ NMR (150 MHz) spectra of **6c** (rt, $CDCl_3$).

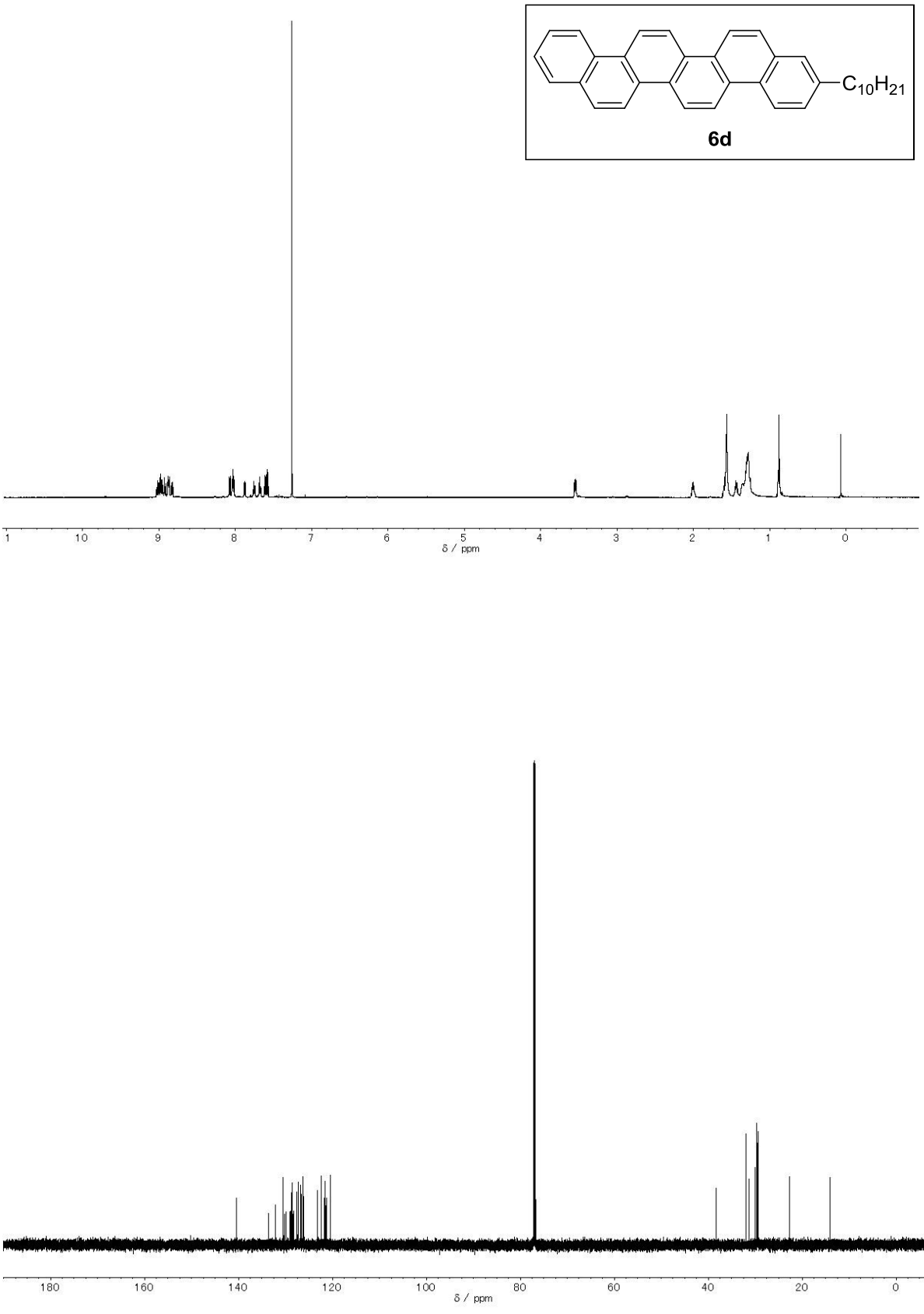

^{1}H (600 MHz) and $^{13}C\{^{1}H\}$ NMR (150 MHz) spectra of **6d** (rt, $CDCl_3$).

3-6 References and Notes

[1] Mallory, F. B.; Butler, K. E.; Evans, A. C.; Mallory, C. W. *Tetrahedron Lett.* **1996**, *37*, 7173.

[2] (a) Okamoto, H.; Kawasaki, N.; Kaji, Y.; Kubozono, Y.; Fujiwara, A.; Yamaji, M. *J. Am. Chem. Soc.* **2008**, *130*, 10470. (b) Kawasaki, N.; Kubozono, Y.; Okamoto, H.; Fujiwara, A.; Yamaji, M. *Appl. Phys. Lett.* **2009**, *94*, 043310. (c) Kaji, Y.; Mitsuhashi, R.; Lee, X.; Okamoto, H.; Kambe, T.; Ikeda, N.; Fujiwara, A.; Yamaji, M.; Omote, K.; Kubozono, Y. *Org. Electron.* **2009**, *10*, 432. (d) Kaji, Y.; Kawasaki, N.; Lee, X.; Okamoto, H.; Sugawara, Y.; Oikawa, S.; Ito, A.; Okazaki, H.; Yokoya, T.; Fujiwara, A.; Kubozono, Y. *Appl. Phys. Lett.* **2009**, *95*, 183302. (e) Kawasaki, N.; Kalb, W. L.; Mathis, T.; Kaji, Y.; Mitsuhashi, R.; Okamoto, H.; Sugawara, Y.; Fujiwara, A.; Kubozono, Y.; Batlogg, B. *Appl. Phys. Lett.* **2010**, *96*, 113305. (f) Kaji, Y.; Ogawa, K.; Eguchi, R.; Goto, H.; Sugawara, Y.; Kambe, T.; Akaike, K.; Gohda, S.; Fujiwara, A.; Kubozono, Y. *Org. Electron.* **2011**, *12*, 2076.

[3] (a) Komura, N.; Goto, H.; He, X.; Mitamura, H.; Eguchi, R.; Kaji, Y.; Okamoto, H.; Sugawara, Y.; Gohda, S.; Sato, K.; Kubozono. Y. *Appl. Phys. Lett.* **2012**, *101*, 083301. (b) He, X.; Eguchi, R.; Goto, H.; Uesugi, E.; Hamao, S.; Takabayashi, Y.; Kubozono. Y. *Org. Electron.* **2013**, *14*, 1673.

[4] (a) Mallory, F. B.; Butler, K. E.; Evans, A. C.; Brondyke, E. J.; Mallory, C. W.; Yang, C.; Ellenstein, A. *J. Am. Chem. Soc.* **1997**, *119*, 2119. (b) Mallory, F. B.; Butler, K. E.; Bérubé, A.; Luzik, Jr., E. D.; Mallory, C. W. E.; Brondyke, J.; Hiremath, R.; Ngo, P.; Carroll. P. J. *Tetrahedron* **2001**, *57*, 3715. (c) Mallory, F. B.; Mallory, C. W.; Regan, C. K.; Aspden, R. J.; Ricks, A. B.; Racowski, J. M.; Nash, A. I.; Gibbons, A. V.; Carroll, P. J.; Bohen. J. M. *J. Org. Chem.* **2013**, *78*, 2040.

[5] Harvey, R. G.; Pataki, J.; Cortez, C.; Raddo, P. D.; Yang. C. *J. Org. Chem.* **1991**, *56*, 1210.

[6] Okamoto, H.; Yamaji, M.; Gohda, S.; Sato, K.; Sugino, H.; Satake. K. *Res. Chem. Intermed.* **2013**, *39*, 147.

[7] Chang, N.-H.; Chen, X.-C.; Nonobe, H.; Okuda, Y.; Mori, H.; Nakajima, K.; Nishihara, Y. *Org. Lett.* **2013**, *15*, 3558.

[8] See Chapter 2.

[9] With $PdCl_2$(dppf) the reaction of **3** with **4a** resulted in a lower yield of **5a** (55%).

[10] (a) Kamikawa, K.; Takemoto, I.; Takemoto, S.; Matsuzaka, H. *J. Org. Chem.* **2007**, *72*, 7406. (b) Umeda, R.; Miyake, S.; Nishiyama, Y. *Chem. Lett.* **2012**, *41*, 215.

[11] Zhao, J.; Oniwa, K.; Asao, N.; Yamamoto, Y.; Jin, T. *J. Am. Chem. Soc.* **2013**, *135*, 10222.

[12] (a) Fery-Forgues, S.; Lavabre, D. *J. Chem. Educ.* **1999**, *76*, 1260. (b) Suzuki, K.; Kobayashi, A.; Kaneko, S.; Takehira, K.; Yoshihara, T.; Ishida, H.; Shiina, Y.; Oishi, S.; Tobita, S. *Phys. Chem. Chem. Phys*. **2009**, *11*, 9850.

[13] Alonso, D. A.; Nájera, C.; Pacheco, M. C. *Adv. Synth. Catal*. **2003**, *345*, 1146.

[14] Feng, Y.-S.; Xie, C.-Q.; Qiao, W.-L.; Xu. H.-J. *Org. Lett*. **2013**, *15*, 936.

[15] Lang, K. F.; Buffleb, H.; Kalowy, J. *Chem. Ber.* **1964**, *97*, 494.

CHAPTER 4

Conclusion and Perspectives

4-1 Conclusion

In this Dissertation, the Author focused on the synthesis of fused polycyclic aromatic compounds, [n]phenacenes, which have attracted a great deal of attention as active layers in organic field-effect transistors (OFETs) because of their advantages in organic materials.

In Chapter 1, the Thesis firstly described an overview of OFETs and the application of [n]phenacenes to OFETs. Because of their importance in organic electronic devices, it is of great interest to develop methods of various [n]phenacenes derivatives. Based on previously reported synthetic methods, the Author proposed a more convenience, and reliable methodology to the synthesis of [n]phenacenes.

In Chapter 2, after exploration and optimization, a novel and versatile synthetic method for [5]phenacenes (picenes) was established using the Pd-catalyzed intramolecular double cyclization of the corresponding 2,3-bis[(1*Z*)-2-phenylethenyl]-1,4-dichlorobenzenes, which were readily prepared by Suzuki-Miyaura cross-coupling reactions of polyhalobenzenes with (*Z*)-arylethenylboronates. Through this methodology, the Author synthesized a series of picene derivatives bearing various functional groups, for instance, trimethylsilane, methoxy, ethyl, decyl as well as trifluoromethyl groups. X-ray diffraction analysis successfully clarified the structure of 3,10-dimethoxypicene and meanwhile confirmed a reliability of the synthetic method.

Physicochemical properties of the obtained picenes were modified by functionalization of the picene framework. All compounds are investigated by UV-vis and fluorescence spectroscopic measurements, CV, and DFT calculations. To the best of his knowledge, these picene derivatives are first occur in organic materials. A more precise elucidation of their physicochemical properties is now in progress.

In Chapter 3, the Author noticed the effect that the increased numbers of the benzene rings in [n]phenacene have potentials to improve the FET characteristics. For the further investigation, a new family of the unsymmetrically substituted [6]phenacenes were synthesized via sequential Suzuki-Miyaura coupling and intramolecular double cyclization

utilizing polyhalobenzene and two alkenylboronates. This methodology addresses a straightforward route to synthesis of [6]phenacenes. An introduction of a methoxy or alkyl group into the [6]phenacene framework increased the solubility of [6]phenacenes, thus implying the possibility to fabricate single crystals FET device in solution process.

Physicochemical properties of four [6]phenacenes were also evaluated by measurements of UV-vis and fluorescence spectra and cyclic voltammogram (CV) as well as DFT calculation. Similar to the [5]phenacene cases, optical and electrochemical data demonstrated that an introduction of substituents into the [6]phenacene framework affected their physical properties. In particular, a substitution effect of two methoxy groups in the 2,4-position is larger than that of alkyl and TMS groups in the 3-position. All investigation indicated that the substituted [6]phenacenes are potential materials for practical high-performance organic field-effect transistors (OFETs).

4-2 Perspectives

This Thesis established a versatile methodology to synthesis of [n]phenacenes. Therefore, this method would also be suitable for the synthesis of other picene analogues, for instance, heteroatom-containing picenes and unsymmetrical fused aromatic compounds (Figure 4-1).

On the other hand, the clear pictures of the effects of the structural variations by substituents on their electronic and electrochemical properties have emerged. In addition, this method has the advantage, i.e., ready introduction of the substituents into [n]phenacene framework. The HOMO/LUMO energies of the [n]phenacene derivatives can be tuned by the functional group modification. In particular, a substitution effect of a *side*-position is larger than that of an *edge*-position of the [n]phenacenes framework. Therefore, the functional groups can be introduced into the side-position of [n]phenacenes (Figure 4-2). A further elucidation of physical properties, in particular, FET characteristics of the synthesized [n]phenacenes is currently in progress. The Author expects that the FET

devices with a high performance can be obtained via the framework modification in the future.

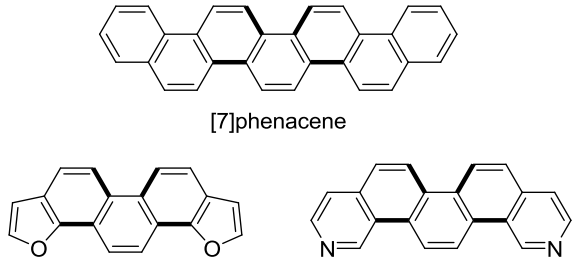

Figure 4-1. Analogous compounds of [n]phenacenes.

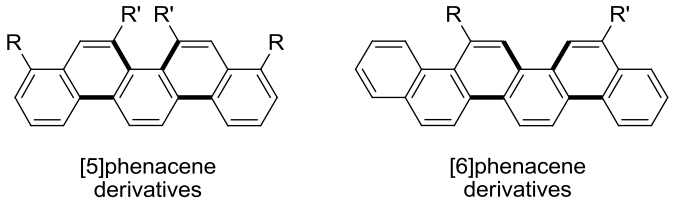

Figure 4-2. Derivatives of [n]phenacenes.

List of Publications

JOURNALS

Chapter 2

1) Synthesis of Substituted Picenes through Pd-Catalyzed Cross-Coupling Reaction/ Annulation Sequences and Their Physicochemical Properties

   Ning-hui Chang, Xi-chao Chen, Hikaru Nonobe, Yasuhiro Okuda, Hiroki Mori, Kiyohiko Nakajima, and Yasushi Nishihara*.

   Org. Lett. **2013**, *15*, 3558–3561.

Chapter 3

2) Synthesis of Substituted [6]Phenacenes through Suzuki-Miyaura Coupling of Polyhalobenzene with Alkenylboronates and Sequential Intramolecular Cyclization via C−H Bond Activation

   Ning-hui Chang, Hiroki Mori, Xi-chao Chen, Yasuhiro Okuda, Takeru Okamoto, and Yasushi Nishihara*.

   Chem. Lett. **2013**, doi:10.1246/cl.130584.

BOOK

Chapter 5, Liquid Crystals, in "Applied Cross-Coupling Reactions"

Ed by Y. Nishihara, Springer (2013)

Yasushi Nishihara, **Ning-hui Chang**, Megumi Kinoshita

ORGANIC LETTERS

2013
Vol. 15, No. 14
3558–3561

Synthesis of Substituted Picenes through Pd-Catalyzed Cross-Coupling Reaction/ Annulation Sequences and Their Physicochemical Properties

Ning-hui Chang,[†] Xi-chao Chen,[†] Hikaru Nonobe,[†] Yasuhiro Okuda,[†] Hiroki Mori,[†] Kiyohiko Nakajima,[‡] and Yasushi Nishihara*[,†,§]

Division of Earth, Life, and Molecular Sciences, Graduate School of Natural Science and Technology, Okayama University, 3-1-1 Tsushimanaka, Kita-ku, Okayama 700-8530, Japan, Japan Science and Technology Agency, ACT-C, 4-1-8 Honcho, Kawaguchi, Saitama 332-0012, Japan, and Department of Chemistry, Aichi University of Education, 1 Hirosawa, Igaya-cho, Kariya, Aichi 448-8542, Japan

ynishiha@okayama-u.ac.jp

Received May 16, 2013

ABSTRACT

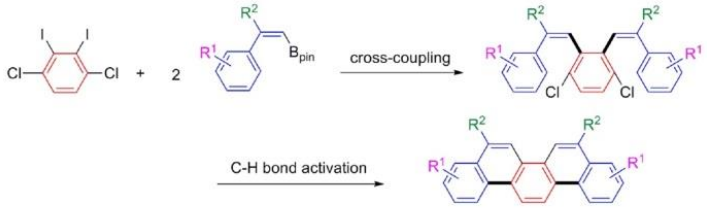

A novel and versatile synthetic method for picene derivatives is developed using the Pd-catalyzed intramolecular double cyclization of the corresponding 2,3-bis[(1*Z*)-2-phenylethenyl]-1,4-dichlorobenzenes, which are readily prepared by Suzuki–Miyaura cross-coupling reactions of polyhalobenzenes with (*Z*)-arylethenylboronates. The physical properties of the obtained picenes can be modified via introducing a variety of functional groups to the picene framework. All compounds are investigated by UV–vis and fluorescence spectroscopic measurements, CV, and DFT calculations as well as X-ray diffraction analysis.

Among the fused polycyclic compounds, [*n*]phenacenes, arm-chair edged benzenoid compounds possessing extended π-conjugation, have attracted a great deal of attention as an active layer in organic field-effect transistors (OFETs)[1] because of their mechanical flexibility, lightweight, large-area coverage, ambipolar property, and low-cost/low-temperature fabrication process. Picene ([5]phenacene; Figure 1) represents a novel and promising class of materials for organic electronics.[2] However, the systematic modification of a picene core has rarely been reported,[3] although the development of methods to prepare various picene derivatives is of great interest because it may adjust their optical and electronic properties as well as their solubility and packing structures in the crystals.[4] In addition, there are several critical drawbacks for the

[†] Okayama University.
[‡] Japan Science and Technology Agency.
[§] Aichi University of Education.

(1) (a) Sugawara, Y.; Kaji, Y.; Ogawa, K.; Eguchi, R.; Oikawa, S.; Gohda, H.; Fujiwara, A.; Kubozono, Y. *Appl. Phys. Lett.* **2011**, *98*, 013303. (b) Komura, N.; Goto, H.; He, X.; Mitamura, H.; Eguchi, R.; Kaji, Y.; Okamoto, H.; Sugawara, Y.; Gohda, S.; Sato, K.; Kubozono, Y. *Appl. Phys. Lett.* **2012**, *101*, 083301.

(2) (a) Okamoto, H.; Kawasaki, N.; Kaji, Y.; Kubozono, Y.; Fujiwara, A.; Yamaji, M. *J. Am. Chem. Soc.* **2008**, *130*, 10470. (b) Kawasaki, N.; Kubozono, Y.; Okamoto, H.; Fujiwara, A.; Yamaji, M. *Appl. Phys. Lett.* **2009**, *94*, 043310. (c) Mitsuhashi, R.; Suzuki, Y.; Yamanari, Y.; Mitamura, H.; Kambe, T.; Ikeda, N.; Okamoto, H.; Fujiwara, A.; Yamaji, M.; Kawasaki, N.; Maniwa, Y.; Kubozono, Y. *Nature* **2010**, *464*, 76. (d) Wang, Y.; Motta, S. D.; Negri, F.; Friedlein, R. *J. Am. Chem. Soc.* **2011**, *133*, 10054. (e) Kawai, N.; Eguchi, R.; Goto, H.; Akaike, K.; Kaji, Y.; Kambe, T.; Fujiwara, A.; Kubozono, Y. *J. Phys. Chem. C* **2012**, *116*, 7983.

(3) (a) Okamoto, H.; Yamaji, M.; Gohda, S.; Kubozono, Y.; Komura, N.; Sato, K.; Sugino, H.; Satake, K. *Org. Lett.* **2011**, *13*, 2758. (b) Kitazawa, K.; Kochi, T.; Nitani, M.; Ie, Y.; Aso, Y.; Kakiuchi, F. *Chem. Lett.* **2011**, *40*, 300. (c) Xia, Y.; Liu, Z.; Xiao, Q.; Qu, P.; Ge, R.; Zhang, Y.; Wang, J. *Angew. Chem., Int. Ed.* **2012**, *51*, 5714. (d) Mallory, F. B.; Mallory, C. W.; Regan, C. K.; Aspden, R. J.; Ricks, A. B.; Racowski, J. M.; Nash, A. I.; Gibbons, A. V.; Carroll, P. J.; Bohen, J. M. *J. Org. Chem.* **2013**, *78*, 2040.

(4) For examples of pentacene, see: (a) Takahashi, T.; Kitamura, M.; Shen, B.; Nakajima, K. *J. Am. Chem. Soc.* **2000**, *122*, 12876. (b) Payne, M. M.; Parkin, S. R.; Anthony, J. E.; Kuo, C.-C.; Jackson, T. N. *J. Am. Chem. Soc.* **2005**, *127*, 4986.

10.1021/ol401375n
Published on Web 07/01/2013

established synthetic methods for picenes, such as limitation of irradiation for large scale,[3a,d] multiple steps for their preparation,[3b,d] and a requirement of unstable precursors.[3c] Therefore, a simple and convenient strategy for the synthesis of various substituted picene derivatives is highly desirable in order to promote further investigations into its use in organic electronics. Herein we report the synthesis, characterization, and physicochemical properties of a series of novel substituted picenes.

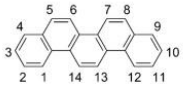

Figure 1. Structure of picene.

An outline for the synthesis of the substituted picene derivatives **4** is shown in Scheme 1. Although there have been no examples of the application of Pd-catalyzed C−H arylation to the picene synthesis, to the best of our knowledge, it would be a powerful method for the construction of the desired framework.[5] In order to obtain picene precursors **3**, Suzuki−Miyaura coupling reaction of 1,4-dichloro-2,3-diiodobenzene (**1**) with the stereodefined (*Z*)-alkenylboronates **2** bearing various substituents was designed.

A series of (*Z*)-alkenylboronates **2a**−**e** were successfully prepared by Rh-catalyzed stereoselective hydroboration of terminal alkynes[6] or the zirconium-mediated synthesis from alkynylboronate.[7] Suzuki−Miyaura coupling reactions of **1** with **2a**−**e** catalyzed by PEPPSI-IPr[8] gave the corresponding **3a**−**e** in moderate to high yields (Table 1).

Scheme 1. Retrosynthetic Route to Picene Derivatives **4**

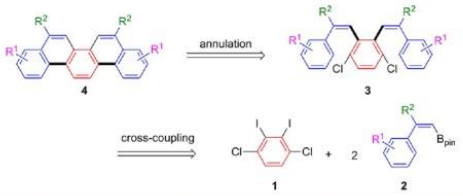

Next, we investigated the Pd-catalyzed double cyclization of **3a** through the C−H functionalization toward the synthesis of picene (**4a**). Among the different catalyst systems, the in situ generated $PdCl_2(PCy_3)_2$ from $PdCl_2(NCPh)_2$ and PCy_3 and pivalic acid as the additive was found to be the best. Encouraged by an identical ^{1}H NMR spectrum of the isolated **4a** to that of the commercial source, a series of picene derivatives **4b**−**e** were synthesized in moderate yields under optimized reaction conditions (Scheme 2).[9]

Table 1. Synthesis of the Picene Precursors **3** through Suzuki−Miyaura Coupling Reactions of **1** with **2**

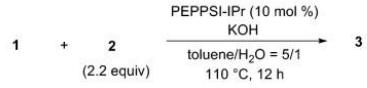

entry	**2**		**3**	yield (%)
1	**2a**	($R^1 = R^2 = H$)	**3a**	57
2	**2b**	(R^1 = 3-SiMe$_3$, $R^2 = H$)	**3b**	68
3	**2c**	(R^1 = 3-OMe, $R^2 = H$)	**3c**	67
4	**2d**	(R^1 = 2,4-OMe, $R^2 = H$)	**3d**	38
5	**2e**	($R^1 = H$, R^2 = Et)	**3e**	67

Scheme 2. Synthesis of Picenes **4a**−**e**

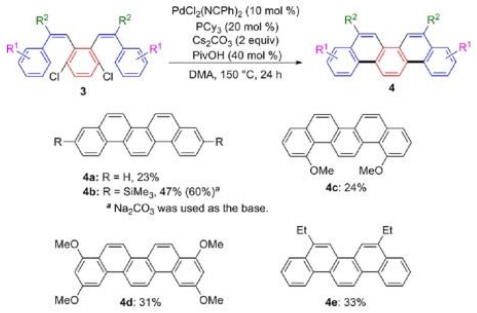

It is noteworthy that the structure of compound **4c** is different from our initial expectation that two methoxy groups would locate in the 3,10-positions by the C−H bond functionalization to avoid a steric congestion. However, as shown in Figure 2, X-ray structural analysis successfully clarified the structure of **4c**, in which two OMe groups are situated at the 1,12-positions.[10] Moreover, the ^{1}H NMR measurement of **4c** showed a characteristic singlet at δ 9.92 ppm.

The optical properties of **4a**−**e** were studied by UV−vis and steady-state fluorescence spectroscopy. The observed optical properties are listed in Table 2. As shown in Figure 3(A), the wavelengths of maximum absorptions (λ_{max}^{abs}) of **4a**−**e** are ca. 290 nm. The substituted picenes **4b**−**e** exhibited absorption peaks at longer wavelengths, but their molar

(5) For reviews, see: (a) Echavarren, A. M.; Gómez-Lor, B.; González, J. J.; Frutos, O. D. *Synlett* **2003**, 585. (b) Alberico, D.; Scott, M. E.; Lautens, M. *Chem. Rev.* **2007**, *107*, 174. (c) Lyons, T. W.; Sanford, M. S. *Chem. Rev.* **2010**, *110*, 1147.

(6) Ohmura, T.; Yamamoto, Y.; Miyaura, N. *J. Am. Chem. Soc.* **2000**, *122*, 4990.

(7) Nishihara, Y.; Miyasaka, M.; Okamoto, M.; Takahashi, H.; Inoue, E.; Tanemura, K.; Takagi, K. *J. Am. Chem. Soc.* **2007**, *129*, 12634.

(8) O'Brien, C. J.; Kantchev, E. A. B.; Valente, C.; Hadei, N.; Chass, G. A.; Lough, A.; Hopkinson, A. C.; Organ, M. G. *Chem.—Eur. J.* **2006**, *12*, 4743.

(9) Although the picene precursor **3** from a (*Z*)-arylethenylboronate bearing an electron-withdrawing CF_3 group in the 3-position was successfully synthesized, Pd-catalyzed double cyclization resulted in the formation of a mixture of structural isomers in a ratio of 46:54.

(10) CCDC-932531 (**4c**) contains the supplementary crystallographic data for this paper. These data can be obtained free of charge from the Cambridge Crystallographic Data Centre via www.ccdc.cam.ac.uk/data_request/cif.

Figure 2. ORTEP drawing of **4c** determined by X-ray crystallography with 30% thermal ellipsoidal plotting. Hydrogen atoms are omitted for simplicity.

extinction coefficient ε values are smaller compared to that of **4a**. These results indicate that an introduction of the substituents into a picene framework can affect the physical properties, since no concentration influence was observed when UV−vis spectra of **4a**−**e** in different concentrations were measured.[3,11] The absorption spectra of the either edged- (as **4b**) or side- (as **4c** and **4e**) substituents are similar in shape, possessing the main transition around 290 nm and at higher wavelengths the other transitions appeared as a shoulder.

Table 2. UV−vis[a] and Fluorescence[b] Data of Picenes **4a**−**e**

picenes	λ_{max}^{abs} (nm)	ε ($M^{-1}cm^{-1}$)	λ_{max}^{eme} (nm)	Stokes shift (cm^{-1})	Φ_f[d]
4a	285	94300	378	212	0.07
4b	293	56800	384	274	0.10
4c	290	49700	388	201	0.06
4d	290	55100	391	331	0.18
4e	290	43700	385	273	0.13

[a] 1×10^{-5} M in CH_2Cl_2. [b] 5×10^{-7} M in CH_2Cl_2. [c] Wavelength of maximum fluorescence emission. [d] *p*-Terphenyl was used as a standard sample.

Since all the compounds **4a**−**e** are fluorescent, we performed the fluorescence spectral measurements by using the diluted CH_2Cl_2 solution (5×10^{-7} M), as shown in Figure 3(B). The results are also summarized in Table 2. Using the λ_{max}^{abs} values of picenes as the 0−0 transition wavelength, the emission maxima (λ_{max}^{em}) displayed Stokes shifts by approximately 4 nm.[12] The relative fluorescence quantum yields (Φ_f) of **4a**−**e** were estimated with Williams' relative method.[13]

The substituents in the picene framework can significantly affect the Φ_f values. The Φ_f values of **4d** and **4e** were 0.18 and 0.13, respectively. An introduction of the methoxy group decreased the Φ_f values for **4c**. It is uncertain at present why the Φ_f value was changed by an introduction of these substituents.

The absorption band edges (λ_{onset}) of picenes **4a**−**e** and the corresponding optical band gaps (E_g^{opt}) calculated

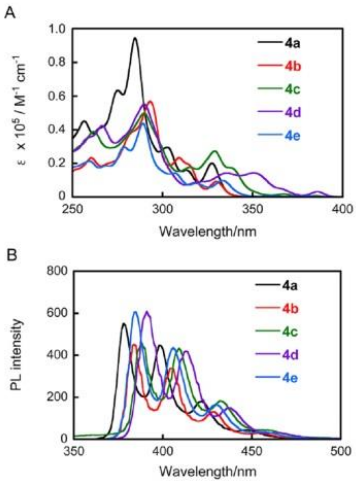

Figure 3. (A) Absorption spectra (1×10^{-5} M) and (B) fluorescence emission spectra with excitation wavelength at λ_{max}^{abs} (5×10^{-7} M) of **4a**−**e** in CH_2Cl_2.

from $1240/\lambda_{onset}$ are summarized in Table 3. The electrochemical properties of **4a**−**e** were also investigated by cyclic voltammetry (CV). The CV curves were recorded versus the potential of the Ag/Ag^+, which was calibrated by the ferrocene−ferrocenium (Fc/Fc^+) redox couple (−4.8 eV below the vacuum level).[14] The electrochemical data are also summarized in Table 3. The highest occupied molecular orbital (HOMO) energy levels were calculated from the CV data and the corresponding LUMO levels were estimated from formula $E_{LUMO} = E_{HOMO} + E_g^{opt}$. The observed oxidation waves and no reduction waves in the CV measurement suggest that all compounds are p-type semiconductors, which have potent applications in organic electronics. Moreover, all picene derivatives exhibited quasi-reversible oxidation wave,[15] reflecting that they possess an excellent electrochemical stability.

Picene derivative **4b** bearing the substituents in the 3,10-positions have the similar HOMO energy levels and slightly narrow optical band gaps than that of a parent picene **4a**. These results indicate that a substitution effect of a picene core in the 3,10-positions is rather small. In sharp contrast, other substituted picenes, **4c**, **4d**, and **4e**, have lower HOMO energy levels and smaller optical band gaps than that of **4a**. Furthermore, their HOMO levels significantly elevate with increasing the number of the substituents. In these cases, alkyl and methoxy groups introduced into the picene framework in the 1,12-, 2,11-, and 4,9-positions act as strong electron-donating groups. New five picenes **4b**−**e** could show better electron transfer capability in electronic devices since they showed relatively smaller the band gaps of than picene (3.23 eV).[16] Thus we calculated

(11) Kato, S.; Noguchi, H.; Kobayashi, A.; Yoshihara, T.; Tobita, S.; Nakamura, Y. *J. Org. Chem.* **2012**, *77*, 9120.
(12) Okamoto, H.; Yamaji, M.; Gohda, S.; Sato, K.; Sugino, H.; Satake, K. *Res. Chem. Intermed.* **2013**, *39*, 147.
(13) (a) Fery-Forgues, S.; Lavabre, D. *J. Chem. Educ.* **1999**, *76*, 1260. (b) Suzuki, K.; Kobayashi, A.; Kaneko, S.; Takehira, K.; Yoshihara, T.; Ishida, H.; Shiina, Y.; Oishi, S.; Tobita, S. *Phys. Chem. Chem. Phys.* **2009**, *11*, 9850.
(14) Liu, S.-Y.; Shi, M.-M.; Huang, J.-C.; Jin, Z.-N.; Hu, X.-L.; Pan, J.-Y.; Li, H.-Y.; Jen, A. K.-Y.; Chen, H.-Z. *J. Mater. Chem. A* **2013**, *1*, 2795.
(15) See the Supporting Information.

Table 3. Physicochemical Properties of Picenes **4a**–**e**

compd	E_{onset}[a] (V)	E_{HOMO} (eV)[b]	E_{LUMO} (eV)[c]	$E_g^{opt}/\lambda_{onset}$[(eV)[d]/nm]	E_{HOMO} (eV)[f]	E_{LUMO} (eV)[f]	E_g (eV)[f]
4a	+0.88	−5.80	−2.57	3.23/384	−5.48	−1.27	4.21
4b	+0.86	−5.78	−2.60	3.18/390	−5.45	−1.25	4.20
4c	+0.59	−5.51	−2.38	3.13/396	−5.12	−1.02	4.10
4d	+0.37	−5.29	−2.21	3.08/402	−4.80	−0.84	3.96
4e	+0.74	−5.67	−2.52	3.15/393	−5.33	−1.19	4.14

[a] Obtained from cyclic voltammograms in CH_2Cl_2. Reference electrode: Ag/Ag^+. [b] All of the potentials were calibrated with the Fc/Fc^+ ($E^{1/2} = -0.12$ V measured under identical conditions). Estimated with the following equation: E_{HOMO} (eV) $= -4.92 - E_{onset}$. [c] Calculated according to the formula $E_{LUMO} = E_{HOMO} + E_g^{opt}$. [d] Optical band gap, $E_g^{opt} = 1240/\lambda_{onset}$. [e] Obtained from theoretical calculations.

molecular reorganization energy (λ), which may potentially affect the transport properties.[17] From the results of λ^h, **4c** should be advantageous for efficient carrier transport. However, the calculated transfer integrals (t_{HOMO}s) of **4c** were found to be fairly small, because packing structure of **4c** is less effective for carrier transport, which was quite different from **4a** with high field-effect mobility.[18]

Electronic structures of novel picenes **4a**–**e** are theoretically investigated through calculation. The molecular geometries of **4a**–**e** were optimized using density functional theory (DFT) at the B3LYP/6-31G(d) level using Gaussian 09, Revision A. 02.[19] The results are also listed in Table 3. The frontier molecular orbitals of the optimized molecules were also calculated, as shown in Figure 4. The theoretically calculated HOMO–LUMO gaps are higher than those obtained in the UV–vis spectroscopic measurements (E_g^{opt}) by ca. 1.0 eV. All the HOMOs and LUMOs of picenes **4a**–**e** are evenly delocalized over the entire molecular π-frameworks. In addition, coefficients of picenes **4c**–**e** reside on the 1,12-, 2,11-, and 4,9-methoxy and 5,8-alkyl groups in the HOMO. On the other hand, the carbon atoms in the 3,10-position in **4b** have nodal planes in the HOMO. These results clearly support the similarity/difference of the energy levels of the frontier orbitals as well as the molecular electronic structures among **4a**–**e**.

In summary, we have developed a novel and versatile synthetic method for the synthesis of various picene derivatives by sequential Suzuki–Miyaura coupling and cyclization via intramolecular C–H bond functionalization. This methodology might also be used for the synthesis of other picene analogues, for instance, heteroatom-containing picenes and unsymmetric fused aromatic compounds such as [6]-phenacene. On the basis of this study, the effects of the structural variations of substituents on their electronic and electrochemical properties have emerged. A further elucidation of their physical properties involving the FET characters is underway in our laboratories.

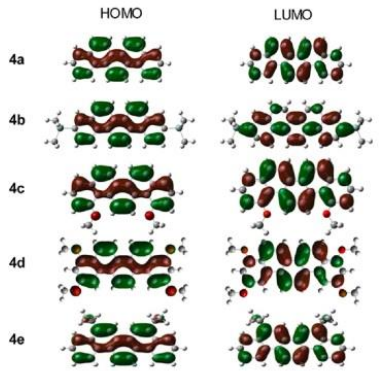

Figure 4. Wave functions for the HOMO and LUMO of **4a**–**e**.

Acknowledgment. We gratefully thank Profs. Koichi Mitsudo and Seiji Suga (Okayama University) for the measurements of CV and Ms. M. Kosaka and Mr. M. Kobayashi at the Department of Instrumental Analysis, Advanced Science Research Center, Okayama University, for the measurements of elemental analyses, respectively. The SC-NMR Laboratory of Okayama University for the NMR spectral measurements is gratefully acknowledged.

Supporting Information Available. Copies of ^1H NMR and $^{13}C\{^1H\}$ NMR spectra for all the new compounds, as well as details on experimental procedures and characterization data. This material is available free of charge via the Internet at http://pubs.acs.org.

The authors declare no competing financial interest.

(16) Li, G.; Wu, Y.; Gao, J.; Wang, C.; Li, J.; Zhang, H.; Zhao, Y.; Zhao, Y.; Zhang, Q. *J. Am. Chem. Soc.* **2012**, *134*, 20298.

(17) (a) Bredas, J.-L.; Beljonne, D.; Coropceanu, V.; Cornil, J. *Chem. Rev.* **2004**, *104*, 4971. (b) Sakanoue, K.; Motoda, M.; Sugimoto, M.; Sakaki, S. *J. Phys. Chem. A* **1999**, *103*, 5551.

(18) Takimiya, K.; Shinamura, S.; Osaka, I.; Miyazaki, E. *Adv. Mater.* **2011**, *23*, 4347.

(19) Frisch, M. J.; Trucks, G. W.; Schlegel, H. B.; Scuseria, G. E.; Robb, M. A.; Cheeseman, J. R.; Scalmani, G.; Barone, V.; Mennucci, B.; Petersson, G. A.; Nakatsuji, H.; Caricato, M.; Li, X.; Hratchian, H. P.; Izmaylov, A. F.; Bloino, J.; Zheng, G.; Sonnenberg, J. L.; Hada, M.; Ehara, M.; Toyota, K.; Fukuda, R.; Hasegawa, J.; Ishida, M.; Nakajima, T.; Honda, Y.; Kitao, O.; Nakai, H.; Vreven, T.; Montgomery, J. A., Jr.; Peralta, J. E.; Ogliaro, F.; Bearpark, M.; Heyd, J. J.; Brothers, E.; Kudin, K. N.; Staroverov, V. N.; Kobayashi, R.; Normand, J.; Raghavachari, K.; Rendell, A.; Burant, J. C.; Iyengar, S. S.; Tomasi, J.; Cossi, M.; Rega, N.; Millam, J. M.; Klene, M.; Knox, J. E.; Cross, J. B.; Bakken, V.; Adamo, C.; Jaramillo, J.; Gomperts, R.; Stratmann, R. E.; Yazyev, O.; Austin, A. J.; Cammi, R.; Pomelli, C.; Ochterski, J. W.; Martin, R. L.; Morokuma, K.; Zakrzewski, V. G.; Voth, G. A.; Salvador, P.; Dannenberg, J. J.; Dapprich, S.; Daniels, A. D.; Farkas, Ö.; Foresman, J. B.; Ortiz, J. V.; Cioslowski, J.; Fox, D. J. Gaussian, Inc., Wallingford, CT, 2009.

Advance Publication Cover Page

Chemistry Letters

Synthesis of Substituted [6]Phenacenes through Suzuki-Miyaura Coupling of Polyhalobenzene with Alkenylboronates and Sequential Intramolecular Cyclization via C−H Bond Activation

Ning-hui Chang, Hiroki Mori, Xi-chao Chen, Yasuhiro Okuda, Takeru Okamoto, and Yasushi Nishihara*

Advance Publication on the web July 11, 2013 by J-STAGE
doi:10.1246/cl.130584

Synthesis of Substituted [6]Phenacenes through Suzuki-Miyaura Coupling of Polyhalobenzene with Alkenylboronates and Sequential Intramolecular Cyclization via C−H Bond Activation

Ning-hui Chang,[1] Hiroki Mori,[1] Xi-chao Chen,[1] Yasuhiro Okuda,[1] Takeru Okamoto,[1] and Yasushi Nishihara*[1,2]
[1]*Division of Earth, Life, and Molecular Sciences, Graduate School of Natural Science and Technology, Okayama University, 3-1-1 Tsushimanaka, Kita-ku, Okayama 700-8530*
[2]*Japan Science and Technology Agency, ACT-C, 4-1-8 Honcho, Kawaguchi, Saitama 332-0012*

E-mail: ynishiha@okayama-u.ac.jp

A series of substituted [6]phenacenes are synthesized through Suzuki-Miyaura coupling and intramolecular double cyclization utilizing polyhalobenzene and two different alkenylboronates. This methodology addresses a straightforward route to unsymmetrical [6]phenacenes. Physicochemical properties of four [6]phenacenes are evaluated by UV−vis and fluorescence spectra as well as cyclic voltammetry (CV).

[n]Phenacenes,[1] where n is the number of fused benzene rings with an arm-chaired structure, have attracted much attention because [5]phenacene (picene)[2] and [6]phenacene (fulminene)[3] are known to exhibit superior FET characteristics (Chart 1). Generally, solubilities of the unsubstituted [n]phenacenes dramatically decrease with increasing n. For instance, [5]phenacene is sparingly soluble in $CHCl_3$, whereas the $^{13}C\{^1H\}$ NMR spectrum of [6]phenacene cannot be obtained due to its extreme insolubility. Typically, this solubility problem can be solved by incorporating suitable substituents into the core.

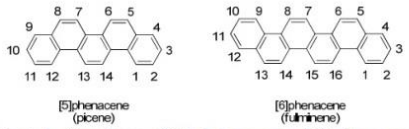

Chart 1. Structures of [5]phenacene and [6]phenacene.

From the synthetic point of view, most of the precedent [n]phenacene synthesis by oxidative photocyclizations of (*Z*)-stilbene skeletons[4] are mainly applicable to the synthesis of symmetrical [n]phenacene (i.e. n = 5 and 7). Notably, although the unsubstituted [6]phenacene has been barely synthesized,[1,5,6] to the best of our knowledge, the synthesis of the substituted [6]phenacenes are unprecedented to date. Herein, we report the synthesis, characterization, and physicochemical properties of unsymmetrically substituted [6]phenacenes for the first time by using our synthetic strategy for the synthesis of [5]phenacenes recently established.[7]

The first set of experiments examined the reaction conditions of Suzuki-Miyaura coupling of 1,4-dichloro-2,3-diiodobenzene (**1**) with a slightly excess of (*Z*)-2-naphthylethenylboronate **2**, prepared by Rh-catalyzed stereoselective hydroboration of terminal alkynes.[8] The results are summarized in Table 1.

Table 1. Optimization of conditions for cross-coupling reaction of **1** with **2**[a]

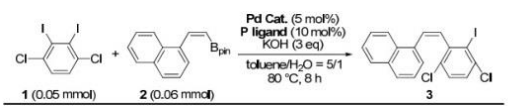

entry	Pd cat.	ligand	yield (%)[b]
1	PEPPSI-IPr	—	22
2	$Pd(OAc)_2$	PCy_3	43
3	$Pd(OAc)_2$	dppe	10
4	$Pd(OAc)_2$	$P[(2,4,6\text{-}(MeO)_3C_6H_2)]_3$	34
5	$Pd(OAc)_2$	RuPhos	32
6	$Pd(OAc)_2$	SPhos	60
7	$Pd(OAc)_2$	$P(3,5\text{-}CF_3C_6H_3)_3$	61
8	$PdCl_2(NCPh)_2$	$P(3,5\text{-}CF_3C_6H_3)_3$	53
9[c]	$PdCl_2$(dppp)	—	60
10[c]	**$PdCl_2$(dppf)**	**—**	**74 (57)**

[a] Reaction conditions: **1** (0.05 mmol), **2** (0.06 mmol), Pd catalyst (5 mol%), and ligand (10 mol%) at 80 °C for 8 h, unless otherwise noted. [b] GC yields. An isolated yield is shown in parenthesis. [c] Aqueous KOH (3 M) as the base and THF as the solvent were employed at 50 °C.

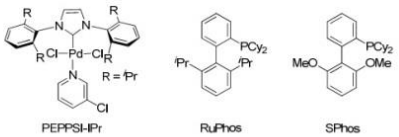

We initially utilized PEPPSI-IPr[9] as the catalyst, which exerts high efficiency in our previous work.[7] However, the desired product **3** was obtained in only 22% due to a concurrent protodeborylation of **2** (Table 1, entry 1). We then exploited other palladium catalysts, mainly, with bulky phosphine ligands. A combination of $Pd(OAc)_2$ with $P(3,5\text{-}CF_3C_6H_3)_3$ gave the desired product **3** in 61% yield (Table 1, entry 7). To our delight, when the bidentate ligands were surveyed, $PdCl_2$(dppf) (dppf = 1,1'-bis(diphenylphosphino)ferrocene) gave the best yield of **3** up to 74% (Table 1, entry 10).

With the synthesized **3** in hand, we conducted the second cross-coupling with the synthesized alkenylboronates **4a-4d** as the coupling partners. The PEPPS-IPr catalyst gave rise to the corresponding [6]phenacene precursors **5a−5d** in 63-83% yields (Table 2).[10]

Table 2. Synthesis of **5a-5d** by Suzuki-Miyaura coupling of **3** with **4a-4d**[a]

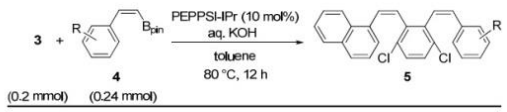

entry	4		product	yield (%)[b]
1		**4a**	**5a**	63
2	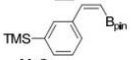	**4b**	**5b**	76
3	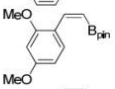	**4c**	**5c**	83
4	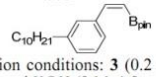	**4d**	**5d**	69

[a] Reaction conditions: **3** (0.2 mmol), **4** (0.24 mmol), PEPPSI-IPr (10 mol%), and KOH (3 M, 1.2 mmol) at 80 °C for 12 h. [b] Isolated yields.

Finally, we performed the Pd-catalyzed double cyclization of **5a-5d** through the C−H activation[11] toward the synthesis of [6]phenacenes **6a-6d** (Scheme 1).[12] The solubility of [6]phenacene **6b** is so poor that its ^{13}C NMR data were not available, whereas the solubility of **6c** and **6d** was obviously improved by introducing the OMe groups and alkyl chains, thus implying the possibility to fabricate single crystals by solution process.

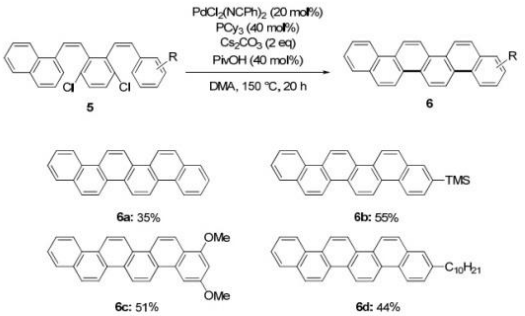

Scheme 1. Synthesis of [6]phenacenes **6a-6d** by intramolecular double cyclization of **5a-5d**.

In order to further survey the potentials toward organic electronic materials, we measured UV-vis and steady-state fluorescence spectroscopy of **6a-6d** and the results are listed in Table 3. As shown in Figure 1, the absorption spectra of **6b-6d** show main transition around 300 nm (λ_{max}^{abs}) and the other transitions appeared at higher wavelengths, which are similar with the parent **6a**. Molar extinction coefficient ε values of substituted [6]phenacenes **6b-6d** are available owing to the increased solubility than that of **6a**. Obviously, these results indicate that an introduction of the substituents into a [6]phenacene framework can affect the physical properties. In particular, a substitution effect of two methoxy groups at the 2,4-position is larger than that of alkyl and TMS groups at the 3-position.

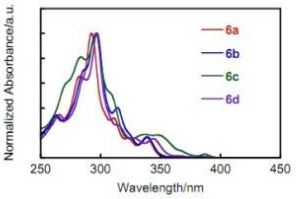

Figure 1. UV-vis absorption spectra of **6a-6d** in CH_2Cl_2.

Fluorescence spectra in diluted CH_2Cl_2 solution (1×10^{-6} M) are shown in Figure S1 in SI[13] and the results are also summarized in Table 3. The Stokes shifts of **6b** and **6d** are ca. 200 cm^{-1}, which are similar to that of parent **6a**.[6] In contrast, the shift of **6c** is higher than that of **6a**. This can be attributed to the slightly large and flexible molecular geometry of **6c**, which can have access to different geometrical configuration. The relative fluorescence quantum yields (Φ_f) of **6a-6d** were estimated with relative method.[14] The Φ_f values of **6c** are more than twice as much as that of **6a**, suggesting that an introduction of two electron-donating methoxy groups increased the Φ_f values.

Table 3. UV-vis[a] and fluorescence[b] data of [6]phenacenes **6a-6d**

[6]phenacenes	λ_{max}^{abs} /nm[a]	ε /M^{-1}cm^{-1}	λ_{max}^{em} /nm[b]	Stokes shift /cm^{-1}	Φ_f[c]
6a	293	nd[d]	385	204	0.07
6b	297	40000	387	202	0.09
6c	296	45000	391	264	0.17
6d	297	55700	389	200	0.09

[a]Absorption maxima in the CH_2Cl_2 solution (1×10^{-5} M). [b]Emission maxima in CH_2Cl_2 solution (1×10^{-6} M) excited at λ_{max}^{abs}. [c]Fluorescence quantum yield were determined by the relative method using *p*-terphenyl ($\Phi_f = 0.87$ in cyclohexane) as a standard. [d]Molar absorption coefficient of parent [6]phenacene **6a** cannot be determined due to its low solubility (saturated solution was used).

The absorption band-edges (λ_{edge}) of [6]phenacene **6a-6d** and the corresponding optical band gaps (E_g^{opt}) are summarized in Table 4. The electrochemical properties of **6a-6d** were also investigated by cyclic voltammetry (CV) (see Figure 2 for **6d** and Figure S2) and the electrochemical data are also listed in Table 4. The observed oxidation waves with oxidation onsets at +0.36-0.84 V (vs Ag/Ag$^+$) and no reduction waves in the CV measurements suggest that all compounds **6a-6d** have a potential for p-channel semiconductors in organic electronics. Moreover, **6d** shows quasi-reversible oxidation peaks at +0.76 V (onset, vs Ag/Ag$^+$). The good reversibility of its voltammograms implies that its oxidized species are electrochemically stable.

Table 4. Physicochemical properties of [6]phenacenes **6a-6d**.

[6]phenacenes	E_{onset} (V)[a]	E_{HOMO} (eV)[b]	E_{LUMO} (eV)[c]	E_g^{opt}/λ_{edge}[(eV)[d]/nm]	E_{HOMO} (eV)[e]	E_{LUMO} (eV)[e]	E_g (eV)[e]
6a	+0.84	−5.76	−2.57	3.19/389	−5.41	−1.39	4.02
6b	+0.81	−5.73	−2.58	3.15/393	−5.39	−1.39	4.00
6c	+0.36	−5.29	−2.17	3.12/397	−5.02	−1.22	3.80
6d	+0.76	−5.68	−2.56	3.12/397	−5.36	−1.34	4.02

[a]Obtained from cyclic voltammograms in CH_2Cl_2. V vs Ag/Ag^+. [b]All the potentials were calibrated with the Fc/Fc^+ ($E^{1/2}$ = -0.12 V measured under identical conditions). Estimated with a following equation: E_{HOMO} (eV) = −4.92 − E_{onset}. [c]Calculated according to the formula $E_{LUMO} = E_{HOMO} + E_g^{opt}$. [d]Optical band gap calculated from λ_{edge}, $E_g^{opt} = 1240/\lambda_{edge}$. [e]Obtained from theoretical calculations.

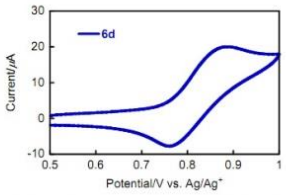

Figure 2. Cyclic voltammograms of **6d** (1 mM) in CH_2Cl_2 solution containing 0.1 M Bu_4NPF_6 as supporting electrolyte at a scan rate of 100 mV/s.

[6]Phenacenes **6b** and **6d** bearing the substituents in the 3-position have the similar HOMO energy levels and slightly narrow optical band gaps than that of **6a**. These results indicate that a substituent effect of the [6]phenacene core in the 3-positions is rather small. In sharp contrast, the methoxy-substituted [6]phenacene **6c** has almost the same optical energy gaps (~3.12 eV), but the higher HOMO energy level than that of **6a**.

In order to understand the difference of the electronic structure, the molecular geometries of **6a**−**6d** were optimized using density functional theory (DFT) at the B3LYP/6-31G(d) level using Gaussian 09, Revision A. 02. The results are also listed in Table 4. The frontier molecular orbitals of the optimized molecules were also calculated (see Figure S3). All the HOMOs and LUMOs of [6]phenacenes except **6c** are evenly delocalized over the entire molecular π-frameworks. The HOMO coefficient of [6]phenacenes in the 3-position is relatively small, implying the small inductive effect of alkyl and TMS groups. On the other hand, the HOMO coefficient is strongly located in the 2,4-positions of a [6]phenacene core of **6c**. In fact, the HOMOs of **6c** partially delocalized to the peripheral groups, whilst the LUMOs were mainly localized on the core. These results are clearly consistent with the similarity/difference of the energy levels of the frontier orbitals as well as the molecular electronic structures among **6a-6d**, as evident from their physicochemical properties.

In summary, we synthesized a new family of the unsymmetrically substituted [6]phenacenes via sequential Suzuki-Miyaura coupling and intramolecular cyclization. An introduction of methoxy and alkyl groups into [6]phenacene framework increased the solubility of [6]phenacenes. A further elucidation of physical properties, in particular, FET characteristics of the obtained [6]phenacenes is currently underway.

The authors gratefully thank Ms. Megumi Kosaka and Mr. Motonari Kobayashi at the Department of Instrumental Analysis, Advanced Science Research Center, Okayama University for the measurements of elemental analyses and the SC-NMR Laboratory of Okayama University for the NMR spectral measurements. Y.N. is grateful to JNC Petrochemical Corporation for generous donation of trimethylsilylacetylene.

References and Notes

1 F. B. Mallory, K. E. Butler, A. C. Evans, C. W. Mallory, *Tetrahedron Lett.* **1996**, *37*, 7173.

2 a) H. Okamoto, N. Kawasaki, Y. Kaji, Y. Kubozono, A. Fujiwara, M. Yamaji, *J. Am. Chem. Soc.* **2008**, *130*, 10470. b) N. Kawasaki, Y. Kubozono, H. Okamoto, A. Fujiwara, M. Yamaji, *Appl. Phys. Lett.* **2009**, *94*, 043310. c) Y. Kaji, R. Mitsuhashi, X. Lee, H. Okamoto, T. Kambe, N. Ikeda, A. Fujiwara, M. Yamaji, K. Omote, Y. Kubozono, *Org. Electron.* **2009**, *10*, 432. d) Y. Kaji, N. Kawasaki, X. Lee, H. Okamoto, Y. Sugawara, S. Oikawa, A. Ito, H. Okazaki, T. Yokoya, A. Fujiwara, Y. Kubozono, *Appl. Phys. Lett.* **2009**, *95*, 183302. e) N. Kawasaki, W. L. Kalb, T. Mathis, Y. Kaji, R. Mitsuhashi, H. Okamoto, Y. Sugawara, A. Fujiwara, Y. Kubozono, B. Batlogg, *Appl. Phys. Lett.* **2010**, *96*, 113305. f) Y. Kaji, K. Ogawa, R. Eguchi, H. Goto, Y. Sugawara, T. Kambe, K. Akaike, S. Gohda, A. Fujiwara, Y. Kubozono, *Org. Electron.* **2011**, *12*, 2076.

3 a) N. Komura, H. Goto, X. He, H. Mitamura, R. Eguchi, Y. Kaji, H. Okamoto, Y. Sugawara, S. Gohda, K. Sato, Y. Kubozono. *Appl. Phys. Lett.* **2012**, *101*, 083301. b) X. He, R. Eguchi, H. Goto, E. Uesugi, S. Hamao, Y. Takabayashi, Y. Kubozono. *Org. Electron.* **2013**, *14*, 1673.

4 a) F. B. Mallory, K. E. Butler, A. C. Evans, E. J. Brondyke, C. W. Mallory, C. Yang, A. Ellenstein, *J. Am. Chem. Soc.* **1997**, *119*, 2119. b) F. B. Mallory, K. E. Butler, A. Bérubé, E. D. Luzik, Jr., C. W. Mallory, E. J. Brondyke, R. Hiremath, P. Ngo, P. J. Carroll. *Tetrahedron* **2001**, *57*, 3715. c) F. B. Mallory, C. W. Mallory, C. K. Regan, R. J. Aspden, A. B. Ricks, J. M. Racowski, A. I. Nash, A. V. Gibbons, P. J. Carroll, J. M. Bohen. *J. Org. Chem.* **2013**, *78*, 2040.

5 R. G. Harvey, J. Pataki, C. Cortez, P. D. Raddo, C. Yang. *J. Org. Chem.* **1991**, *56*, 1210.

6 H. Okamoto, M. Yamaji, S. Gohda, K. Sato, H. Sugino, K. Satake, *Res Chem Intermed* **2013**, *39*, 147.

7 N.-H. Chang, X.-C. Chen, H. Nonobe, Y. Okuda, H. Mori, K. Nakajima, Y. Nishihara, *Org. Lett.* in press. DOI: 10.1021/ol401375n.

8 T. Ohmura, Y. Yamamoto, N. Miyaura, *J. Am. Chem. Soc.* **2000**, *122*, 4990.

9 C. J. O'Brien, E. A. B. Kantchev, C. Valente, N. Hadei, G. A. Chass, A. Lough, A. C. Hopkinson, M. G. Organ, *Chem. Eur. J.* **2006**, *12*, 4743.

10 With $PdCl_2$(dppf) the reaction of **3** with **4a** resulted in a lower yield of **5a** (55%). In addition, the reaction of **1** with an equimolar amount of **4** in place of **2** gave a mixture of mono-coupled and di-coupled products. This result strongly indicates that the sequence of the reagent addition is very critical.

11 a) K. Kamikawa, I. Takemoto, S. Takemoto, H. Matsuzaka, *J. Org. Chem.* **2007**, *72*, 7406. b) R. Umeda, S. Miyake, Y. Nishiyama, *Chem. Lett.* **2012**, *41*, 215.

12 The main by-product in the cyclization step is the protodechlorinated compound.

13 Supporting Information is available electronically on the CSJ-Journal Web site, http://www.csj.jp/journals/chem-lett/index.html.

14 a) S. Fery-Forgues, D. Lavabre, *J. Chem. Educ.* **1999**, *76*, 1260. b) K. Suzuki, A. Kobayashi, S. Kaneko, K. Takehira, T. Yoshihara, H. Ishida, Y. Shiina, S. Oishi, S. Tobita, *Phys. Chem. Chem. Phys*. **2009**, *11*, 9850.

Presentations

1) Fine Synthesis of Conjugated Molecular Applied to Organic Thin Film Solar Cell (poster) **Ning-hui Chang**, Megumi Kinoshita, Masayuki Iwasaki, and Yasushi Nishihara.

   The 6th Meeting and Exchange Research between High School Students and Graduate Students, P-29, Okayama University, July 29, 2011.

2) Fine Synthesis of Conjugated Molecular Applied to Organic Thin Film Solar Cell (poster) **Ning-hui Chang**, Megumi Kinoshita, Masayuki Iwasaki, and Yasushi Nishihara.

   Exhibition of Wisdom in Okayama University 2011, P-19, Okayama University, Nov 2, 2011.

3) Efficient Synthesis of Substituted Picene Derivatives by Cross-Coupling Reactions (poster) **Ning-hui Chang**, Megumi Kinoshita, Hikaru Nonobe, Xi-chao Chen, Masayuki Iwasaki, and Yasushi Nishihara.

   The 59th Symposium on Organometallic Chemistry, P2C-03, Osaka University, Suita Campus, Osaka, Sep 13-15, 2012.

4) Synthesis of Substituted [5]- and [6]Phenacenes through Pd-Catalyzed Cross-Coupling Reactions and Their Physicochemical Properties (poster)

   Ning-hui Chang, Xi-chao Chen, Hikaru Nonobe, Yasuhiro Okuda, Hiroki Mori, Kiyohiko Nakajima, and Yasushi Nishihara.

   The 60th Symposium on Organometallic Chemistry, P3B-05, Gakushuin University, Tokyo, Sep 12-14, 2013. (expected)

5) Synthesis of Substituted Picene Derivatives through Cross-Coupling Reactions (oral)

   Ning-hui Chang, Hikaru Nonobe, Xi-chao Chen, Megumi Kinoshita, Masayuki Iwasaki, Kiyohiko Nakajima, and Yasushi Nishihara.

2013 BK21 Symposium on Chemical Materials Science, OP-01, Diamante Hall, Vivaldi Park, Hongcheon-gun, Korea, Feb 14-15, 2013.

Acknowledgements

On the occasion of the completed Thesis, the Author is deeply grateful to his supervisor: Professor Yasushi Nishihara for patiently and thoughtfully taking him through this chemistry research in the past three years in Japan. Prof. Nishihara, his mentor, gave him an opportunity to conduct this research and the Author obtained lots of sincere instruction, valuable suggestions, and constant encouragement in science research as well as in life.

The Author also would like to express his sincerest appreciation to Assistant Profs. Masayuki Iwasaki and Hiroki Mori for their practical guidance, fruitful discussions, and considerate suggestions.

The Author wish to acknowledge Prof. Kiyohiko Nakajima for measurements of X-ray, Profs. Koichi Mitsudo and Seiji Suga for measurements of CV, Ms. Megumi Kosaka and Mr. Motonari Kobayashi for measurements of elemental analyses, respectively. The SC-NMR Laboratory of Okayama University for the NMR spectral measurements is gratefully acknowledged.

The Author would like to take this opportunity to thank all the persons who have contributed in the different aspects of this study. They have all made it possible for him to commence and complete this task.

The Author gratefully thanks his fellow lab mates, including the persons who have graduated from this lab. He has been blessed with a friendly and cheerful group of fellow students. The Author is able to quickly integrate into new life owing to their generous and hospitably help. They taught him master the basic experimental skill, and made his daily life rich and colorful in Japan. The Author also shows his gratefully thanks to his Chinese friends in Japan. Their positive attitude and help have taken him ahead and will also sustain the vitality of his study in the future.

The Author's special appreciation goes to his wife, Jiao Jiao. This achievement would not be possible without her continuous company, understanding, and supporting.

Finally, the Author would like to acknowledge his family, relatives and friends in China for supporting him throughout all his studies at Okayama University.

Ning-hui CHANG

2013.09